

Supporting Information

Simultaneous Discovery of Chiral and Achiral Dyes: Elucidating Optical Functions of Helical and Flag-Hinged Boron-Tetridentate Complexes

Luxia Cui,^[a] Ryoji Furuta,^[a] Takunori Harada,^[b] Takeru Konta,^[b] Yu Hoshino,^[a, c] and Toshikazu Ono^{*[a, c]}

[a] Department of Chemistry and Biochemistry, Graduate School of Engineering, Kyushu University
744 Motooka, Nishi-ku, Fukuoka 819-0395, Japan. E-mail: tono@mail.cstm.kyushu-u.ac.jp.

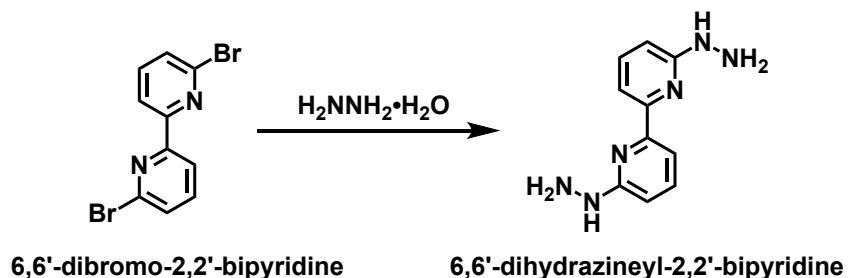
[b] Faculty of Science and Technology, Graduate School of Engineering, Oita University 700
Danno-haru, Oita City 870-1192, Japan.

[c] Center for Molecular Systems (CMS), Kyushu University 744 Motooka, Nishi-ku, Fukuoka 819-
0395, Japan.

Materials and measurements

All chemical reagents and solvents used in this study were obtained from commercial sources and used as received unless otherwise stated. The NMR spectra (^1H , ^{13}C , ^{19}F , and ^{11}B NMR) were recorded by using a Bruker Avance 400 NMR spectrometer. The chemical shifts (in ppm) of ^1H NMR were referenced relative to tetramethylsilane ($\text{CH}_3)_4\text{Si}$, with the residual solvent peak of dimethyl sulfoxide- d_6 ($\text{DMSO}-d_6$) at 2.50 ppm, chloroform- d (CDCl_3) at 7.26 ppm or dichloromethane- d_2 (CD_2Cl_2) at 5.32 ppm, as an internal standard, respectively. The chemical shifts (in ppm) of ^{13}C NMR were referenced relative to the residual solvent peak of CDCl_3 at 77.2 ppm or CD_2Cl_2 at 53.8 ppm. The chemical shifts (in ppm) of ^{19}F and ^{11}B NMR were referenced relative to hexafluorobenzene (C_6F_6) at -162.90 ppm and boron trifluoride-ethyl ether complex ($\text{BF}_3\bullet\text{OEt}_2$) at 0.0 ppm in CDCl_3 or CD_2Cl_2 , respectively. The coupling constants, J are reported in Hertz (Hz). Multiplicity is abbreviated as follows: s = singlet, d = doublet, t = triplet, m = multiplet, and dd = double doublet. The high-resolution mass spectra (HRMS, FAB-MS) were performed with a JEOL JMS-700 instrument. Melting points (m.p.) were measured with a DTM-01 melting point meter (AS ONE Corporation). UV-vis absorption spectra were recorded using a Hitachi U-3900H spectrophotometer. Fluorescence excitation and emission spectra were collected on a Hitachi F-7000 fluorescence spectrophotometer at room temperature or 77 K (liquid N_2). Emission spectra were collected in the range between 300–800 nm, with a scan speed of 240 nm/min, and the slits were set at 5.0 nm (excitation slit) and 5.0 nm (emission slit). The absolute photoluminescence quantum yields (Φ_{PL}) were determined using absolute PL quantum yields measurement system C9920-02 (Hamamatsu photonics) after excitation at maximum absorption wavelength ($\lambda_{\text{abs}}^{\text{max}}$). Time-resolved photoluminescence lifetimes were carried out by using time-correlated single photon counting lifetime spectroscopy system, Quantaurus-Tau C11367-05 (Hamamatsu photonics). The decay constants and fitting parameters (τ_1 , τ_2 , A_1 , A_2) for transient decays were determined using the embedded software of Quantaurus-Tau. Circular Dichroism (CD) spectra were recorded on JASCO J-1500 spectrometer at 25°C. Circularly polarized luminescence (CPL) and DC (= nonpolarized fluorescence) spectra were measured by using a Comprehensive Chiroptical Spectrophotometer (CCS) equipped with Stokes-Mueller matrix analysis system. The excitation wavelength was set to 330 nm and the emission wavelengths were recorded over a wavelength range of 800–300 nm with 33 mm slit width and 10 nm spectral bandwidth for the excitation and emission monochromators, respectively. All the products were isolated by silica-gel column chromatography (Kanto Chemicals, 60N); and then isolated products were identified by HRMS (FAB-MS), ^1H , ^{13}C , ^{19}F , and ^{11}B NMR.

(1) Synthesis of compound 6,6'-dihydrazineyl-2,2'-bipyridine¹



Scheme S1. Synthesis of compound 6,6'-dihydrazineyl-2,2'-bipyridine.

Compound 6,6'-dibromo-2,2'-bipyridine (1 g, 3.18 mmol) was suspended in 40 mL of hydrazine monohydrate ($\text{N}_2\text{H}_4 \cdot \text{H}_2\text{O}$) under a nitrogen atmosphere. The reaction mixture was then heated to dissolve 6,6'-dibromo-2,2'-bipyridine and refluxed at 120 °C for 6 hours. After cooling to room temperature, the resulting precipitate was collected and washed with a small amount of water. Finally, the desired product 6,6'-dihydrazineyl-2,2'-bipyridine was obtained as a yellow solid (0.65 g, 90 %).

¹H NMR (400 MHz, DMSO-*d*₆): δ = 7.59-7.52 (m, 4H), 7.39 (s, 2H), 6.70 (dd, *J* = 7.9, 1.1 Hz, 2H), 4.15 (brs, 4H).

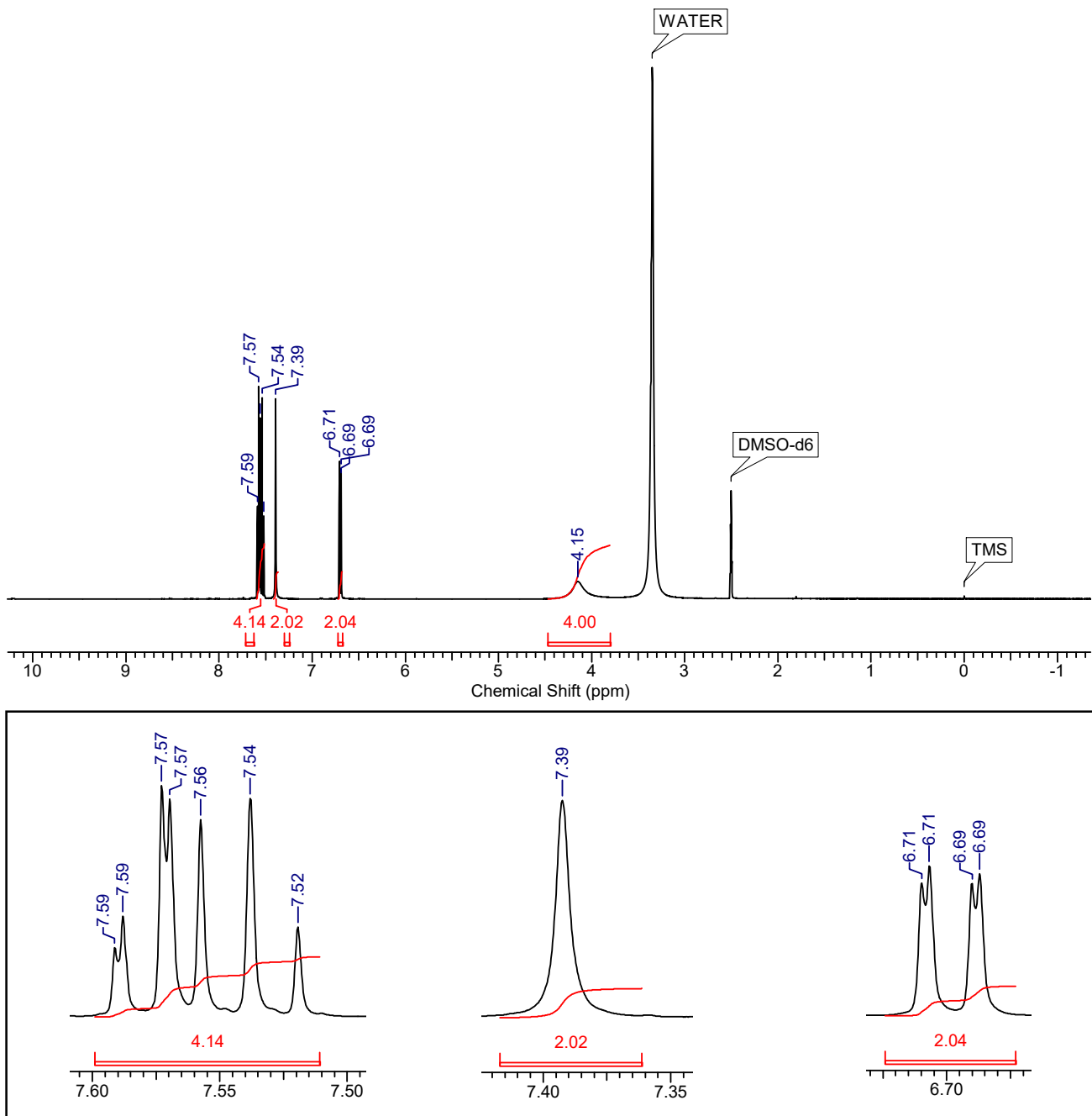
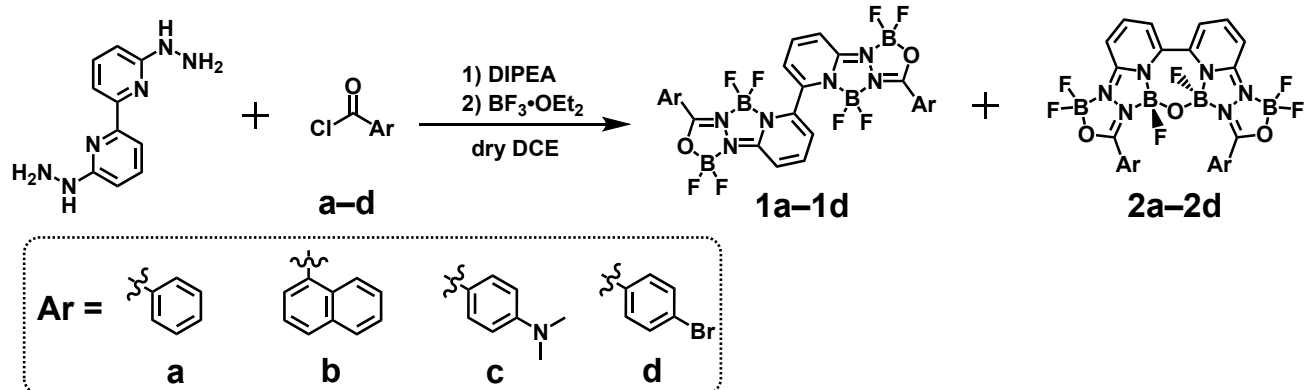


Figure S1. ^1H NMR spectrum of compound 6,6'-dihydrazineyl-2,2'-bipyridine in $\text{DMSO}-d_6$ at room temperature.

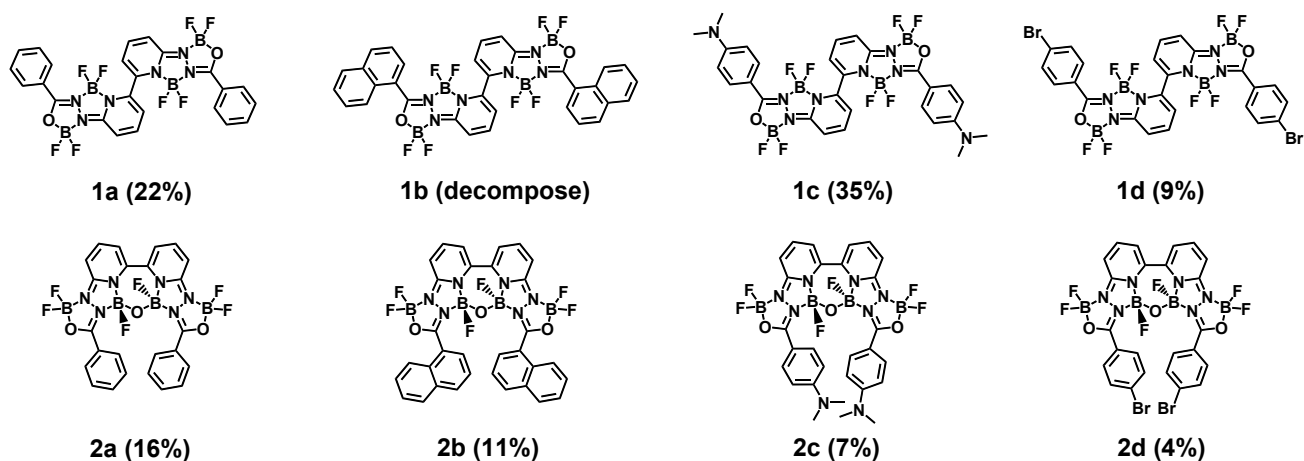
General procedure

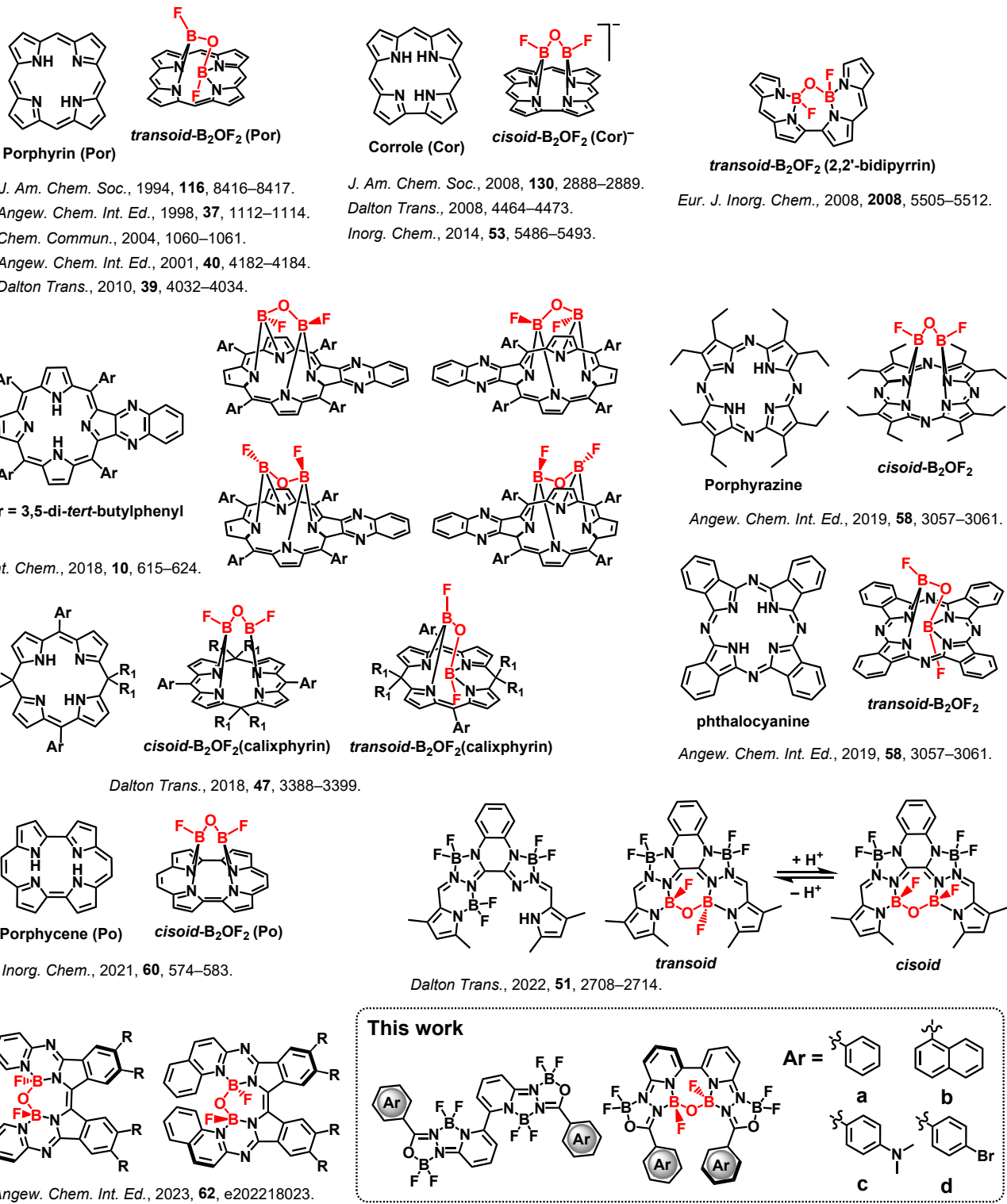


Scheme S2. Synthesis of **1a–1d** and **2a–2d** in this work.

To 6,6'-dihydrazineyl-2,2'-bipyridine (108 mg, 0.5 mmol) suspended in dry 1,2-dichloroethane (DCE, 60 mL), *N,N*-diisopropylethylamine (DIPEA, 2 mL, 12 mmol) was slowly added under a nitrogen atmosphere. Subsequently, acyl chloride derivatives (**a–d**, 1.1 mmol) in 10 mL of dry DCE were then added dropwise in an ice-water bath and stirred for 0.5 h. The reaction mixture was then stirred for 1 h at r.t. before subsequent addition of $\text{BF}_3\cdot\text{OEt}_2$ (3 mL, 24 mmol) in an ice-water bath, and further refluxed at 90 °C for 4 h under a nitrogen atmosphere. After that, the dichloromethane (DCM, 40 mL) was added into the cooled reaction mixture. The mixture was poured into water (100 mL) and extracted with DCM. The extracted organic layer was washed with water, dried over anhydrous sodium sulphate (Na_2SO_4), and concentrated under reduced pressure to obtain the crude product. The crude product was then purified by silica-gel column chromatography using DCM and hexane as eluent. The corresponding pure products were finally obtained by recrystallization from dichloromethane and hexane.

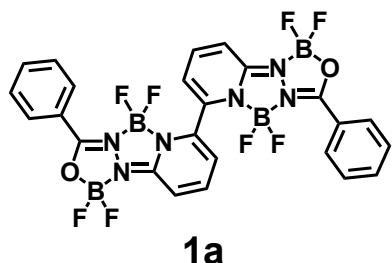
Chemical structures of **1a–1d** and **2a–2d**





Scheme S3. Chemical structures of previously reported FB–O–BF bridged organoboron complexes based on various ligands and developed organoboron complexes in this work.

Synthesis of compounds **1a** and **2a**



The reaction was performed following the general procedure starting with 6,6'-dihydrazineyl-2,2'-bipyridine (108 mg, 0.5 mmol) and benzoyl chloride (155 mg, 1.1 mmol). Compound **1a** was obtained as a yellow solid (66 mg, 22 %).

m.p. > 300°C.

^1H NMR (400 MHz, CDCl_3): δ = 8.10-8.09 (m, 2H), 8.08-8.07 (m, 2H), 7.96 (m, 2H), 7.65 (m, 2H), 7.50 (m, 4H), 7.23 (d, J = 9.5 Hz, 2H), 7.06 (d, J = 7.5 Hz, 2H).

^{13}C NMR (101 MHz, CDCl_3): No analyzable ^{13}C spectrum could be recorded due to the low solubility.

^{19}F NMR (377 MHz, CDCl_3): δ = (-131.25)-(-131.59) (m, 2F), (-143.40)-(-143.55) (m, 2F), (-145.92)-(-146.14) (m, 2F), (-147.43)-(-147.63) (m, 2F).

^{11}B NMR (128 MHz, CDCl_3): No analyzable ^{11}B spectrum could be recorded due to the low solubility.

HRMS (FAB, positive): m/z calcd. for $\text{C}_{24}\text{H}_{16}\text{B}_4\text{F}_8\text{N}_6\text{O}_2$ [M] $^+$ 616.1579; found: 616.1579.

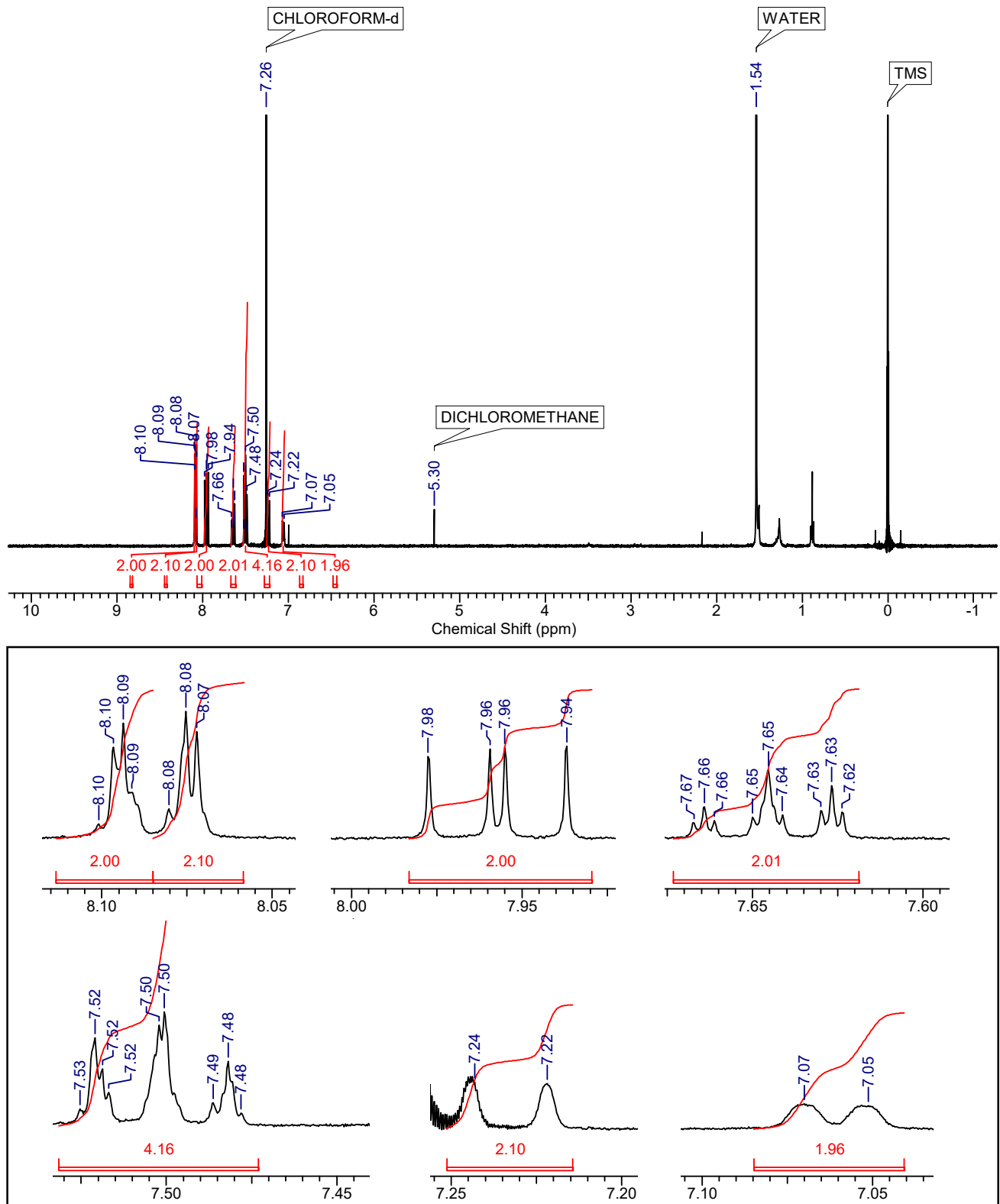


Figure S2-1. ^1H NMR spectrum of compound **1a** in CDCl_3 at room temperature.

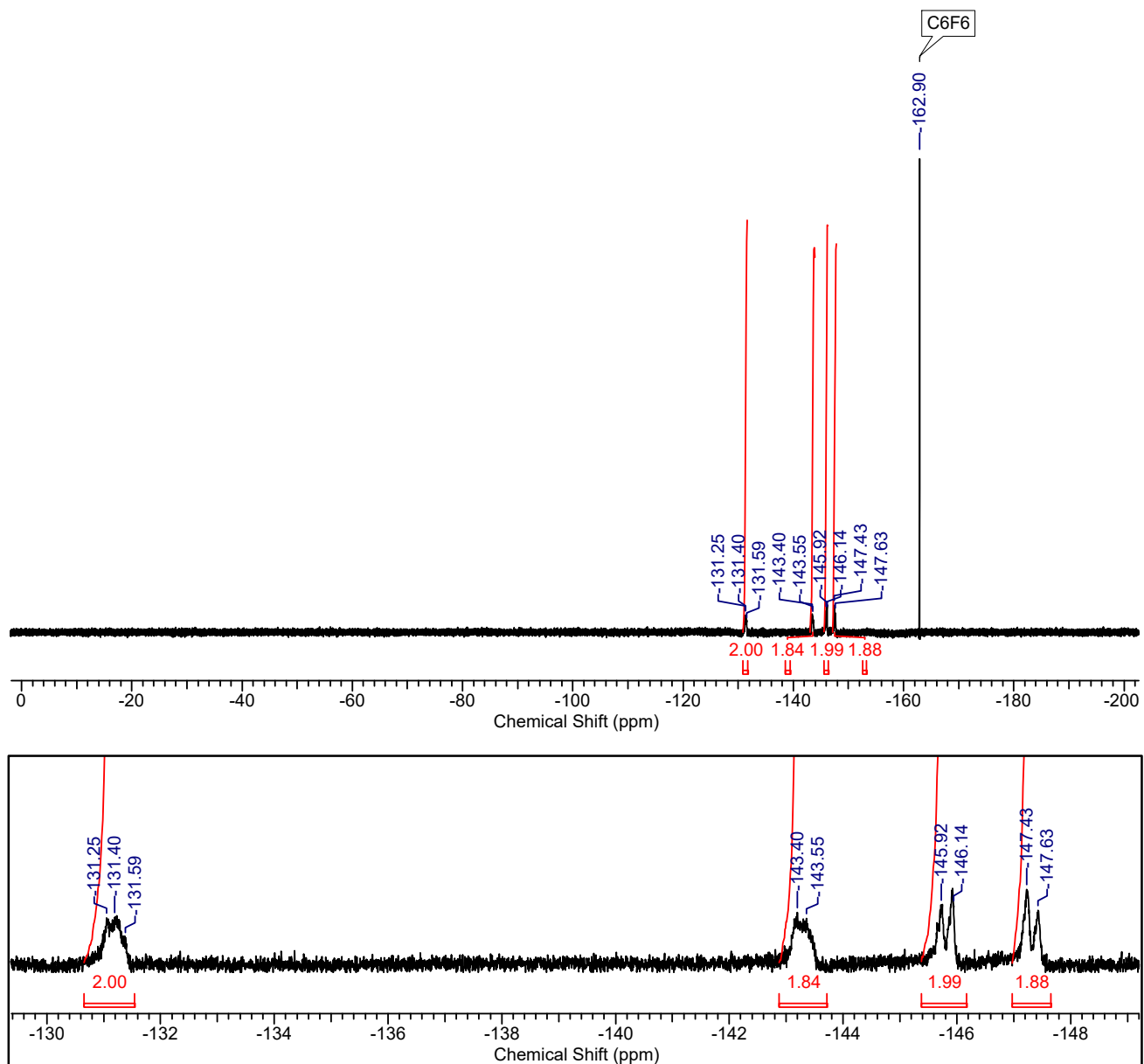
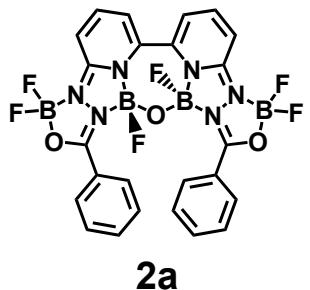


Figure S2-2. ^{19}F NMR spectrum of compound **1a** in CDCl_3 at room temperature.



Following the synthesis procedure of compound **1a**, compound **2a** was simultaneously obtained as a yellow solid (47 mg, 16 %).

m.p. > 300°C.

¹H NMR (400 MHz, CDCl₃): δ = 8.11-8.10 (m, 2H), 8.09-8.08 (m, 2H), 7.92 (m, 2H), 7.42 (m, 2H), 7.23-7.18 (m, 6H), 7.10 (dd, *J* = 7.3, 0.9 Hz, 2H).

¹³C NMR (101 MHz, CDCl₃): δ = 162.4, 150.1, 143.1, 142.3, 134.5, 129.6, 128.9, 123.0, 115.1, 111.2.

¹⁹F NMR (377 MHz, CDCl₃): δ = -135.22 (s, 2F), -146.18 (m, 1F), -146.39 (m, 1F), -147.70 (m, 1F), -147.90 (s, 1F).

¹¹B NMR (128 MHz, CDCl₃): δ = 3.48 (brs).

HRMS (FAB, positive): *m/z* calcd. for C₂₄H₁₆B₄F₆N₆O₃ [M]⁺ 594.1560; found: 594.1559.

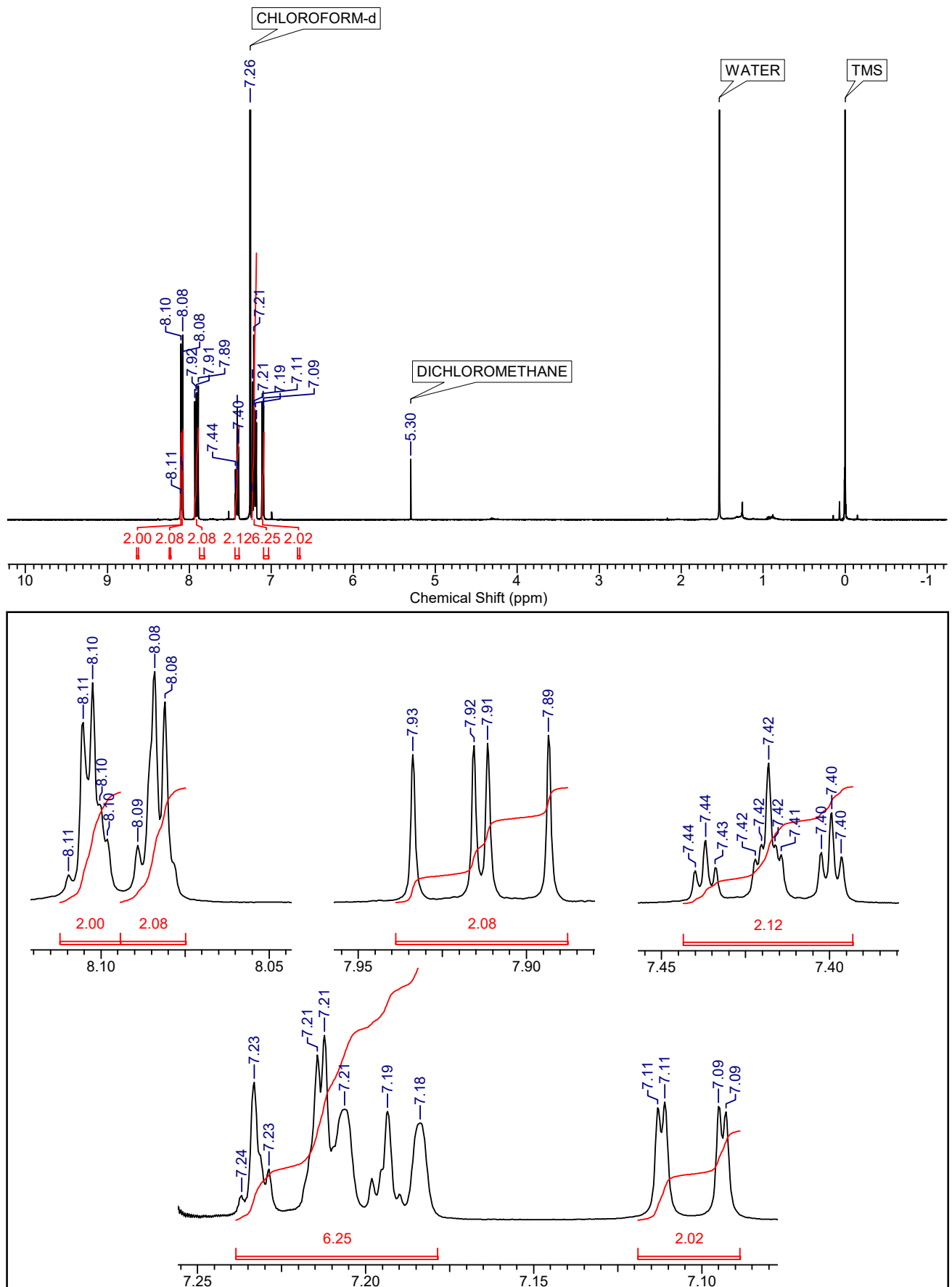


Figure S3-1. ^1H NMR spectrum of compound **2a** in CDCl_3 at room temperature.

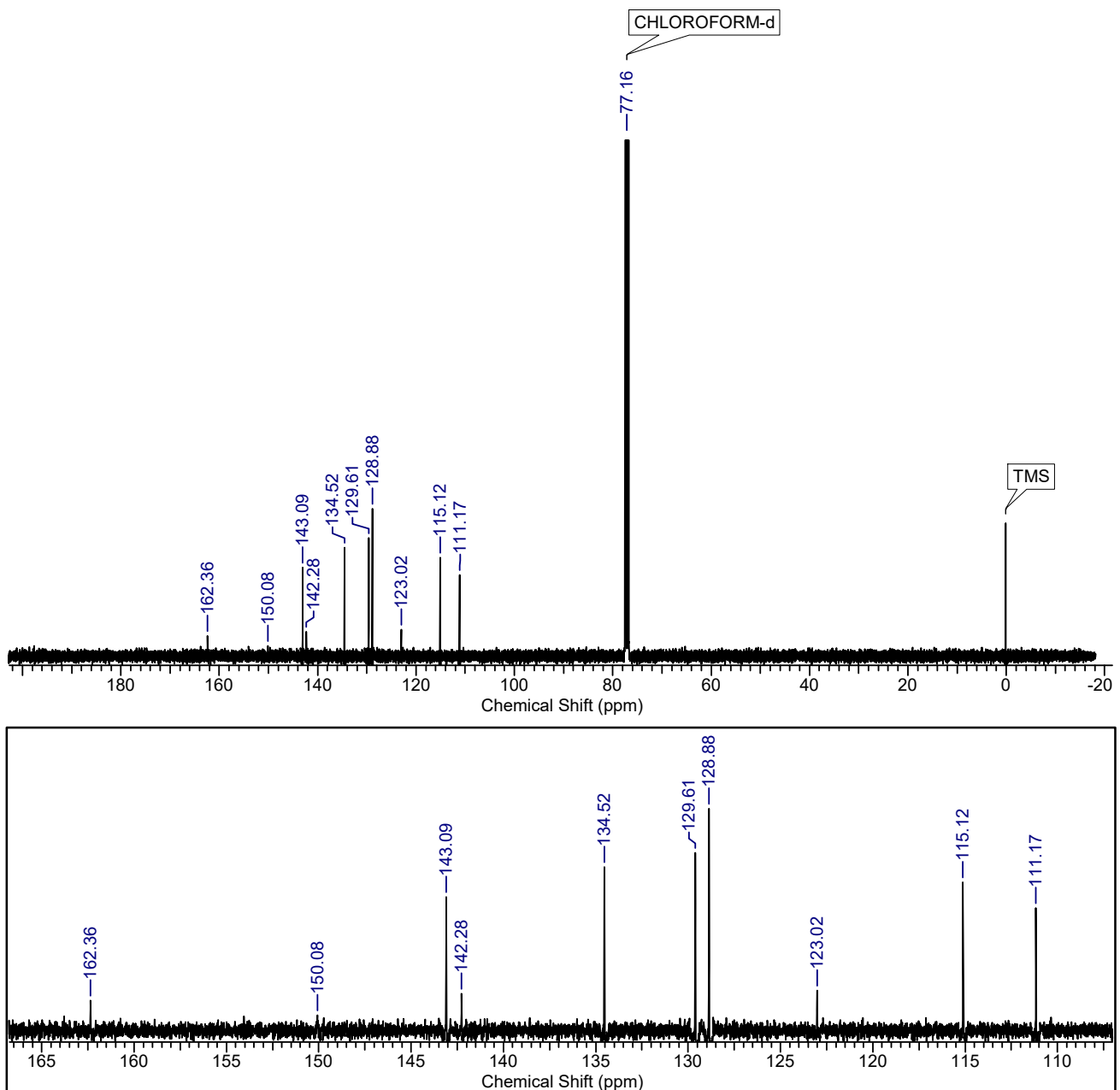


Figure S3-2. ^{13}C NMR spectrum of compound **2a** in CDCl_3 at room temperature.

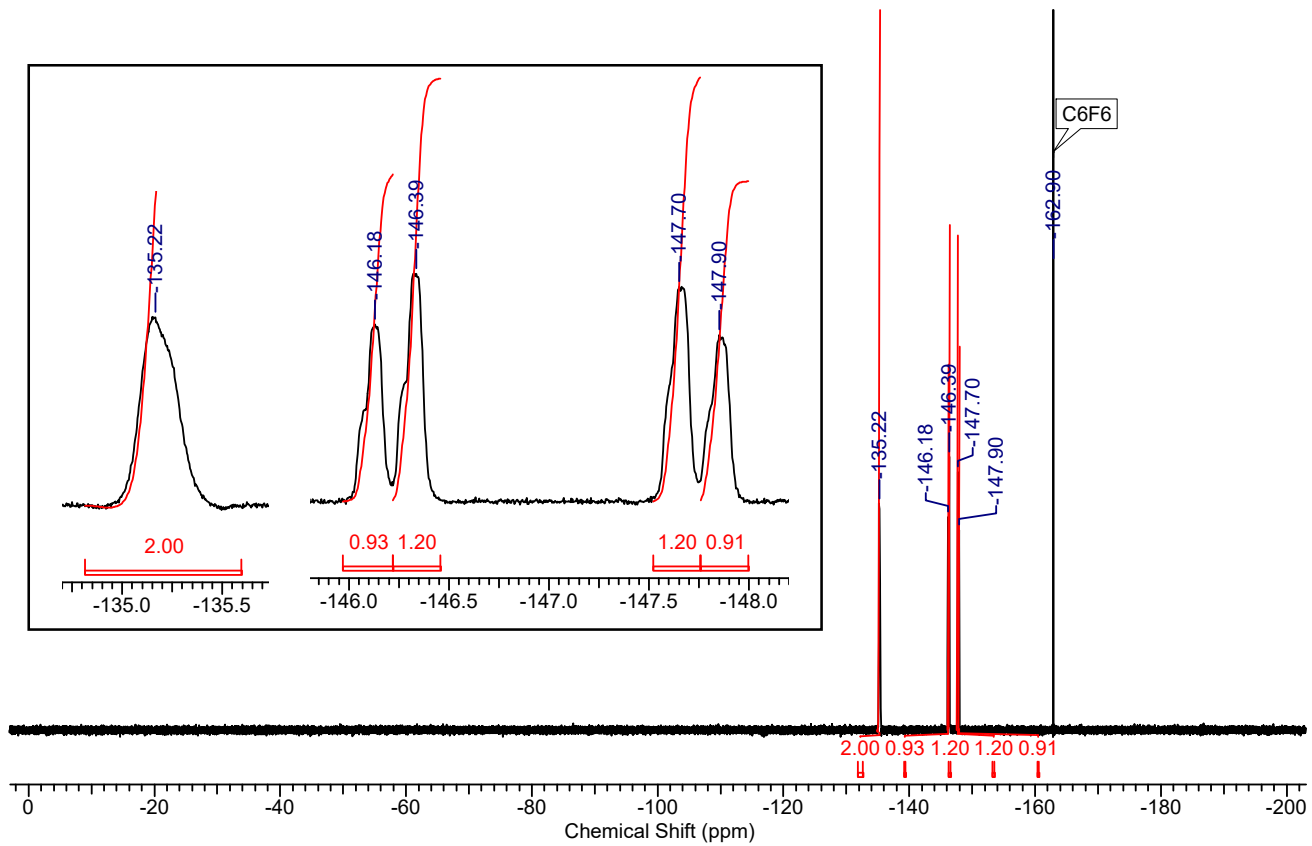


Figure S3-3. ^{19}F NMR spectrum of compound **2a** in CDCl_3 at room temperature.

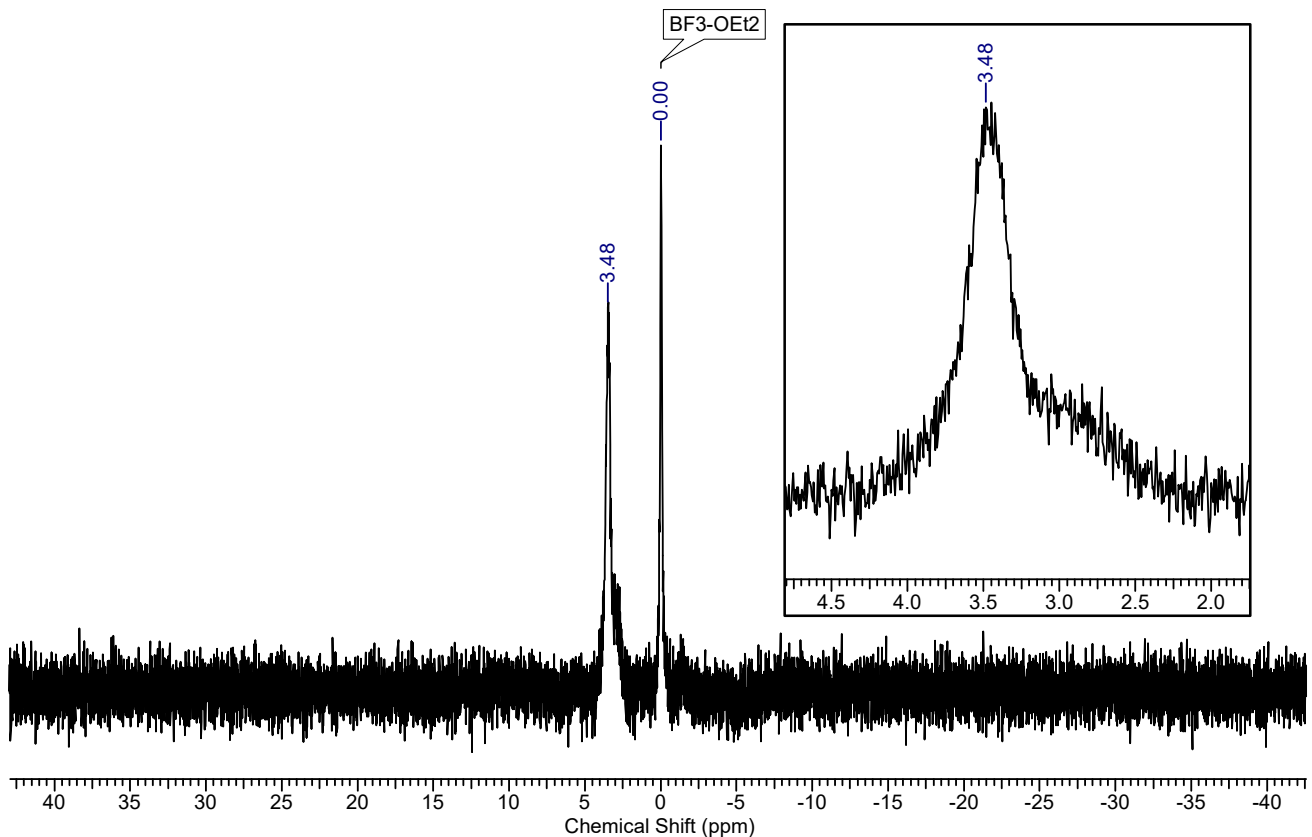
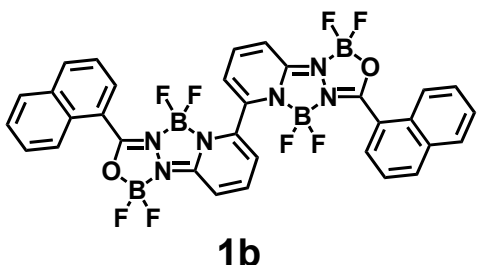


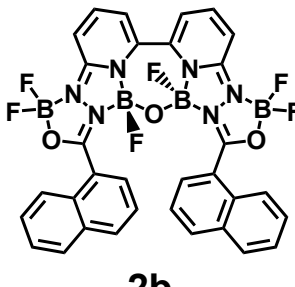
Figure S3-4. ^{11}B NMR spectrum of compound **2a** in CDCl_3 at room temperature.

Synthesis of compound **1b**



The product **1b** seems to be synthesized by TLC monitoring, however, during the purification by silica-gel column chromatography in DCM/hexane, **1b** appeared to decompose so that it cannot be isolated.

Synthesis of compound **2b**



The reaction was performed following the general procedure starting with 6,6'-dihydrazineyl-2,2'-bipyridine (108 mg, 0.5 mmol) and 1-naphthoyl chloride (210 mg, 1.1 mmol). Compound **2b** was obtained as a yellow solid (37 mg, 11 %).

m.p. > 300°C.

¹H NMR (400 MHz, CDCl₃): δ = 8.55 (m, 1H), 8.53 (m, 1H), 7.93 (d, *J* = 7.3 Hz, 1H), 7.91 (d, *J* = 7.3 Hz, 1H), 7.84-7.83 (m, 2H), 7.82-7.81 (m, 2H), 7.69-7.61 (m, 4H), 7.56 (d, *J* = 8.3 Hz, 2H), 7.21 (d, *J* = 8.5 Hz, 2H), 7.10 (dd, *J* = 7.4, 0.9 Hz, 2H), 6.49-6.45 (m, 2H).

¹³C NMR (101 MHz, CDCl₃): δ = 164.2, 150.3, 143.1, 142.4, 134.5, 133.5, 130.8, 130.4, 129.0, 128.4, 127.0, 125.4, 124.3, 120.0, 115.2, 111.2.

¹⁹F NMR (377 MHz, CDCl₃): δ = -132.37 (s, 2F), -145.21 (m, 1F), -145.41 (m, 1F), -146.72 (m, 1F), -146.91 (m, 1F).

¹¹B NMR (128 MHz, CDCl₃): δ = 3.91 (s).

HRMS (FAB, positive): *m/z* calcd. for C₃₂H₂₀B₄F₆N₆O₃ [M]⁺ 694.1873; found: 694.1877.

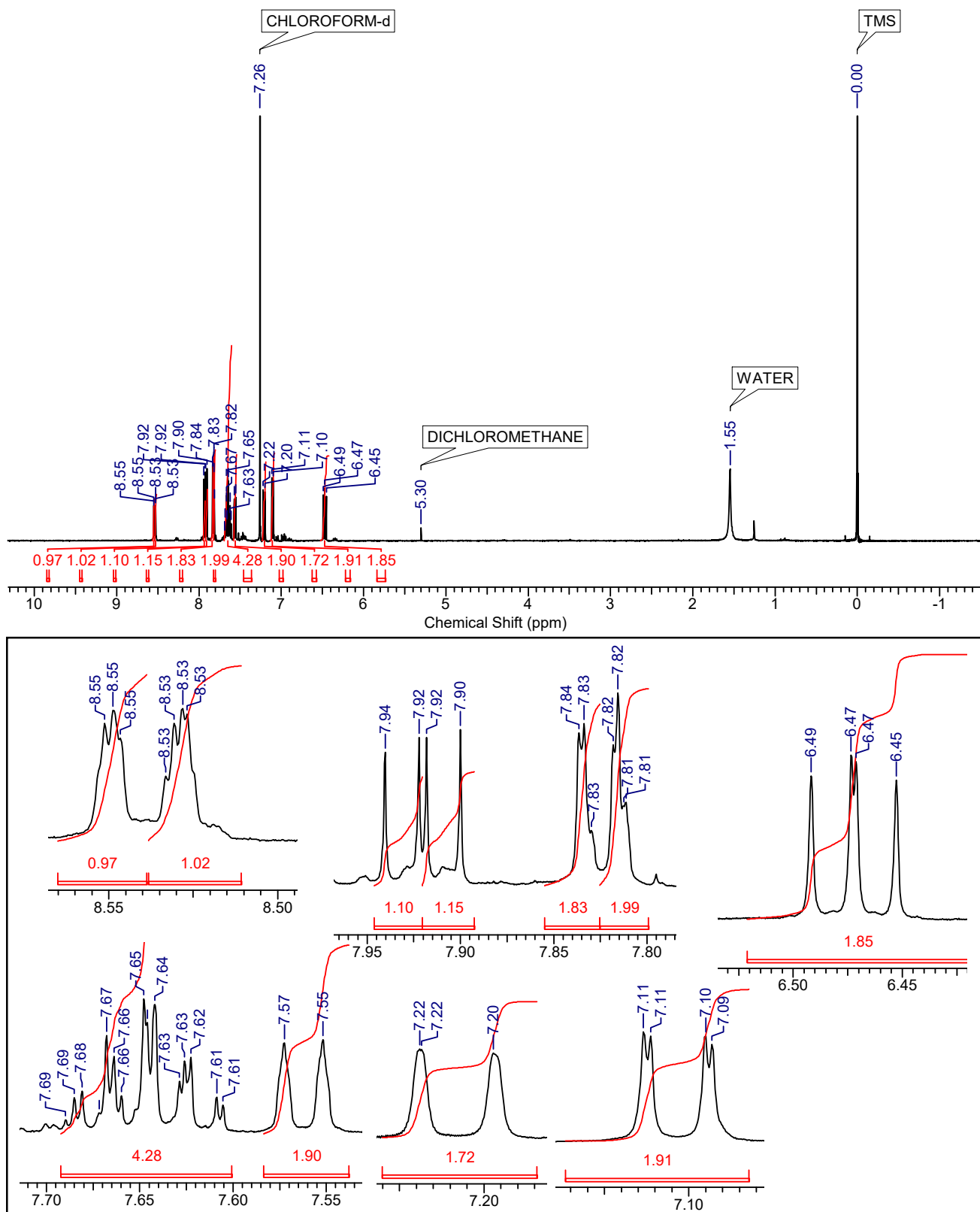


Figure S4-1. ^1H NMR spectrum of compound **2b** in CDCl_3 at room temperature.

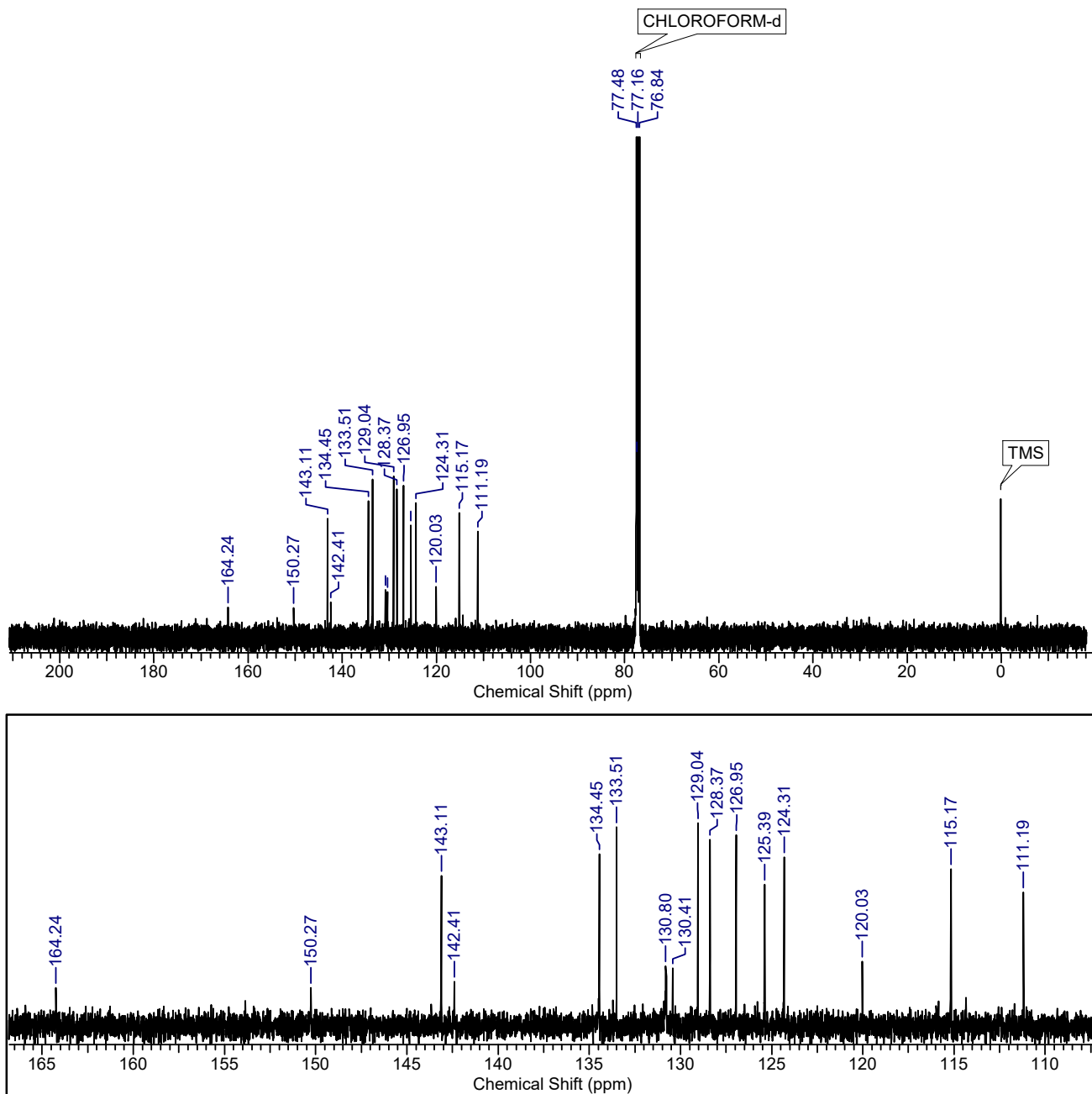


Figure S4-2. ^{13}C NMR spectrum of compound **2b** in CDCl_3 at room temperature.

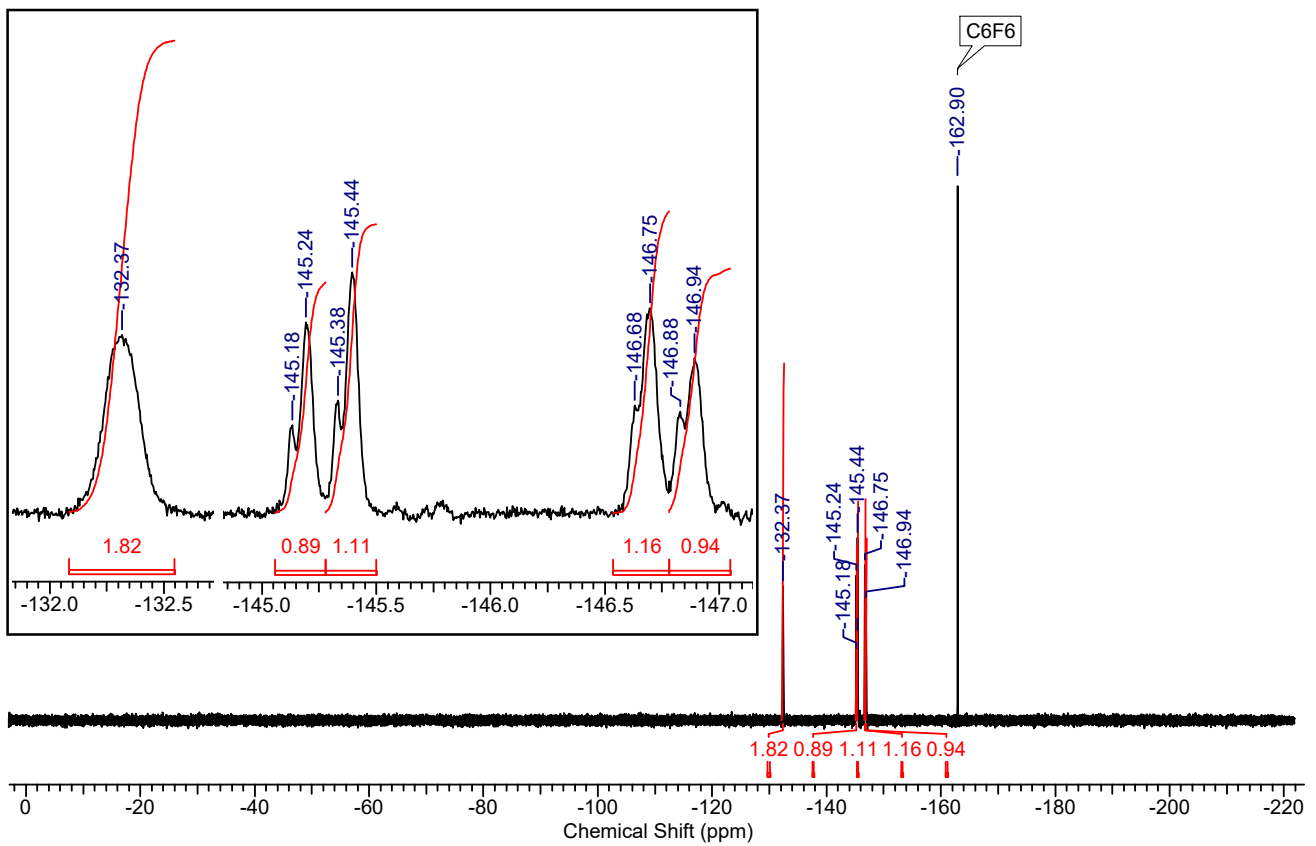


Figure S4-3. ^{19}F NMR spectrum of compound **2b** in CDCl_3 at room temperature.

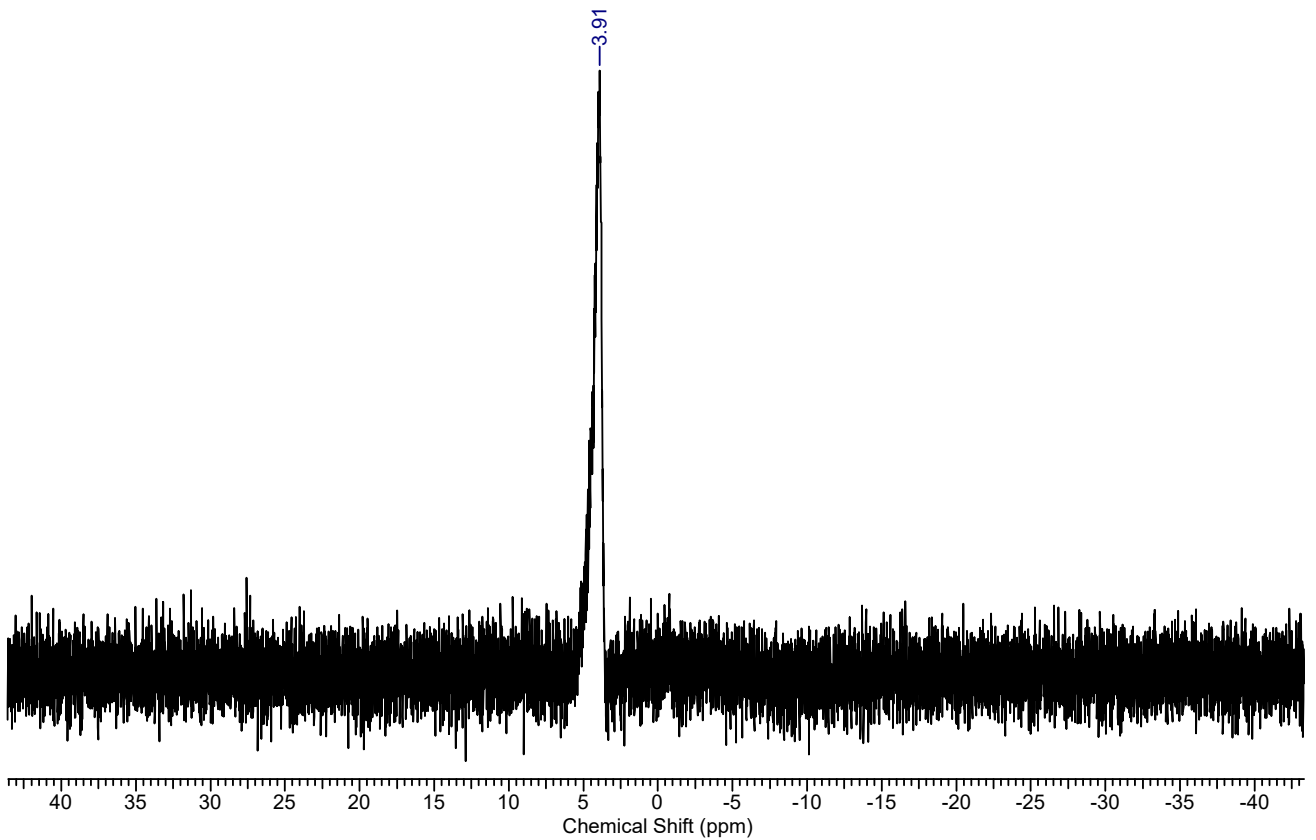
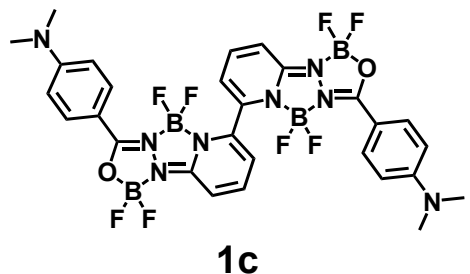


Figure S4-4. ^{11}B NMR spectrum of compound **2b** in CDCl_3 at room temperature.

Synthesis of compounds **1c** and **2c**

Note: 4-(dimethylamino)benzoyl chloride was synthesized according to the reported method.²



The reaction was performed following the general procedure starting with 6,6'-dihydrazineyl-2,2'-bipyridine (108 mg, 0.5 mmol) and 4-(dimethylamino)benzoyl chloride (202 mg, 1.1 mmol). Compound **1c** was obtained as a yellow solid (121 mg, 35 %).

m.p. > 300°C.

¹H NMR (400 MHz, CDCl₃): δ = 7.96-7.95 (m, 2H), 7.93-7.92 (m, 2H), 7.83 (m, 2H), 7.14 (d, *J* = 9.0 Hz, 2H), 6.96 (d, *J* = 7.0 Hz, 2H), 6.67-6.65 (m, 2H), 6.64-6.63 (m, 2H), 3.07 (s, 12H).

¹³C NMR (101 MHz, CDCl₃): 159.2, 157.1, 154.6, 141.9, 140.4, 131.8, 111.3, 110.8, 110.3, 110.1, 108.4, 53.6, 40.1.

¹⁹F NMR (377 MHz, CDCl₃): δ = (-131.52)-(-131.68) (m, 2F), (-143.45)-(-143.61) (m, 2F), (-147.69)-(-147.90) (m, 2F), (-149.06)-(-149.25) (m, 2F).

¹¹B NMR (128 MHz, CDCl₃): δ = 3.38-2.99 (m).

HRMS (FAB, positive): *m/z* calcd. for C₂₈H₂₆B₄F₈N₈O₂ [M]⁺ 702.2423; found: 702.2422.

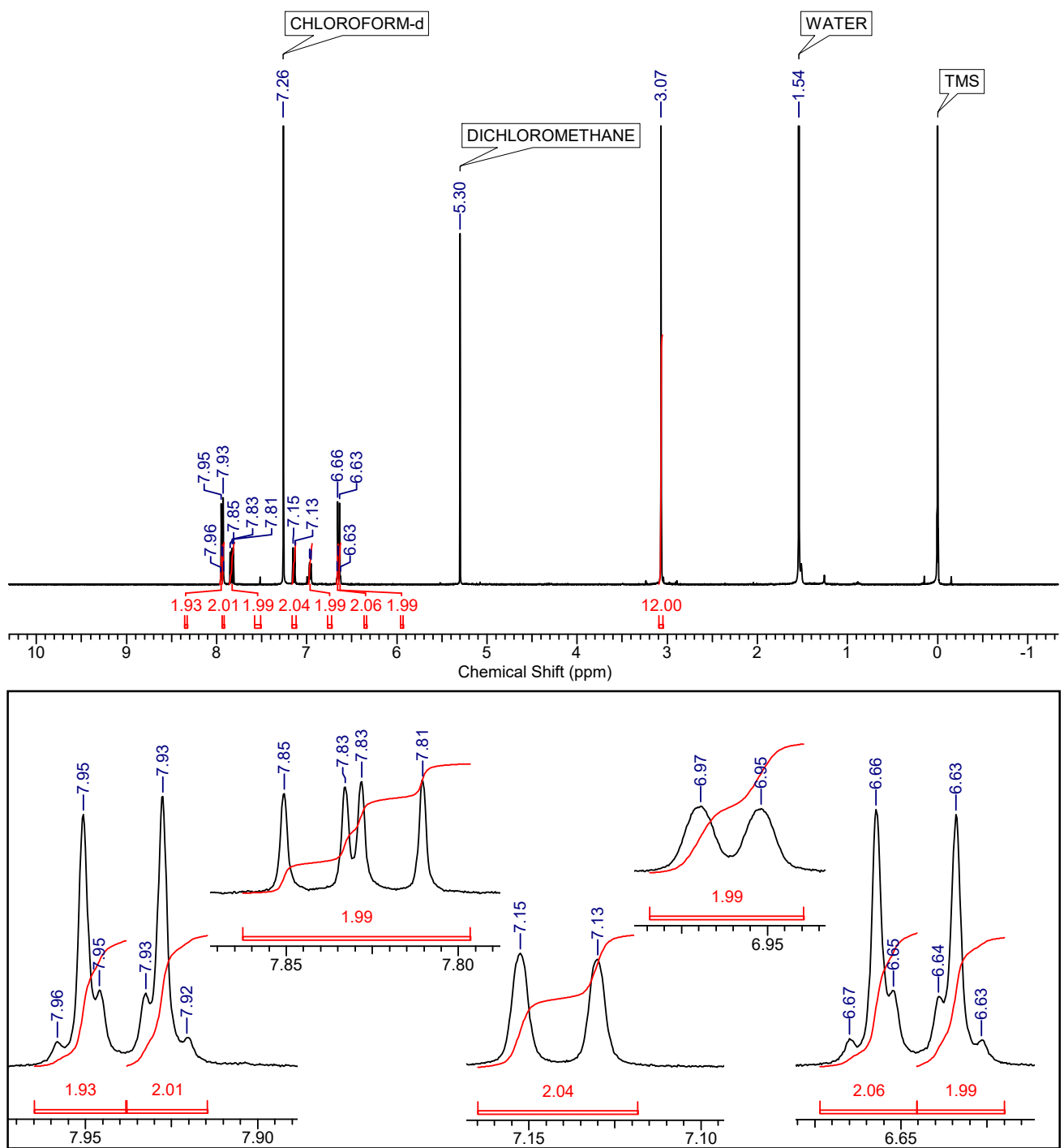


Figure S5-1. ^1H NMR spectrum of compound **1c** in CDCl_3 at room temperature.

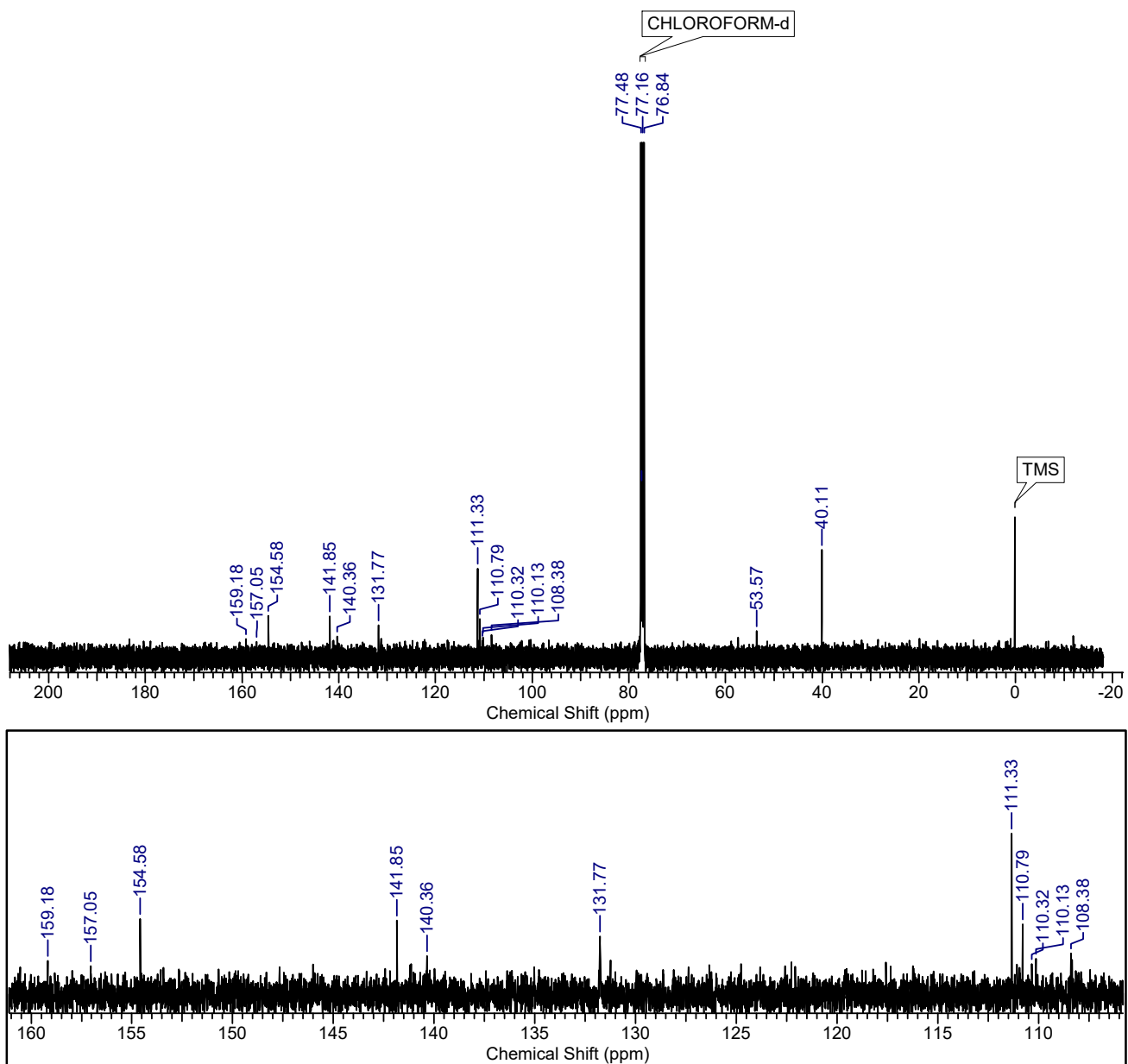


Figure S5-2. ^{13}C NMR spectrum of compound **1c** in CDCl_3 at room temperature.

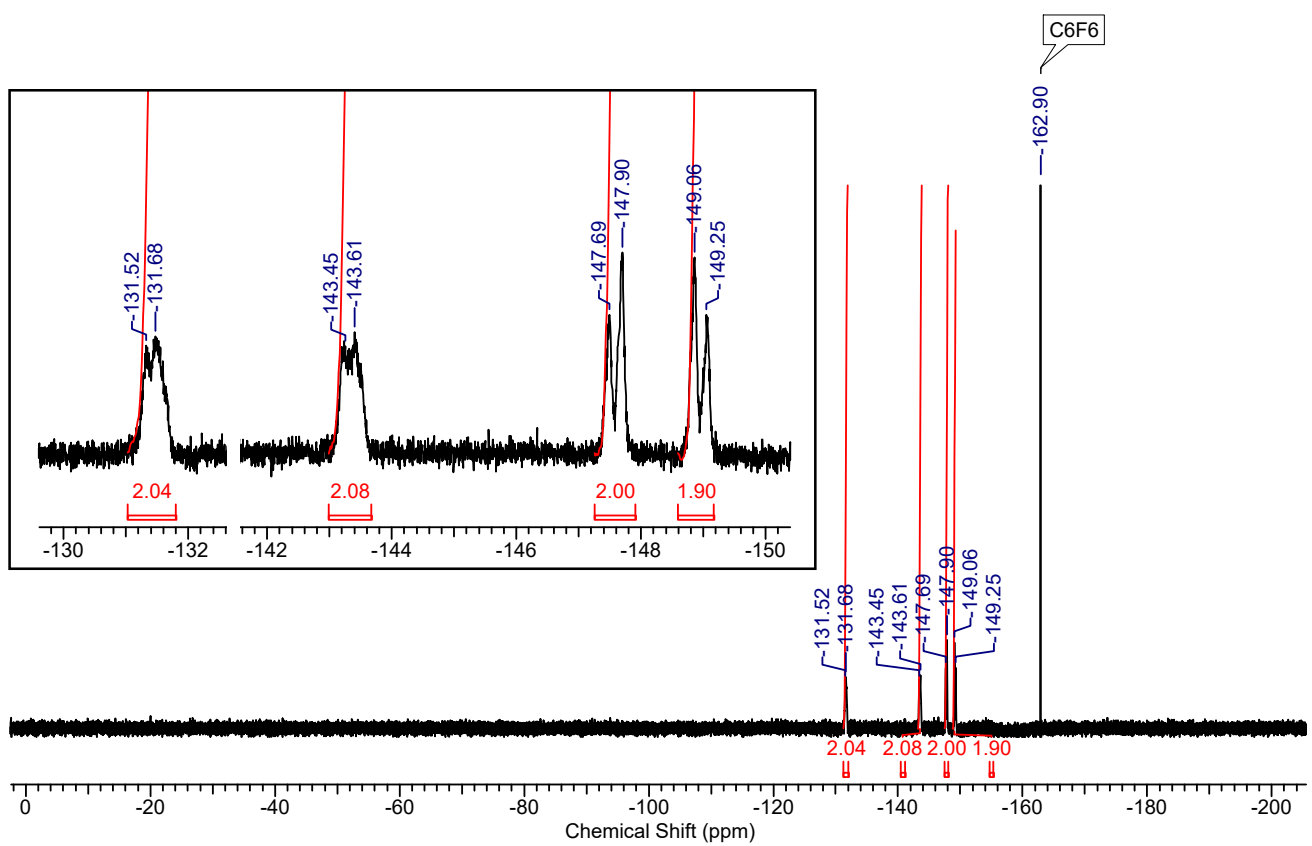


Figure S5-3. ${}^{19}\text{F}$ NMR spectrum of compound **1c** in CDCl_3 at room temperature.

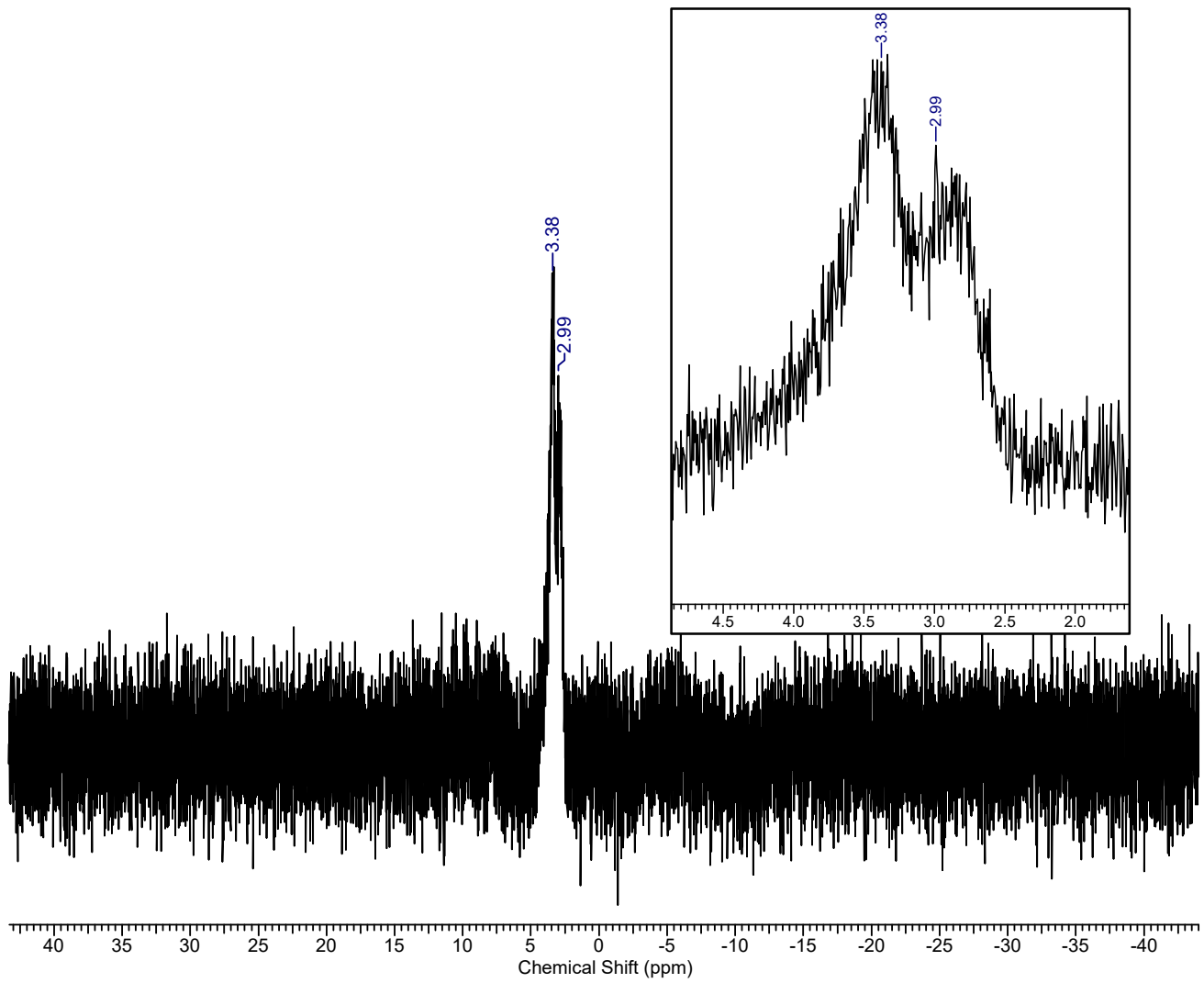
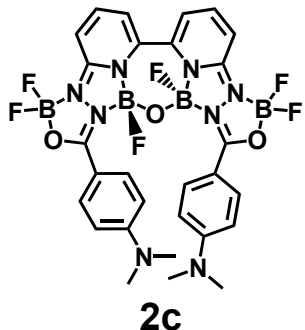


Figure S5-4. ^{11}B NMR spectrum of compound **1c** in CDCl_3 at room temperature.



Following the synthesis procedure of compound **1c**, compound **2c** was simultaneously obtained as a red solid (23 mg, 7 %).

m.p.: ~ 280°C.

¹H NMR (400 MHz, CD₂Cl₂): δ = 7.99-7.98 (m, 2H), 7.96-7.95 (m, 2H), 7.85 (m, 2H), 7.11 (s, 1H), 7.09 (d, *J* = 3.1 Hz, 2H), 7.06 (s, 1H), 6.40-6.39 (m, 2H), 6.37-6.36 (m, 2H), 2.94 (s, 12H)

¹³C NMR (101 MHz, CD₂Cl₂): δ = 162.4, 154.4, 149.8, 142.8, 142.6, 131.9, 129.2, 114.9, 111.2, 111.0, 108.8, 40.1.

¹⁹F NMR (377 MHz, CD₂Cl₂): δ = -135.50 (s, 2F), -147.62 (m, 1F), -147.83 (m, 1F), -149.87 (m, 1F), -150.07 (m, 1F).

¹¹B NMR (128 MHz, CD₂Cl₂): δ = 3.43 (s).

HRMS (FAB, positive): *m/z* calcd. for C₂₈H₂₆B₄F₆N₈O₃ [M]⁺ 680.2404; found: 680.2407.

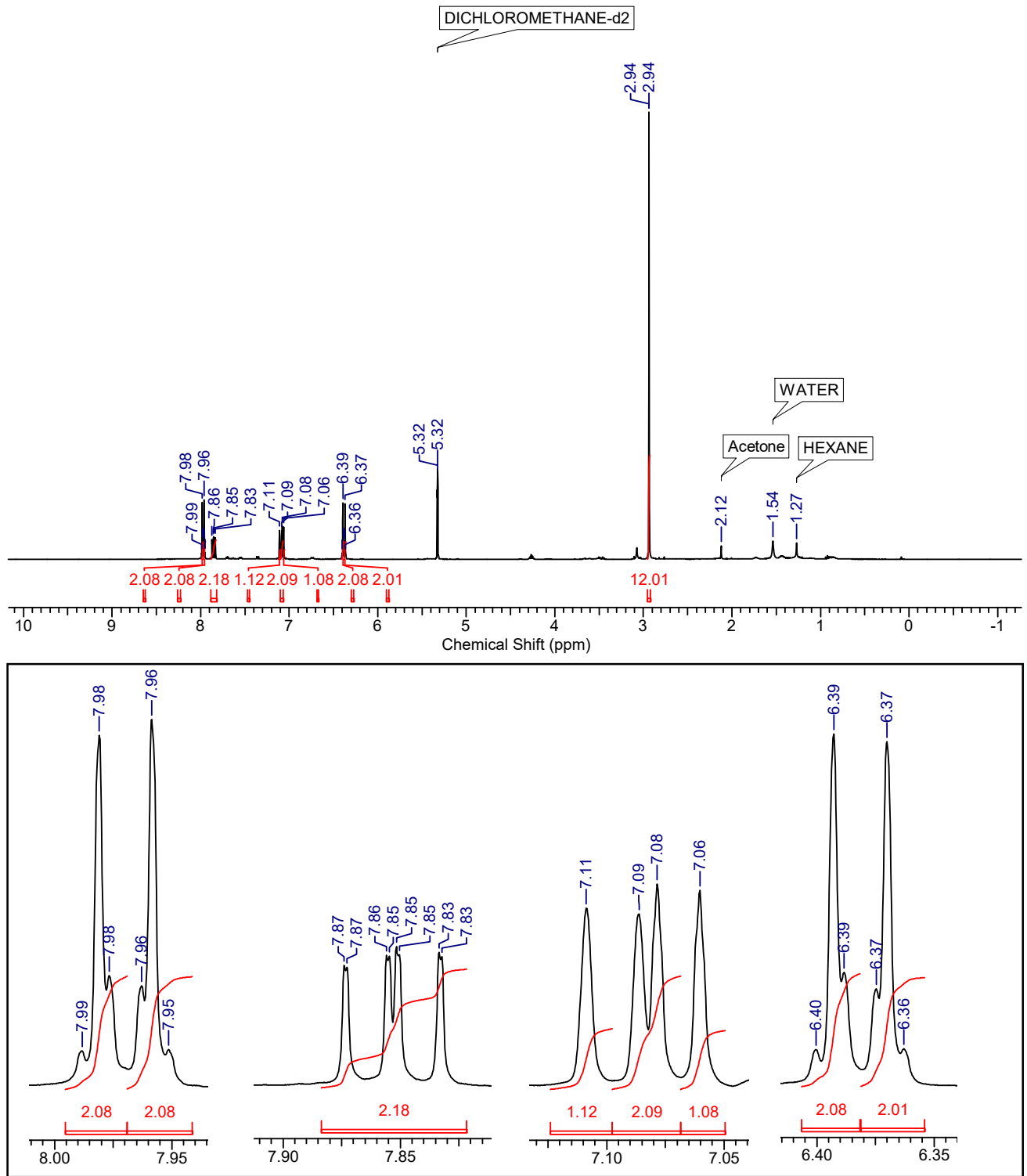


Figure S6-1. ¹H NMR spectrum of compound **2c** in CD₂Cl₂ at room temperature.

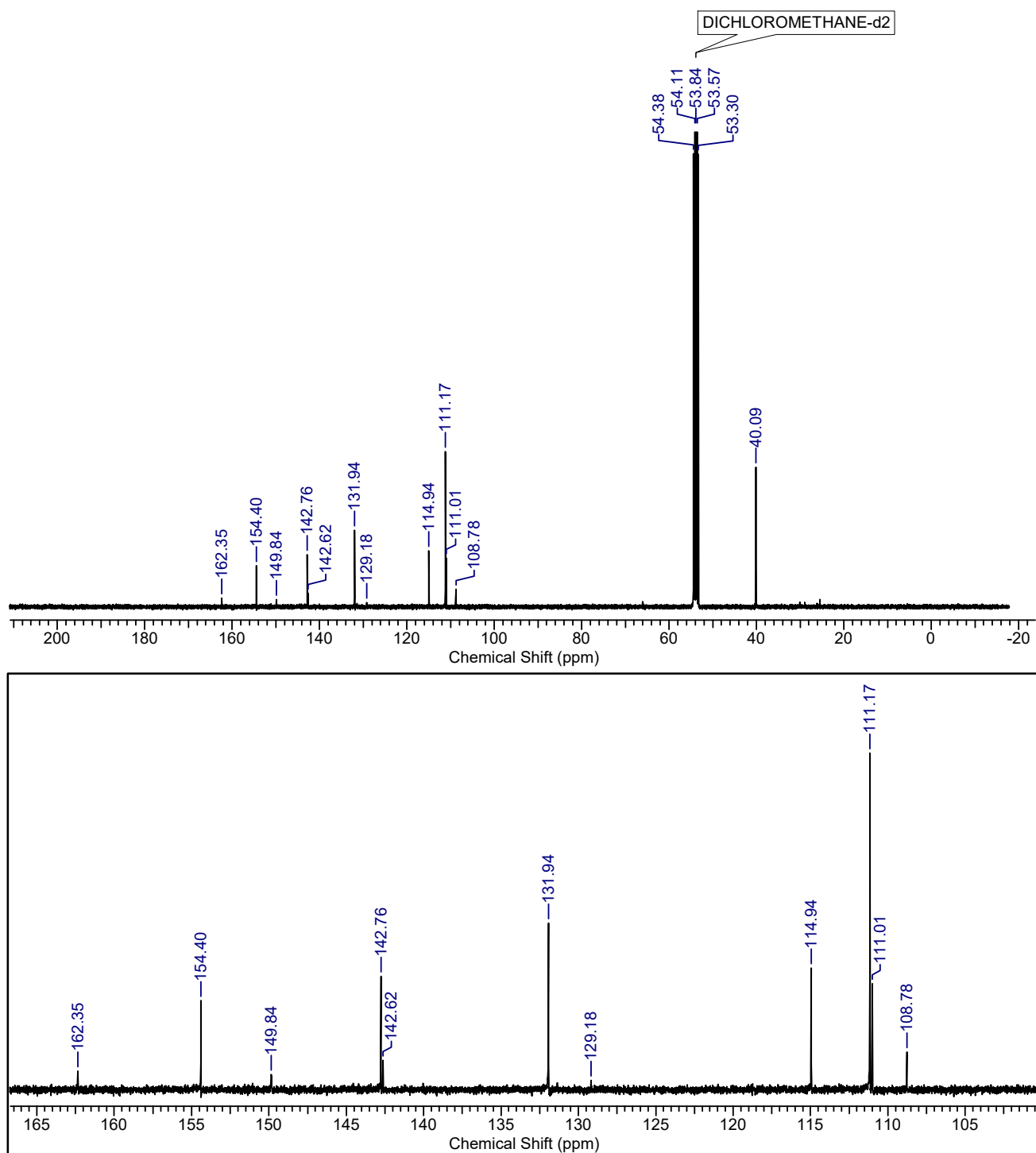


Figure S6-2. ^{13}C NMR spectrum of compound **2c** in CD_2Cl_2 at room temperature.

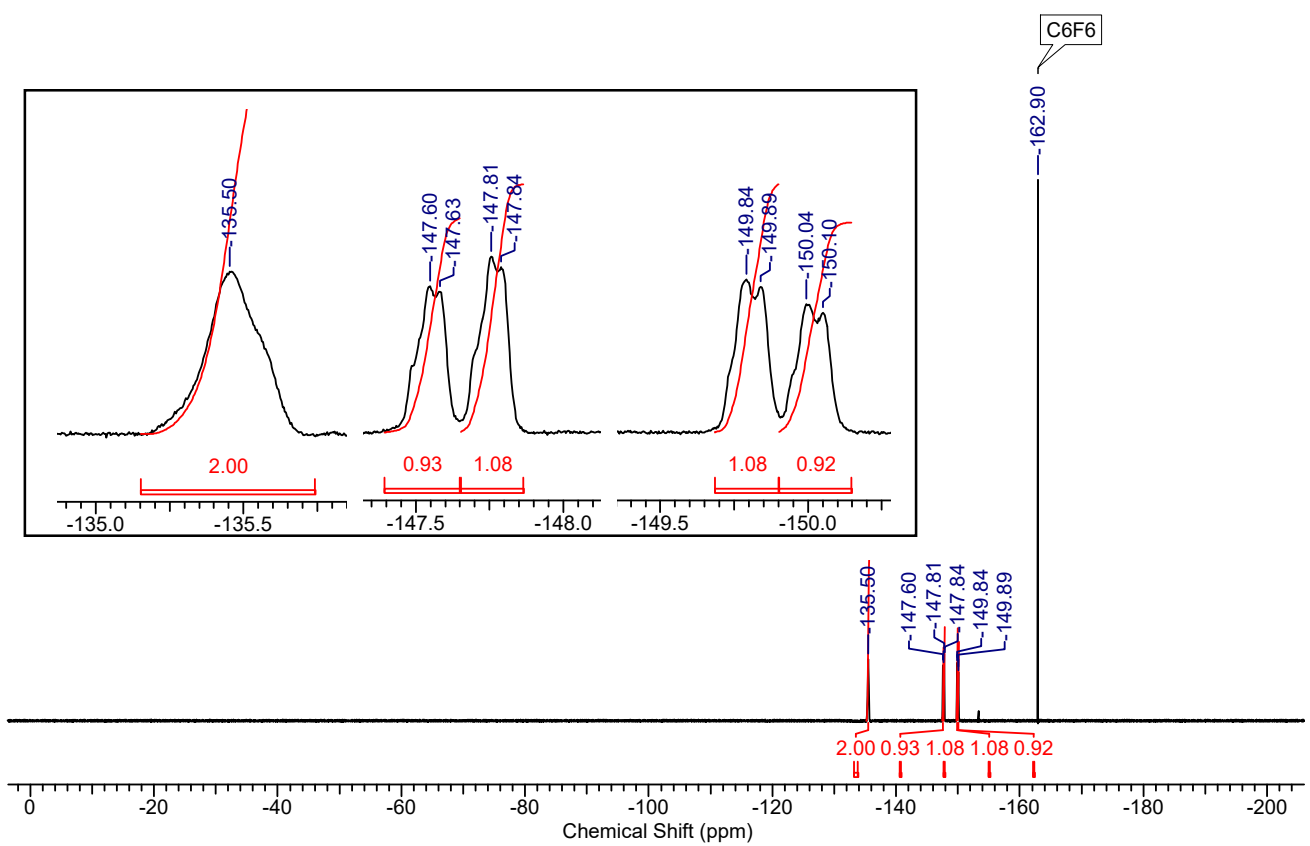


Figure S6-3. ^{19}F NMR spectrum of compound **2c** in CD_2Cl_2 at room temperature.

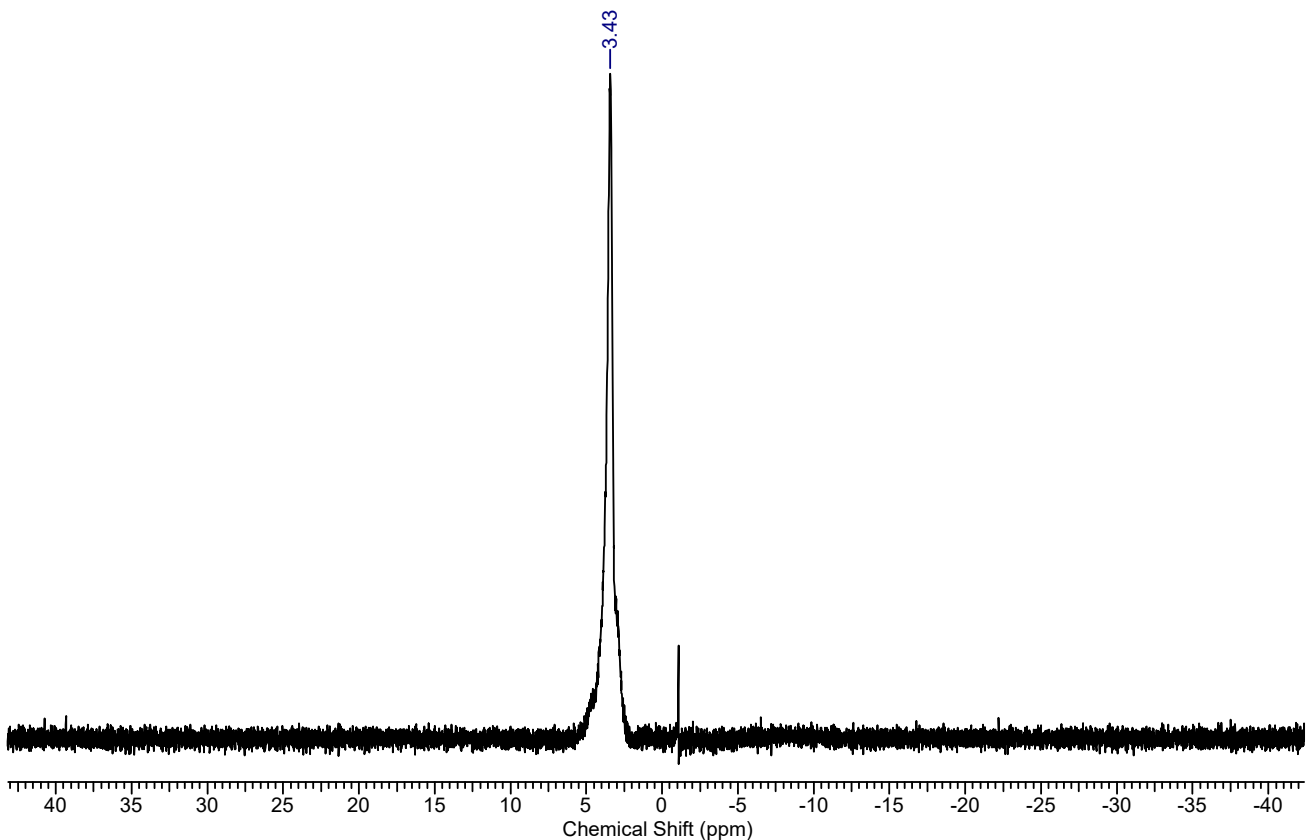
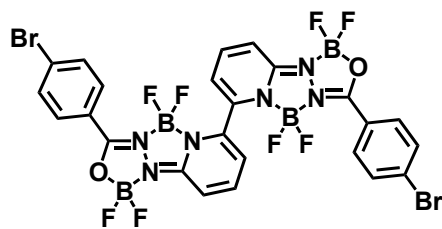


Figure S6-4. ^{11}B NMR spectrum of compound **2c** in CD_2Cl_2 at room temperature.

Synthesis of compounds **1d** and **2d**



1d

The reaction was performed following the general procedure starting with 6,6'-dihydrazineyl-2,2'-bipyridine (216 mg, 1.0 mmol) and 4-bromobenzoyl chloride (483 mg, 2.2 mmol). Compound **1d** was obtained as a yellow solid (70 mg, 9 %).

m.p. > 300 °C.

¹H NMR (400 MHz, CDCl₃): δ = 7.99 (d, *J* = 7.1 Hz, 1H), 7.97 (d, *J* = 7.3 Hz, 1H), 7.95-7.94 (m, 2H), 7.93-7.92 (m, 2H), 7.67-7.66 (m, 2H), 7.64-7.63 (m, 2H), 7.24 (d, *J* = 9.3 Hz, 2H), 7.07 (d, *J* = 7.4 Hz, 2H).

¹³C NMR (101 MHz, CDCl₃): δ = 162.7, 150.5, 143.2, 140.1, 132.9, 130.8, 121.7, 117.3, 111.2.

¹⁹F NMR (377 MHz, CDCl₃): δ = (-128.25)-(-128.34) (m, 2F), (-140.06)-(-140.25) (m, 2F), (-142.41)-(-142.60) (m, 2F), (-143.86)-(-144.04) (m, 2F).

¹¹B NMR (128 MHz, CDCl₃): δ = 3.47 (brs, 2B), 2.66 (brs, 2B).

HRMS (FAB, positive): *m/z* calcd. for C₂₄H₁₄B₄Br₂F₈N₆O₂ [M]⁺ 771.9789; found: 771.9791.

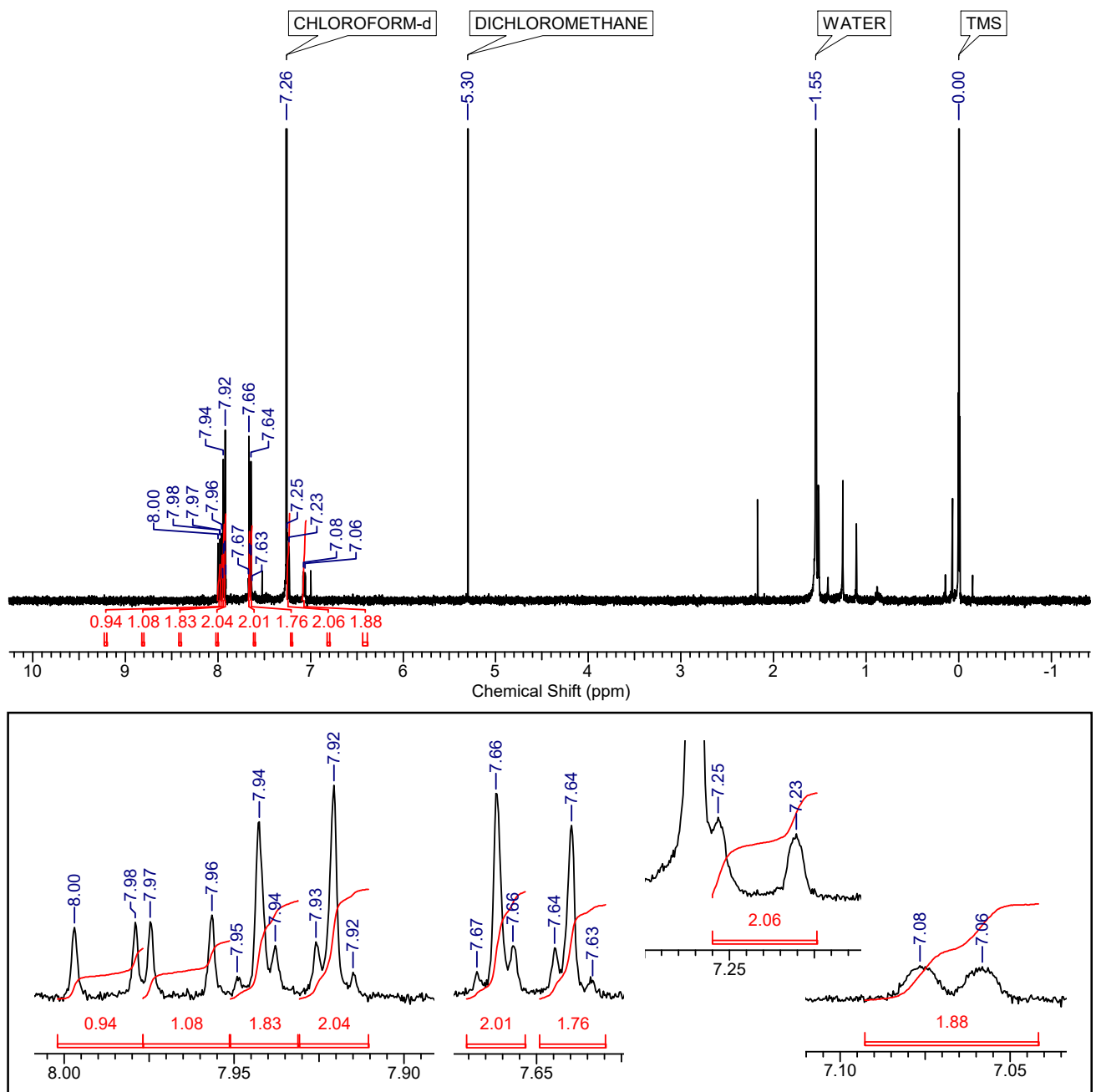


Figure S7-1. ^1H NMR spectrum of compound **1d** in CDCl_3 at room temperature.

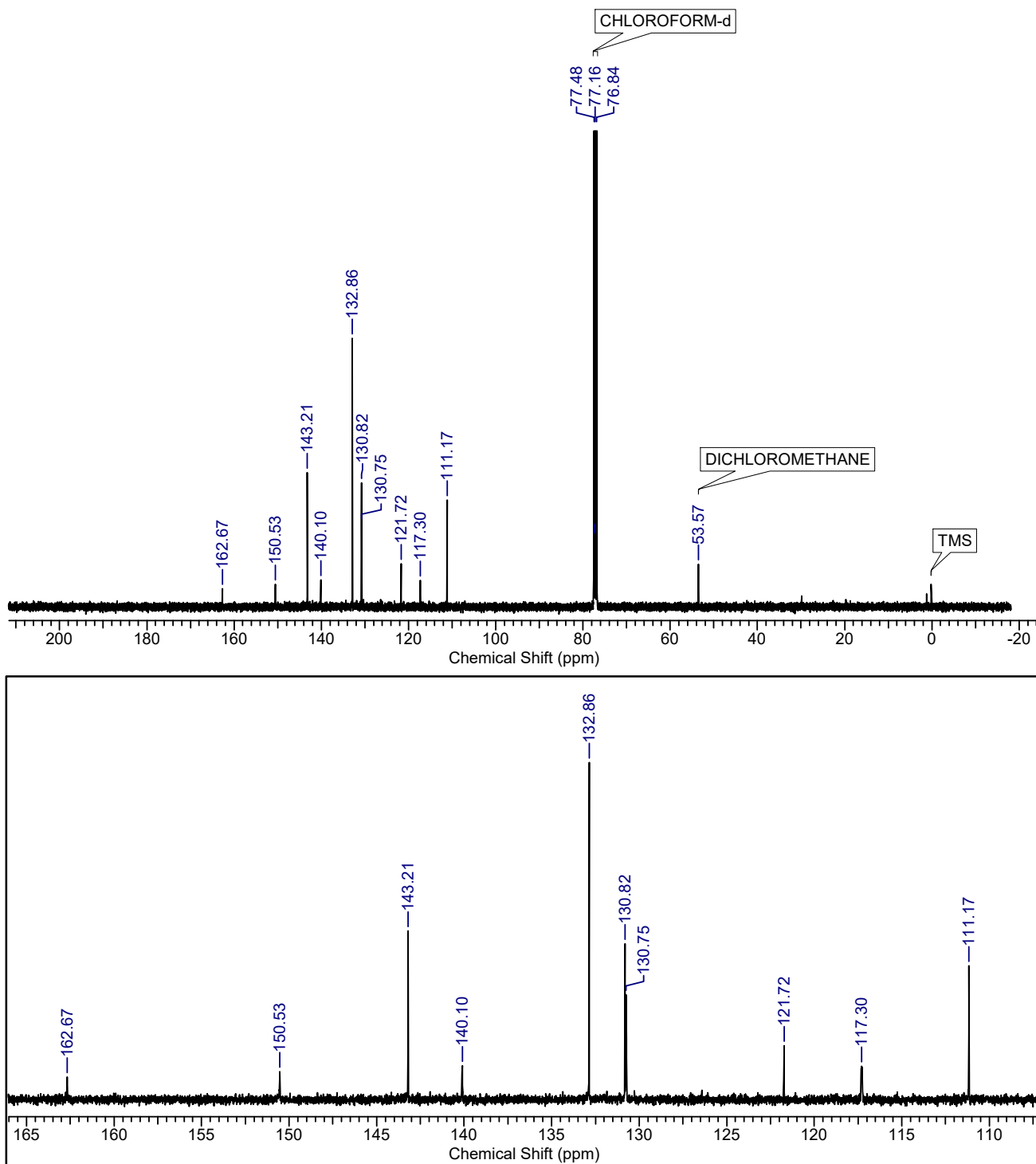


Figure S7-2. ^{13}C NMR spectrum of compound **1d** in CDCl_3 at room temperature.

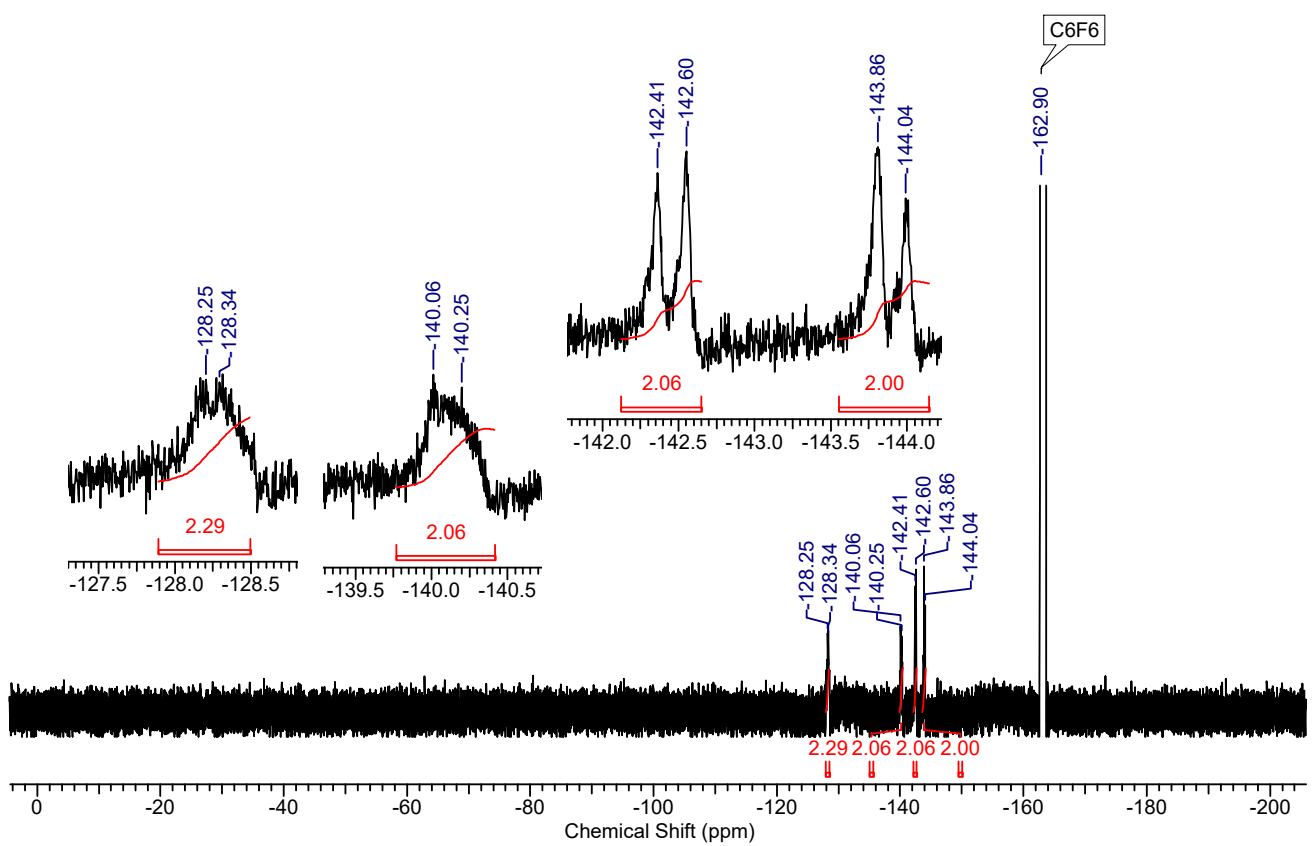


Figure S7-3. ^{19}F NMR spectrum of compound **1d** in CDCl_3 at room temperature.

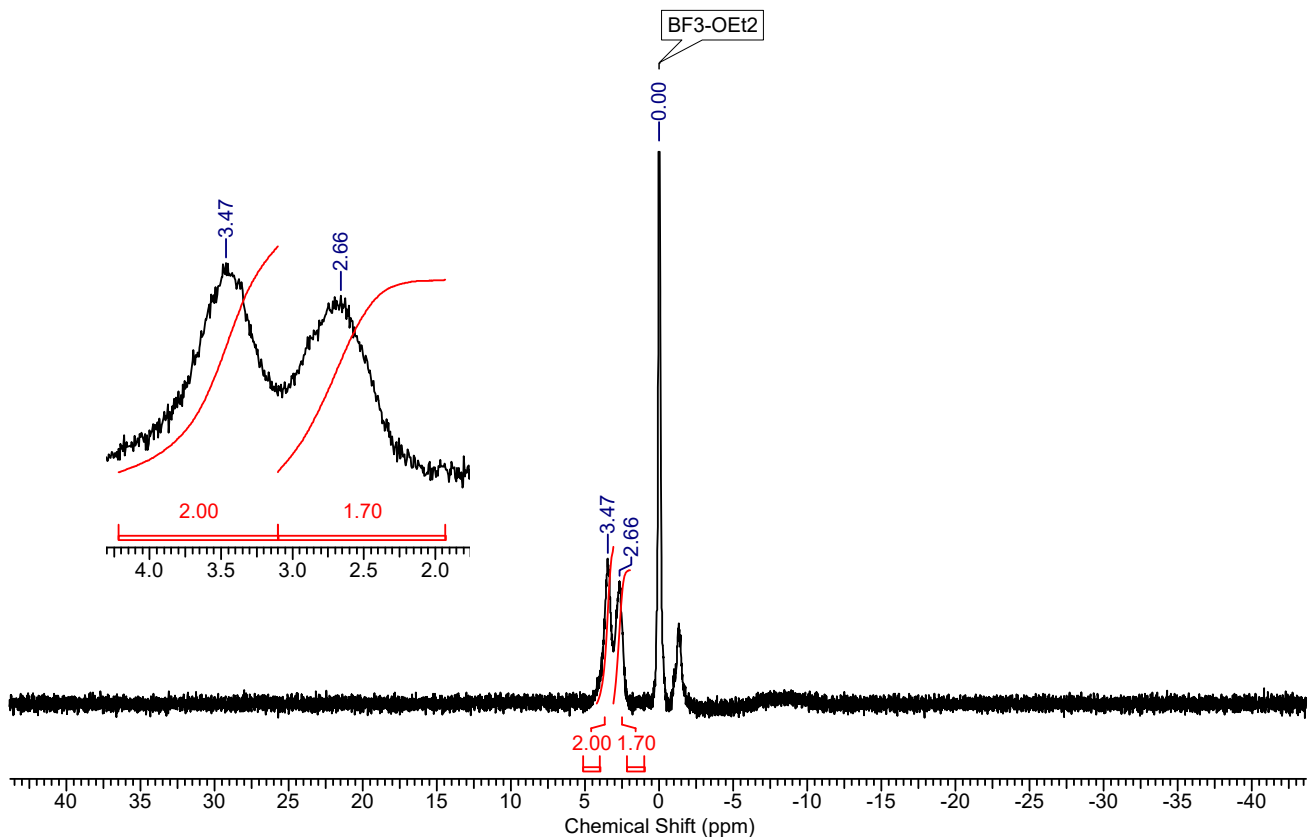
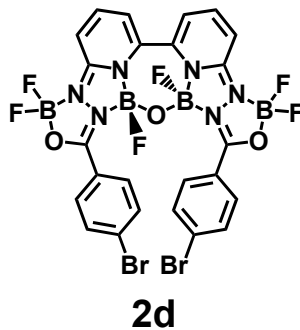


Figure S7-4. ^{11}B NMR spectrum of compound **1d** in CDCl_3 at room temperature.



Following the synthesis procedure of compound **1d**, compound **2d** was simultaneously obtained as a yellow solid (30 mg, 4 %).

m.p. > 300 °C.

¹H NMR (400 MHz, CDCl₃): δ = 7.95 (d, *J* = 7.3 Hz, 1H), 7.93 (d, *J* = 7.3 Hz, 1H), 7.88-7.87 (m, 2H), 7.86-7.85 (m, 2H), 7.39-7.38 (m, 2H), 7.36-7.35 (m, 2H), 7.21 (d, *J* = 9.0 Hz, 2H), 7.13 (dd, *J* = 7.3, 0.9 Hz, 2H).

¹³C NMR (101 MHz, CDCl₃): No analyzable ¹³C spectrum could be recorded due to the low solubility.

¹⁹F NMR (377 MHz, CDCl₃): δ = -134.29 (s, 2F), -145.12 (s, 1F), -145.32 (s, 1F), -147.86 (s, 1F), -148.06 (s, 1F).

¹¹B NMR (128 MHz, CDCl₃): No analyzable ¹¹B spectrum could be recorded due to the low solubility.

HRMS (FAB, positive): *m/z* calcd. for C₂₄H₁₄B₄Br₂F₆N₆O₃ [M]⁺ 749.9771; found: 749.9775.

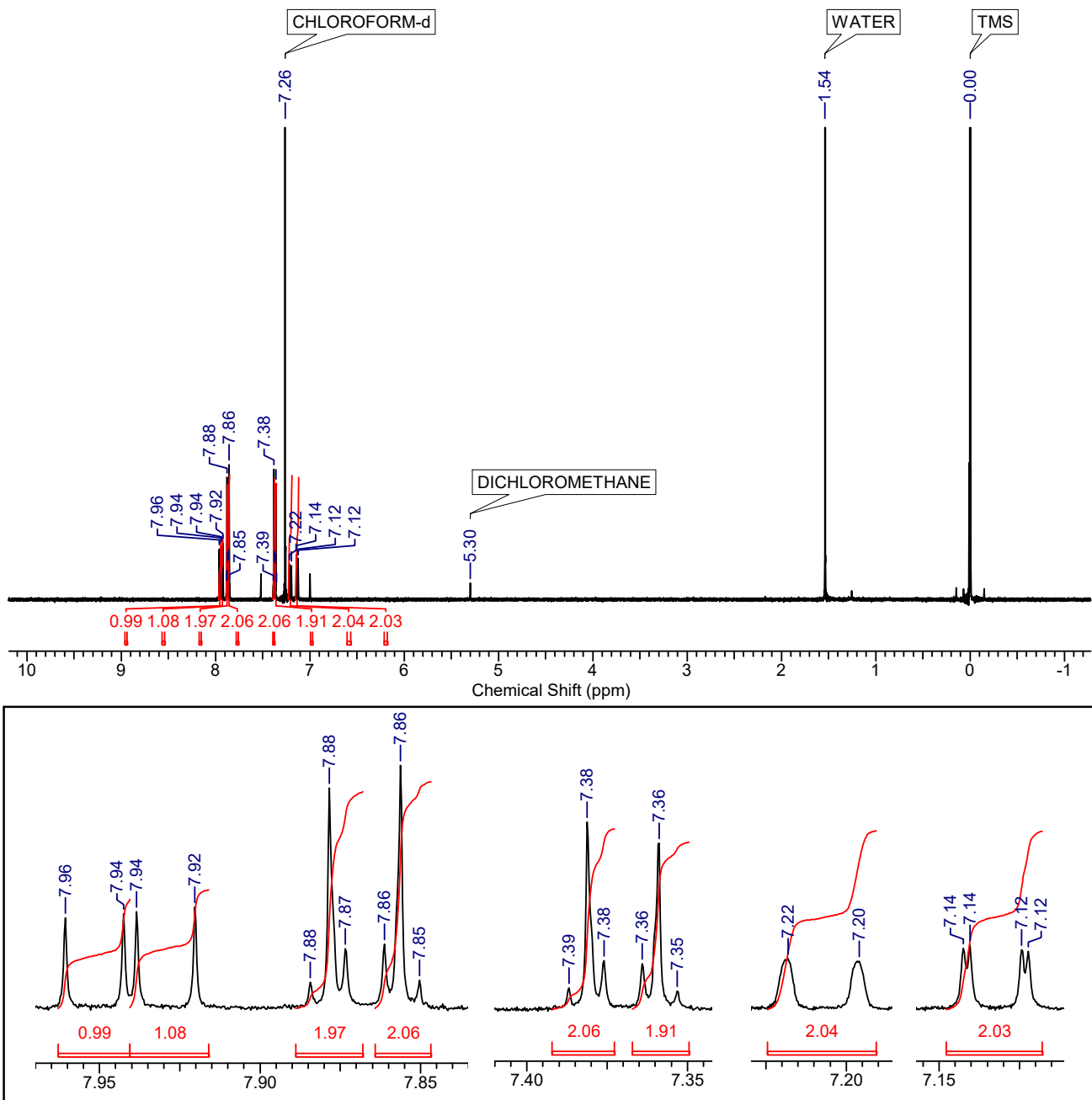


Figure S8-1. ^1H NMR spectrum of compound **2d** in CDCl_3 at room temperature.

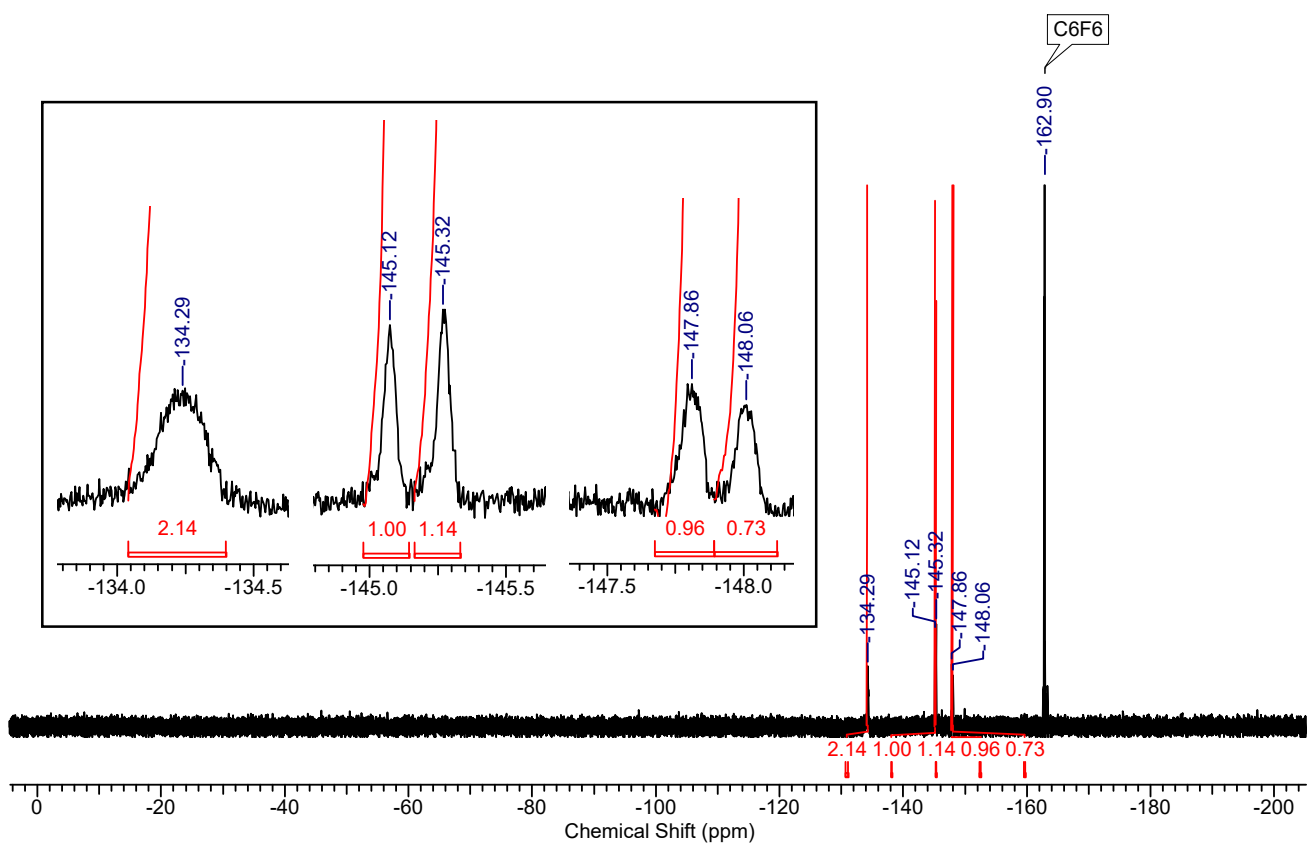


Figure S8-2. ^{19}F NMR spectrum of compound **2d** in CDCl_3 at room temperature.

X-ray crystallographic analysis

The crystals were mounted on a loop. Diffraction data of crystal samples were collected using a Rigaku XtaLABmini CCD diffractometer equipped with graphite-monochromated Mo K α radiation ($\lambda = 0.71073 \text{ \AA}$) or XtaLAB Synergy R/DW system, HyPix diffractometer using Cu K α radiation ($\lambda = 1.54184 \text{ \AA}$). Collected data were integrated, corrected, and scaled using CrysAlisPro.³ The structures were refined using SHELXT (Sheldrick, 2015)⁴ Intrinsic phasing and SHELXL (Sheldrick, 2015).⁵ All nonhydrogen atoms were refined anisotropically. Hydrogen atoms were located at calculated positions and included in the structure factor calculation but were not refined. The program Olex 2 was used as a graphical interface.⁶ Crystallographic data have been deposited with the joint Cambridge Crystallographic Data Centre and Fachinformationszentrum Karlsruhe Access Structures service. The data can be obtained free of charge on application to CCDC, 12 Union Road, Cambridge CB21EZ, UK (fax: (+44) 1223-336-033; email: deposit@ccdc.cam.ac.uk). The CCDC numbers for crystal structures of **1a**, **2a**, **1c**, **1d**, and **2d** are 2322217, 2322218, 2322219, 2322220, and 2322221, respectively.

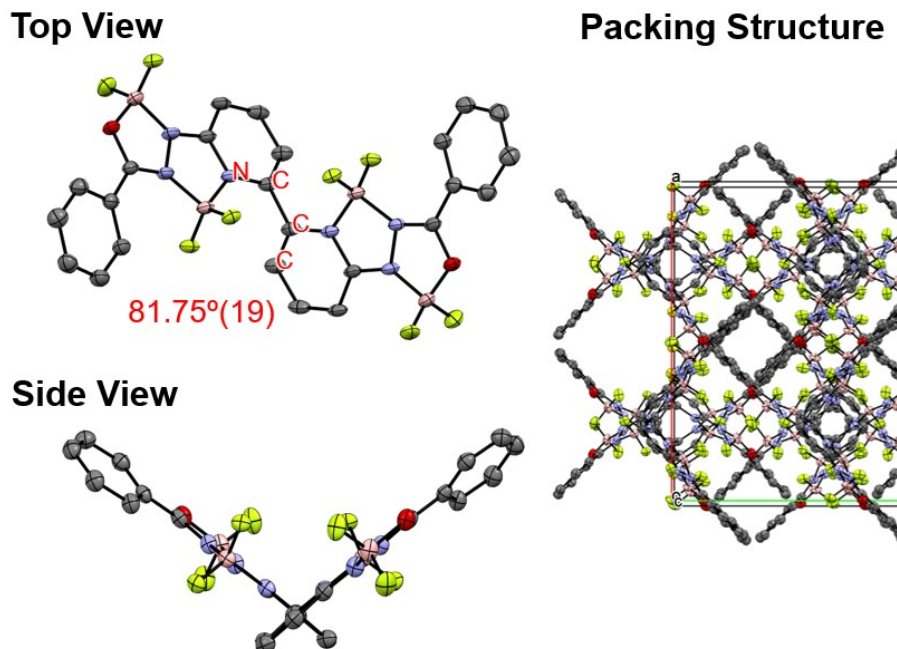


Figure S9. Crystal structure and packing mode of **1a** at 123 K determined by X-ray diffraction. Ellipsoids are plotted at the 50% probability level. Hydrogen atoms are omitted for clarity. Color code: C, gray; N, blue; O, red; B, pink; F, yellow-green. The dihedral angle (N–C–C–C) is $81.75^\circ(19)$.

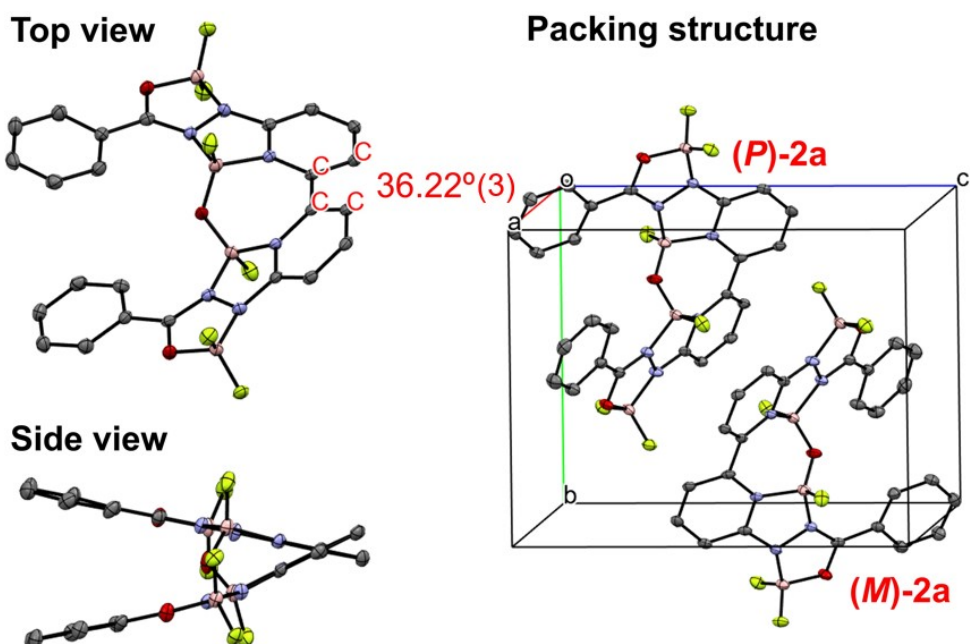


Figure S10. Crystal structure and packing mode of **2a** at 100 K determined by X-ray diffraction. Ellipsoids are plotted at the 50% probability level. Hydrogen atoms are omitted for clarity. Color code: C, gray; N, blue; O, red; B, pink; F, yellow-green. The dihedral angle (C–C–C–C) is $36.22^\circ(3)$.

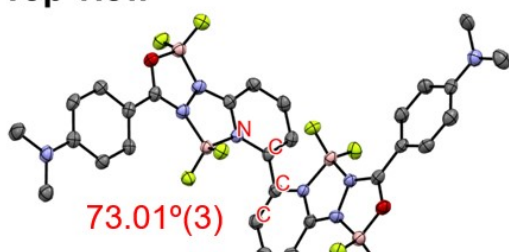
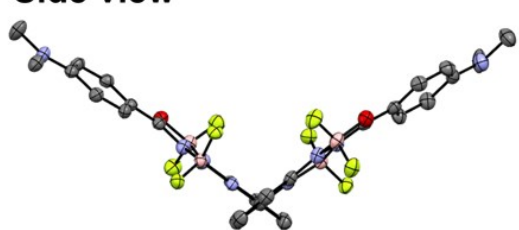
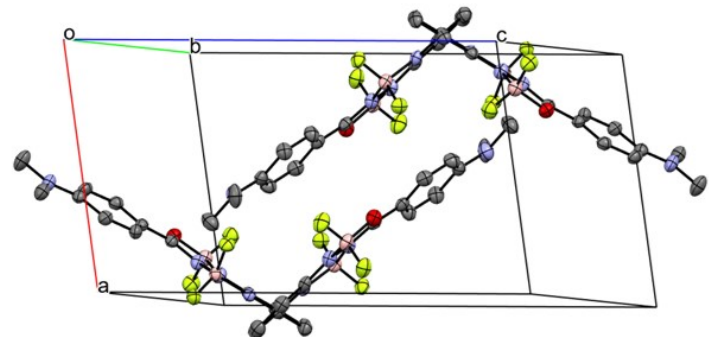
Top view**Side view****Packing structure**

Figure S11. Crystal structure and packing mode of **1c** at 123 K determined by X-ray diffraction. Ellipsoids are plotted at the 50% probability level. Hydrogen atoms are omitted for clarity. Color code: C, gray; N, blue; O, red; B, pink; F, yellow-green. The dihedral angle (N–C–C–C) is $73.01^\circ(3)$.

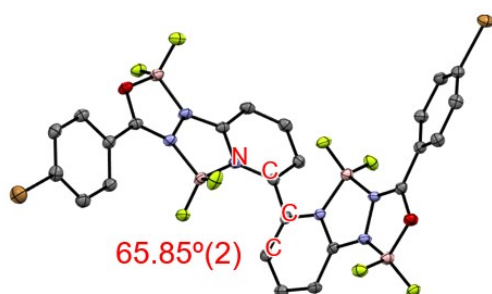
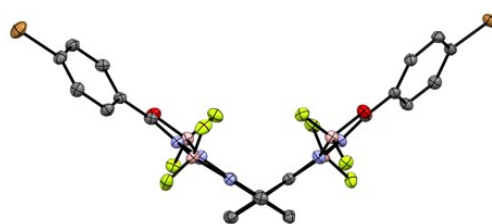
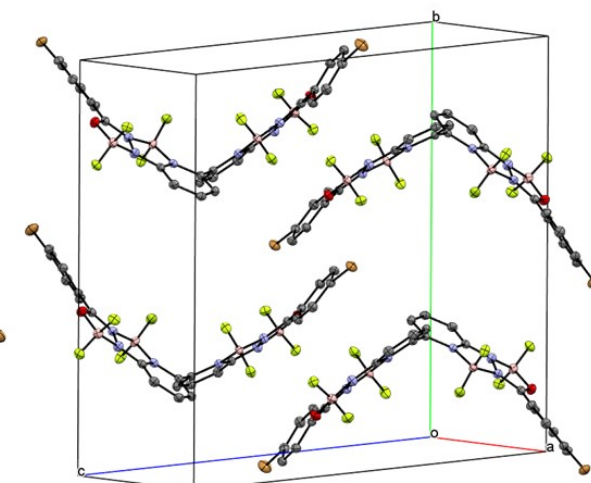
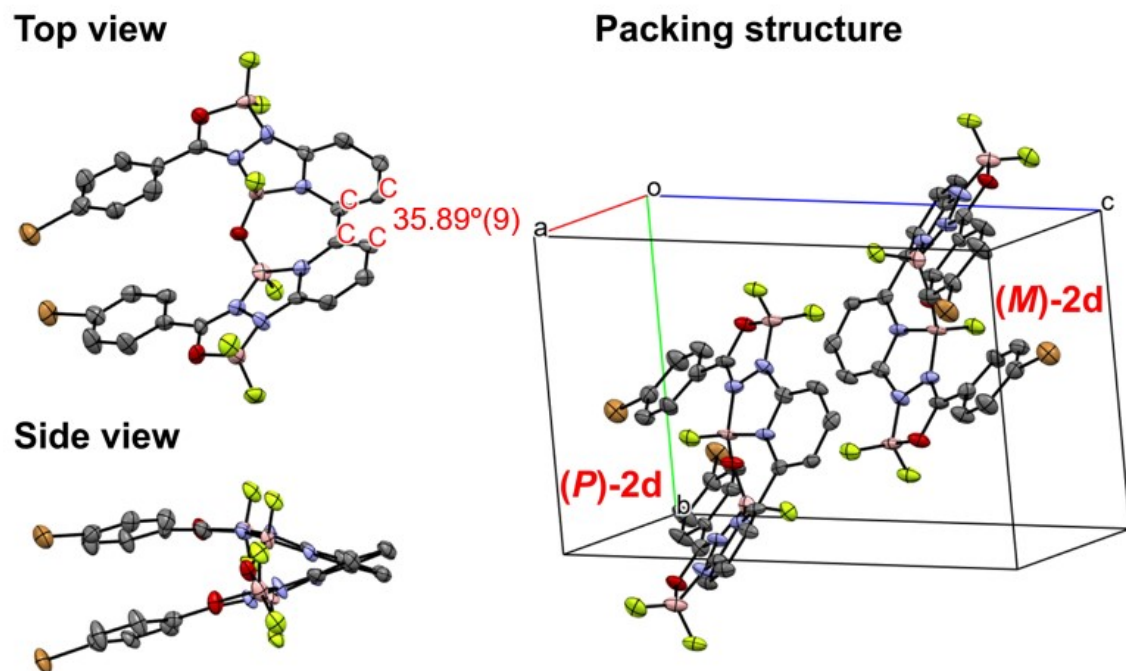
Top View**Side View****Packing Structure**

Figure S12. Crystal structure and packing mode of **1d** at 123 K determined by X-ray diffraction. Ellipsoids are plotted at the 50% probability level. Hydrogen atoms and solvent molecules (CH_2Cl_2) are omitted for clarity. Color code: C, gray; N, blue; O, red; Br, brown; B, pink; F, yellow-green. The



dihedral angle ($\text{N}-\text{C}-\text{C}-\text{C}$) is $65.85^{\circ}(2)$.

Figure S13. Crystal structure and packing mode of **2d** at 123 K determined by X-ray diffraction. Ellipsoids are plotted at the 50% probability level. Hydrogen atoms are omitted for clarity. Color code: C, gray; N, blue; O, red; Br, brown; B, pink; F, yellow-green. The dihedral angle ($\text{C}-\text{C}-\text{C}-\text{C}$) is $35.89^{\circ}(9)$.

Table S1. Crystallographic data for **1a** at 100 K determined by X-ray diffraction.

Compound	1a
CCDC No.	2322217
empirical formula	C ₂₄ H ₁₆ B ₄ F ₈ N ₆ O ₂
formula weight	615.67
temperature [K]	100
wavelength [Å]	1.54184
crystal system	tetragonal
space group	I4 ₁ /acd
<i>a</i> [Å]	18.9140(2)
<i>b</i> [Å]	18.9140(2)
<i>c</i> [Å]	27.7587(4)
α [°]	90
β [°]	90
γ [°]	90
Volume [Å ³]	9930.4(3)
<i>Z</i>	16
Density (calculated) [g/cm ³]	1.647
Absorption coefficient [mm ⁻¹]	1.283
<i>F</i> (000)	4960.0
θ [°]	4.091 to 75.976
Reflections collected	16042
Independent reflections	2542 [$R_{\text{int}} = 0.0276$, $R_{\text{sigma}} = 0.0185$]
Data/restraints/parameters	2542/0/199
Goodness-of-fit on <i>F</i> ²	1.081
<i>R</i> 1 [$I > 2\sigma(I)$]	0.0418
<i>wR</i> 2 (all data)	0.1270
Largest diff. peak and hole [e.Å ⁻³]	0.44/-0.24

Table S2. Crystallographic data for **2a** at 100 K determined by X-ray diffraction.

Compound	2a
CCDC No.	2322218
empirical formula	C ₂₄ H ₁₆ B ₄ F ₆ N ₆ O ₃
formula weight	593.67
temperature [K]	100
wavelength [Å]	0.71073
crystal system	triclinic
space group	P-1
<i>a</i> [Å]	8.4265(4)
<i>b</i> [Å]	10.5693(4)
<i>c</i> [Å]	13.8392(6)
α [°]	89.215(3)
β [°]	85.014(4)
γ [°]	79.567(3)
Volume [Å ³]	1207.58(9)
<i>Z</i>	2
Density (calculated) [g/cm ³]	1.633
Absorption coefficient [mm ⁻¹]	0.139
<i>F</i> (000)	600.0
θ [°]	2.451 to 27.499
Reflections collected	7777
Independent reflections	7777 [R _{int} = ?, R _{sigma} = 0.0366]
Data/restraints/parameters	7777/0/389
Goodness-of-fit on <i>F</i> ²	1.039
<i>R</i> 1 [<i>I</i> >2σ(<i>I</i>)]	0.0443
<i>wR</i> 2 (all data)	0.1183
Largest diff. peak and hole [e.Å ⁻³]	0.27/-0.30

Table S3. Crystallographic data for **1c** at 123 K determined by X-ray diffraction.

Compound	1c
CCDC No.	2322219
empirical formula	C ₂₈ H ₂₆ B ₄ F ₈ N ₈ O ₂
formula weight	701.81
temperature [K]	123
wavelength [Å]	0.71073
crystal system	triclinic
space group	P-1
<i>a</i> [Å]	9.2962(7)
<i>b</i> [Å]	9.8661(7)
<i>c</i> [Å]	17.0113(12)
α [°]	84.337(6)
β [°]	83.855(6)
γ [°]	80.627(6)
Volume [Å ³]	1525.30(19)
<i>Z</i>	2
Density (calculated) [g/cm ³]	1.528
Absorption coefficient [mm ⁻¹]	0.131
<i>F</i> (000)	716.0
θ [°]	2.508 to 26.368
Reflections collected	16242
Independent reflections	6239 [$R_{\text{int}} = 0.0496$, $R_{\text{sigma}} = 0.0658$]
Data/restraints/parameters	6239/0/455
Goodness-of-fit on <i>F</i> ²	1.019
<i>R</i> 1 [$I > 2\sigma(I)$]	0.0546
<i>wR</i> 2 (all data)	0.1479
Largest diff. peak and hole [e.Å ⁻³]	0.51/-0.27

Table S4. Crystallographic data for **1d** at 100 K determined by X-ray diffraction.

Compound	1d
CCDC No.	2322220
empirical formula	C ₂₅ H ₁₆ B ₄ Br ₂ Cl ₂ F ₈ N ₆ O ₂
formula weight	858.40
temperature [K]	100
wavelength [Å]	1.54184
crystal system	monoclinic
space group	P2 ₁ /n
<i>a</i> [Å]	7.36860(10)
<i>b</i> [Å]	18.9186(4)
<i>c</i> [Å]	21.9266(4)
α [°]	90
β [°]	91.991(2)
γ [°]	90
Volume [Å ³]	3054.80(9)
<i>Z</i>	4
Density (calculated) [g/cm ³]	1.866
Absorption coefficient [mm ⁻¹]	5.779
<i>F</i> (000)	1680.0
θ [°]	3.086 to 76.273
Reflections collected	20800
Independent reflections	6127 [$R_{\text{int}} = 0.0335$, $R_{\text{sigma}} = 0.0343$]
Data/restraints/parameters	6127/0/442
Goodness-of-fit on <i>F</i> ²	1.043
<i>R</i> 1 [$I > 2\sigma(I)$]	0.0301
<i>wR</i> 2 (all data)	0.0830
Largest diff. peak and hole [e.Å ⁻³]	0.56/-0.50

Table S5. Crystallographic data for **2d** at 123 K determined by X-ray diffraction.

Compound	2d
CCDC No.	2322221
empirical formula	C ₂₄ H ₁₄ B ₄ Br ₂ F ₆ N ₆ O ₃
formula weight	751.47
temperature [K]	123
wavelength [Å]	0.71073
crystal system	triclinic
space group	P-1
<i>a</i> [Å]	8.1074(11)
<i>b</i> [Å]	10.5772(17)
<i>c</i> [Å]	15.807(3)
α [°]	91.309(14)
β [°]	91.058(14)
γ [°]	99.216(13)
Volume [Å ³]	1337.3(4)
<i>Z</i>	2
Density (calculated) [g/cm ³]	1.866
Absorption coefficient [mm ⁻¹]	3.116
<i>F</i> (000)	736.0
θ [°]	2.578 to 26.37
Reflections collected	12044
Independent reflections	5464 [$R_{\text{int}} = 0.1101$, $R_{\text{sigma}} = 0.1811$]
Data/restraints/parameters	5464/0/406
Goodness-of-fit on <i>F</i> ²	0.987
<i>R</i> 1 [$I > 2\sigma(I)$]	0.0756
<i>wR</i> 2 (all data)	0.1877
Largest diff. peak and hole [e.Å ⁻³]	1.42/-0.70

Optical properties in various solvents

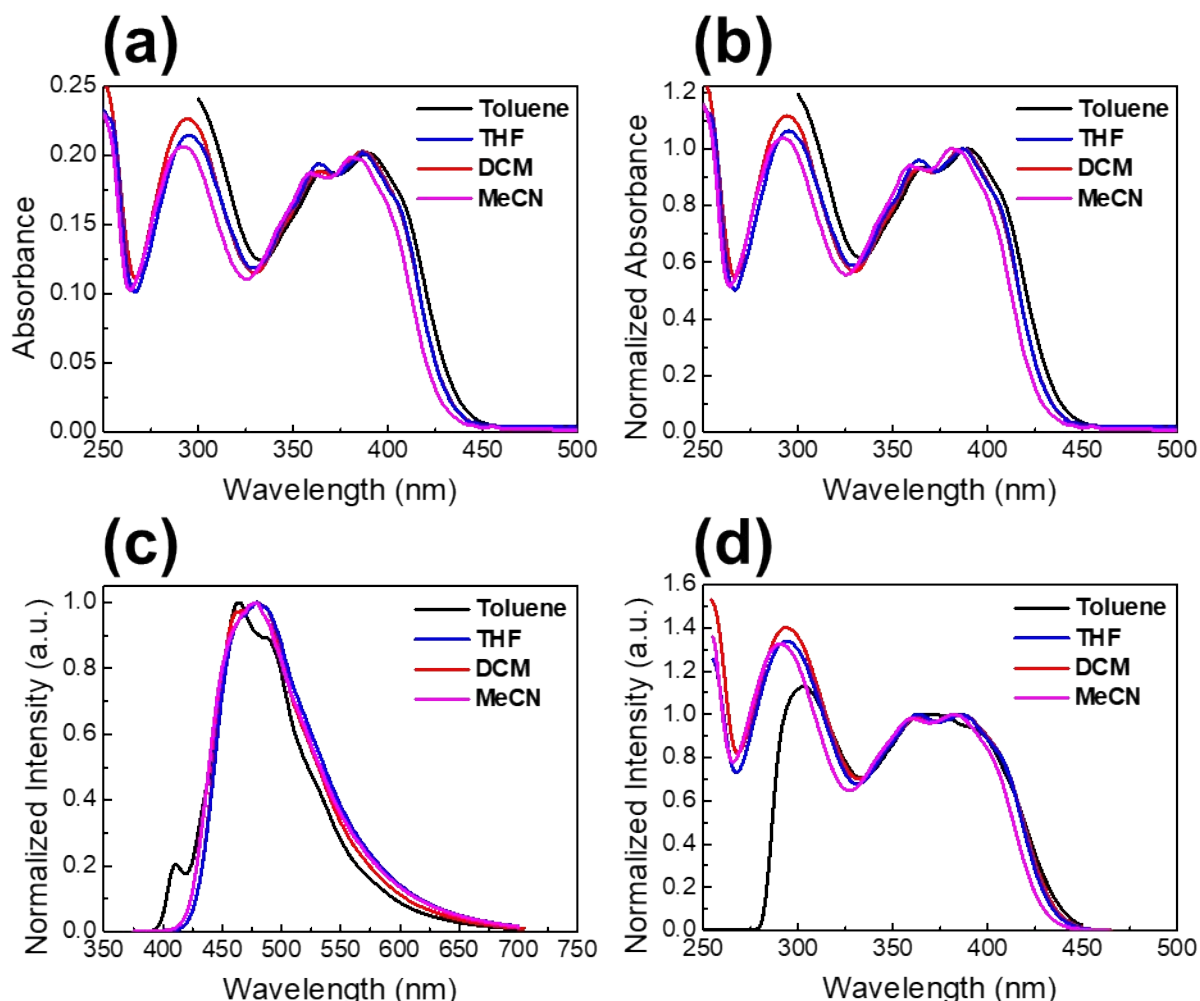
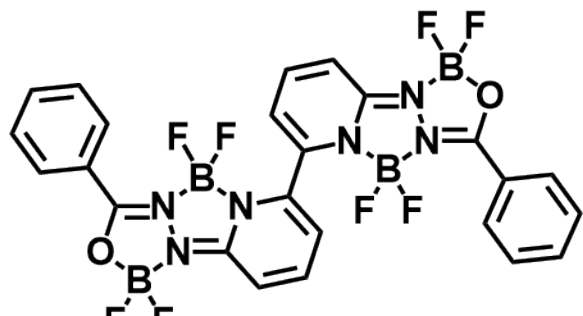


Figure S14. (a) UV-vis absorption spectra of **1a** in various solvents ($c = 10^{-6}$ M). Normalized (b) UV-vis absorption spectra, (c) emission spectra (excited at $\lambda_{\text{abs}}^{\text{max}}$), and (d) excitation spectra (emission wavelength at $\lambda_{\text{em}}^{\text{max}}$) of **1a** in various solvents ($c = 10^{-6}$ M).

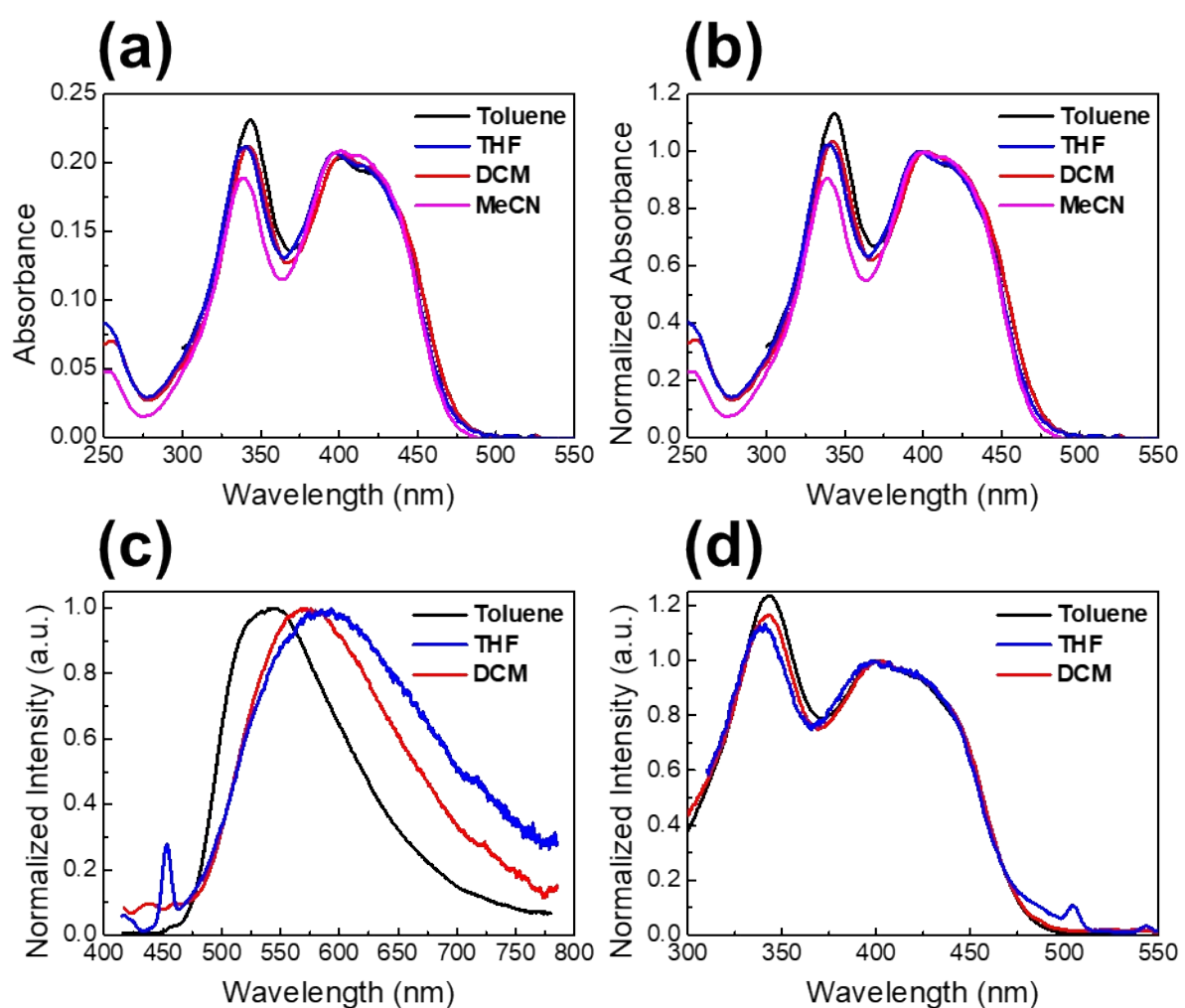
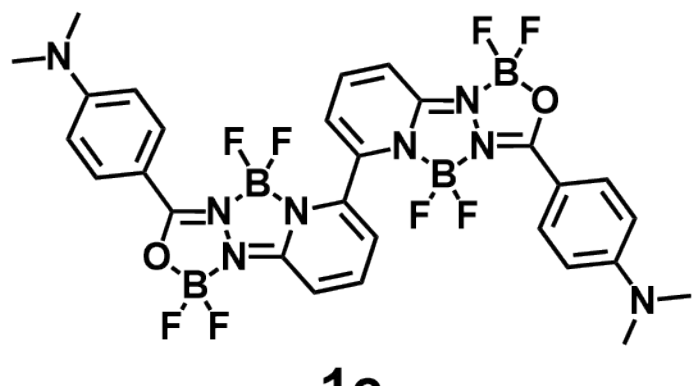


Figure S15. (a) UV-vis absorption spectra of **1c** in various solvents ($c = 10^{-6}$ M). Normalized (b) UV-vis absorption spectra, (c) emission spectra (excited at $\lambda_{\text{abs}}^{\text{max}}$), and (d) excitation spectra (emission wavelength at $\lambda_{\text{em}}^{\text{max}}$) of **1c** in various solvents ($c = 10^{-6}$ M).

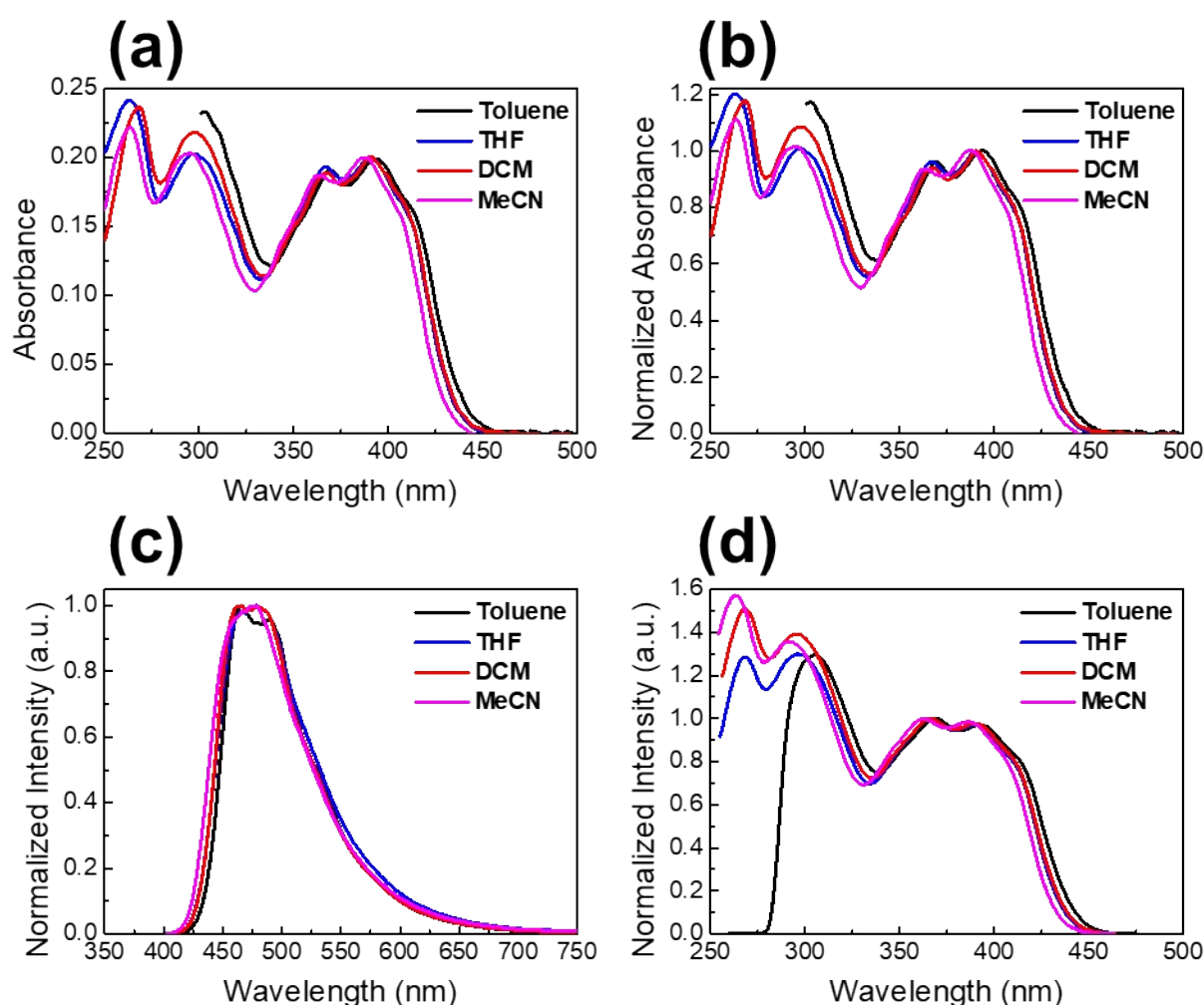
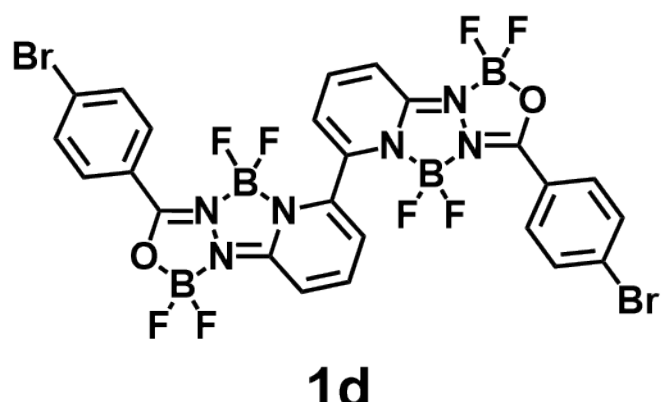
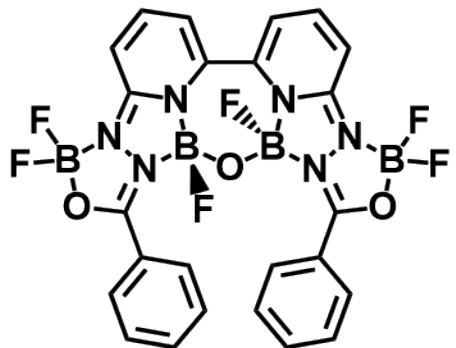


Figure S16. (a) UV-vis absorption spectra of **1d** in various solvents ($c = 10^{-6}$ M). Normalized (b) UV-vis absorption spectra, (c) emission spectra (excited at $\lambda_{\text{abs}}^{\text{max}}$), and (d) excitation spectra (emission wavelength at $\lambda_{\text{em}}^{\text{max}}$) of **1d** in various solvents ($c = 10^{-6}$ M).



2a

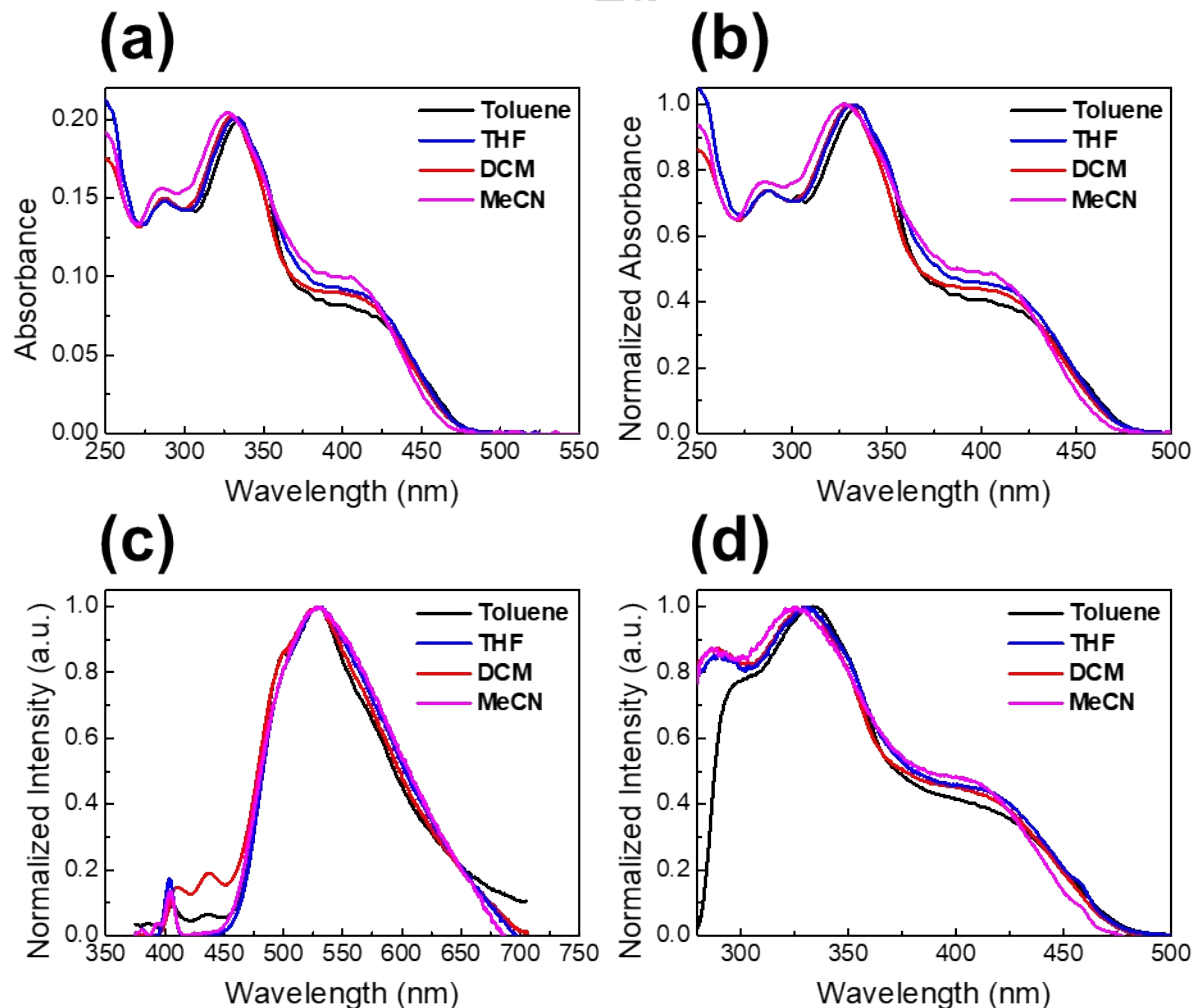
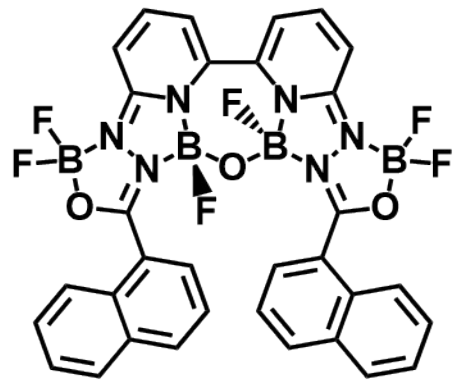


Figure S17. (a) UV-vis absorption spectra of **2a** in various solvents ($c = 10^{-6}$ M). Normalized (b) UV-vis absorption spectra, (c) emission spectra (excited at $\lambda_{\text{abs}}^{\text{max}}$), and (d) excitation spectra (emission wavelength at $\lambda_{\text{em}}^{\text{max}}$) of **2a** in various solvents ($c = 10^{-6}$ M).



2b

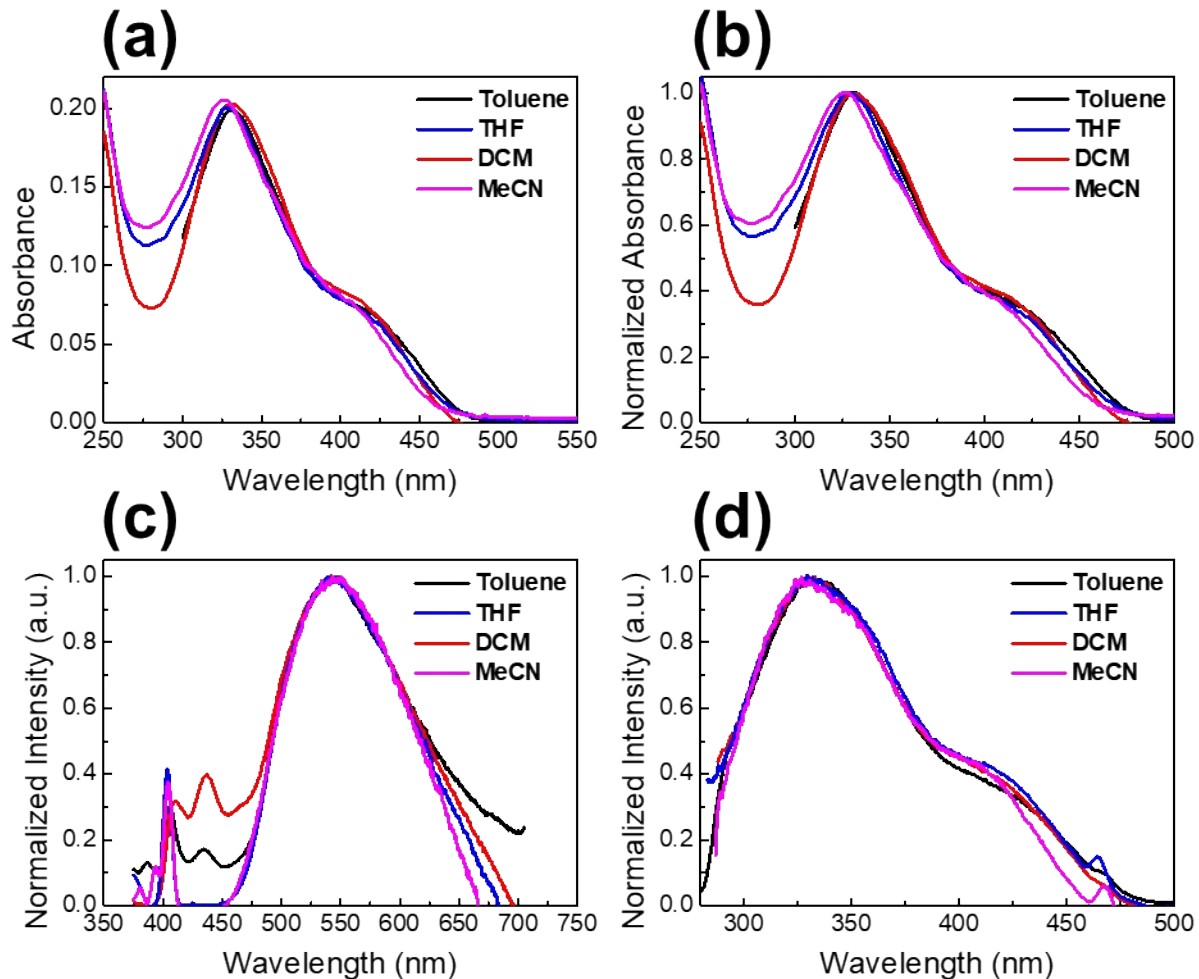
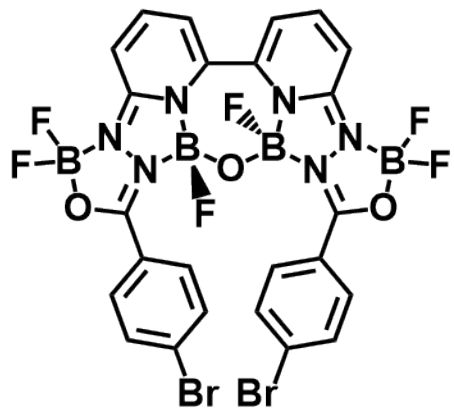


Figure S18. (a) UV-vis absorption spectra of **2b** in various solvents ($c = 10^{-6}$ M). Normalized (b) UV-vis absorption spectra, (c) emission spectra (excited at $\lambda_{\text{abs}}^{\text{max}}$), and (d) excitation spectra (emission wavelength at $\lambda_{\text{em}}^{\text{max}}$) of **2b** in various solvents ($c = 10^{-6}$ M).



2d

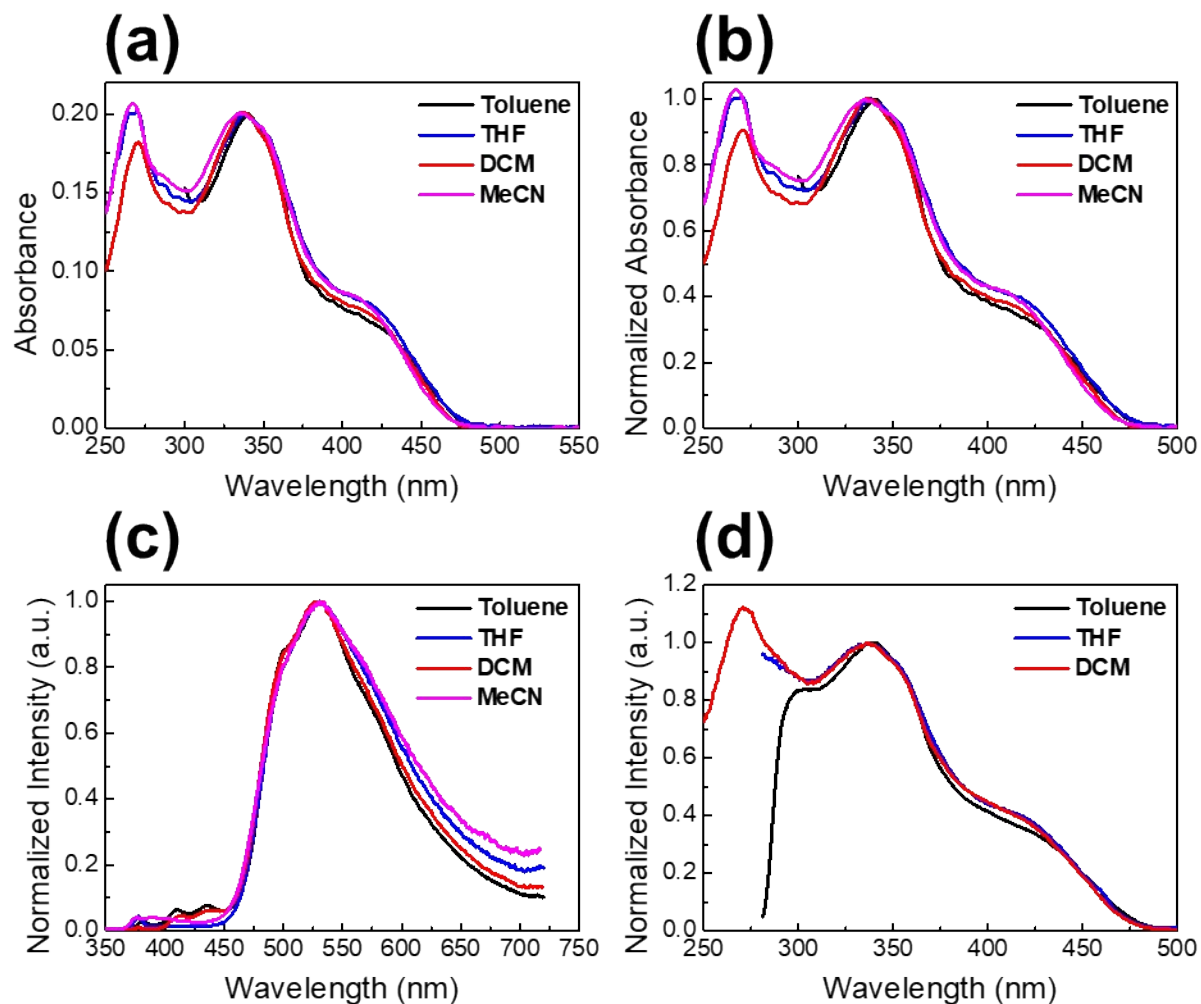
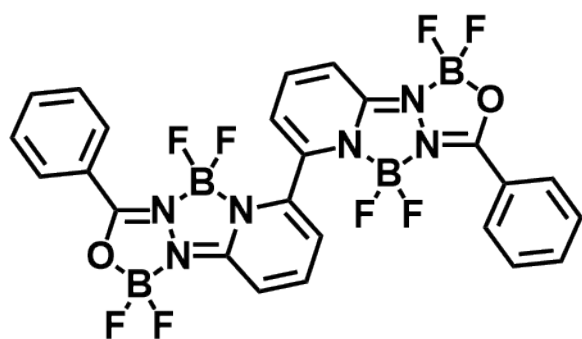


Figure S19. (a) UV-vis absorption spectra of **2d** in various solvents ($c = 10^{-6}$ M). Normalized (b) UV-vis absorption spectra, (c) emission spectra (excited at $\lambda_{\text{abs}}^{\text{max}}$), and (d) excitation spectra (emission wavelength at $\lambda_{\text{em}}^{\text{max}}$) of **2d** in various solvents ($c = 10^{-6}$ M).

Table S6. Photophysical properties of all compounds in various solvents.

Compd.^[a]	Solvent	$\lambda_{\text{abs}}^{\text{max}} / \text{nm}^{\text{[b]}}$	$\lambda_{\text{em}}^{\text{max}} / \text{nm}^{\text{[c]}}$	$\Phi_{\text{PL}}^{\text{[d]}}$	$\tau_{\text{av}} / \text{ns}$	Stokes shift / cm⁻¹
1a	Toluene	390	465, 487	0.23	1.64	4100
	THF	295, 363, 387	479	0.088	1.18	5000
	DCM	294, 364, 386	466, 480	0.20	1.66	4400
	MeCN	292, 359, 384	478	0.088	1.14	5100
1c	Toluene	344, 401	545	0.040	0.36	6600
	THF	341, 399	585, 593	0.007	0.16	8000, 8200
	DCM	342, 402	570	0.012	0.13	7300
	MeCN	339, 401	—	—	—	—
1d	Toluene	393	466, 489	0.27	2.12	4000, 5000
	THF	391	467, 479	0.13	1.53	4200, 4700
	DCM	391	466, 479	0.24	2.06	4100, 4700
	MeCN	388	478	0.15	1.57	4900
2a	Toluene	334	530	0.039	0.50	11100
	THF	286, 333	530	0.013	0.078	11200
	DCM	286, 330	531	0.018	0.25	11500
	MeCN	285, 328	531	0.010	0.12	11700
2b	Toluene	332	545	0.017	0.24	11800
	THF	328	539	0.010	0.094	11900
	DCM	330	545	0.011	0.065	12000
	MeCN	327	543	0.009	0.11	12200
2d	Toluene	340	531	0.078	0.59	10600
	THF	338	534	0.031	0.21	10900
	DCM	336	532	0.018	0.38	11000
	MeCN	335	534	0.013	0.15	11000

[a] $c = 10^{-6}$ M in solutions. [b] Absorption maxima. [c] Emission maxima, excited at $\lambda_{\text{abs}}^{\text{max}}$. [d] Absolute photoluminescence quantum yields, excited at $\lambda_{\text{abs}}^{\text{max}}$.



1a

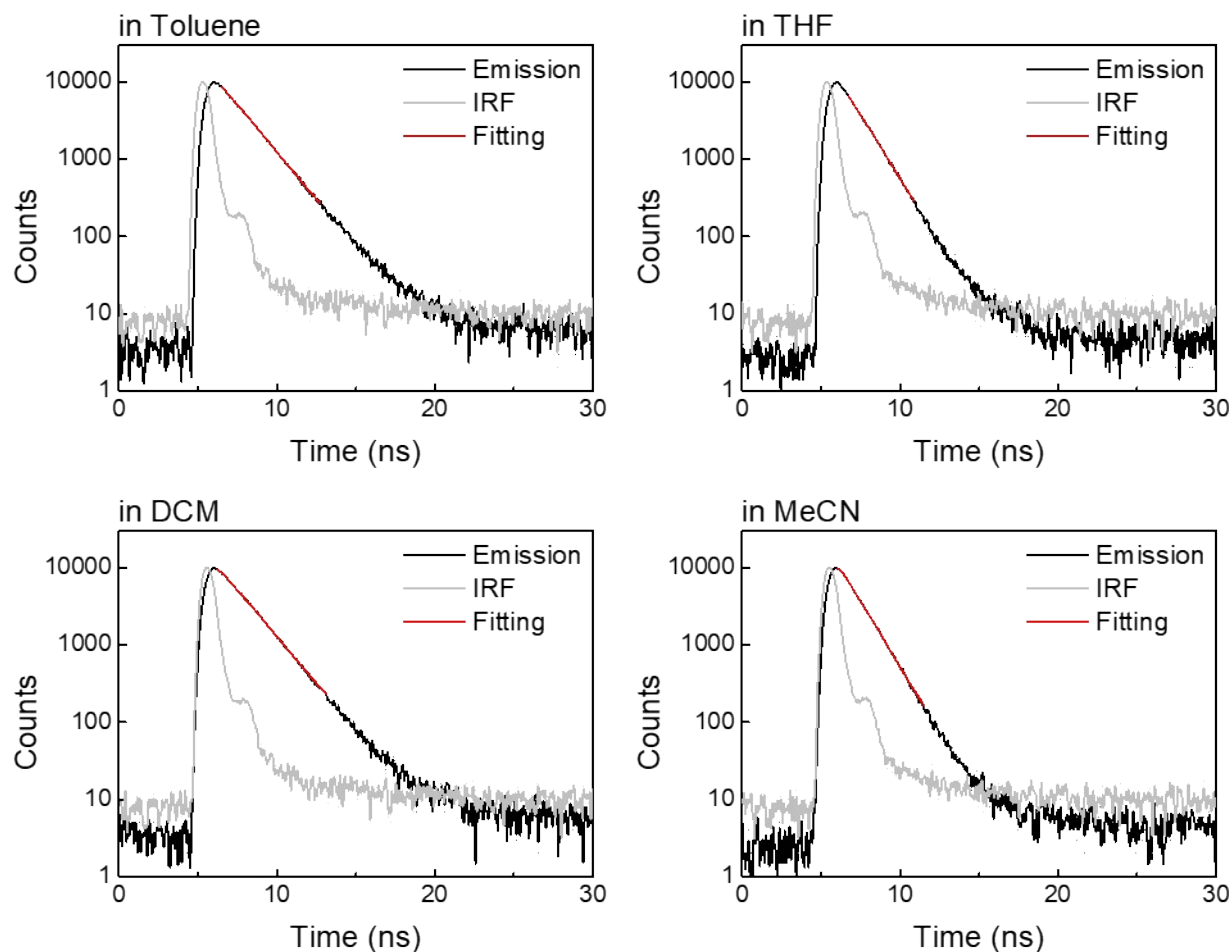


Figure S20. Emission decay curves (black line), fits (red line), and instrument response function (IRF) (gray line) of **1a** in various solvents. Excited at 365 nm and emission wavelength at $\lambda_{\text{em}}^{\text{max}}$.

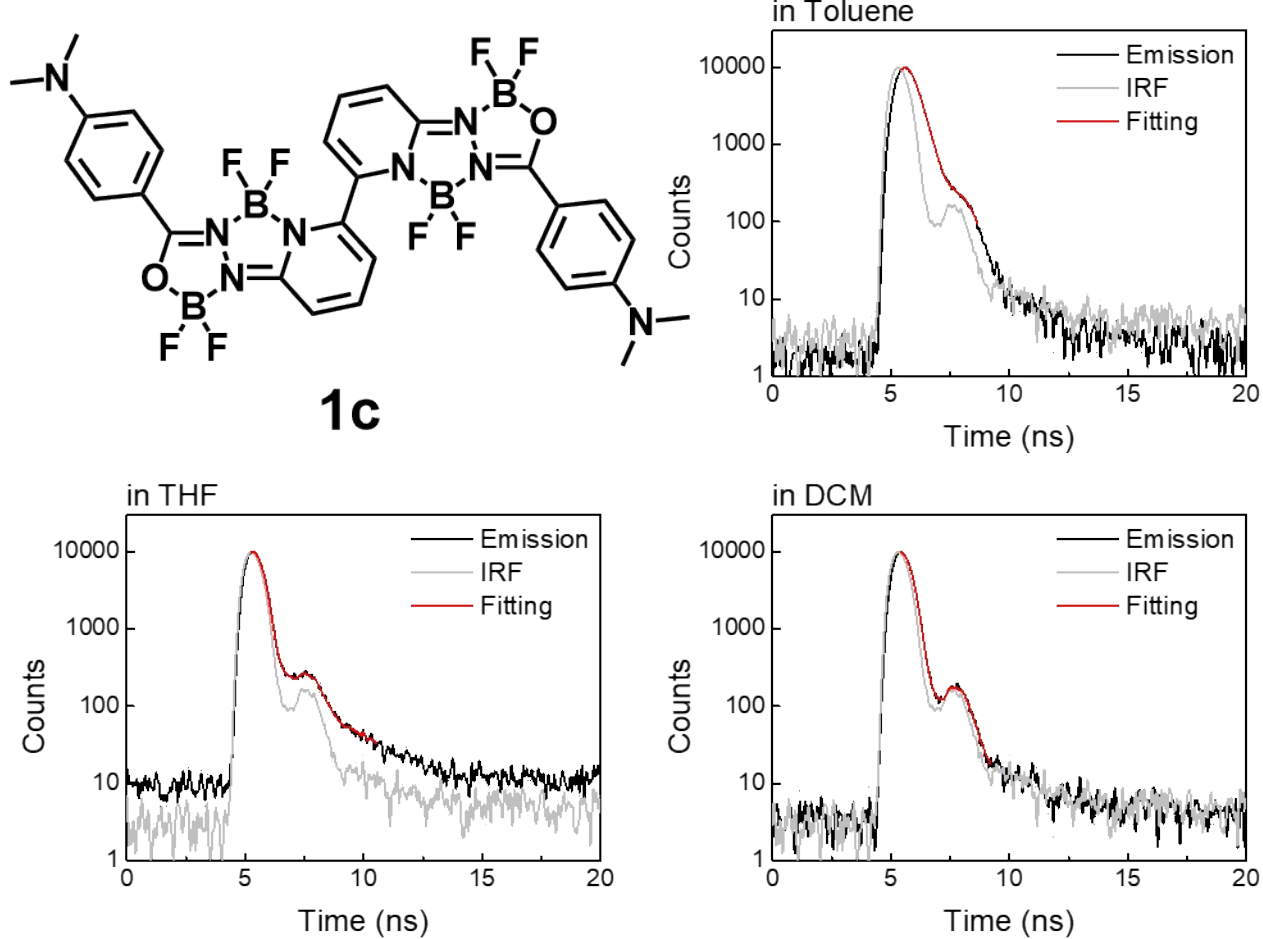
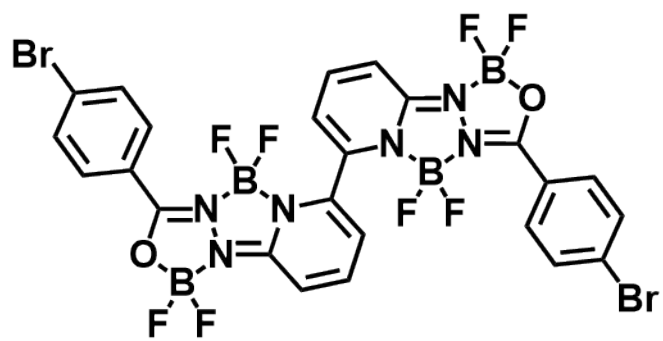


Figure S21. Emission decay curves (black line), fits (red line), and instrument response function (IRF) (gray line) of **1c** in various solvents. Excited at 405 nm and emission wavelength at $\lambda_{\text{em}}^{\text{max}}$.



1d

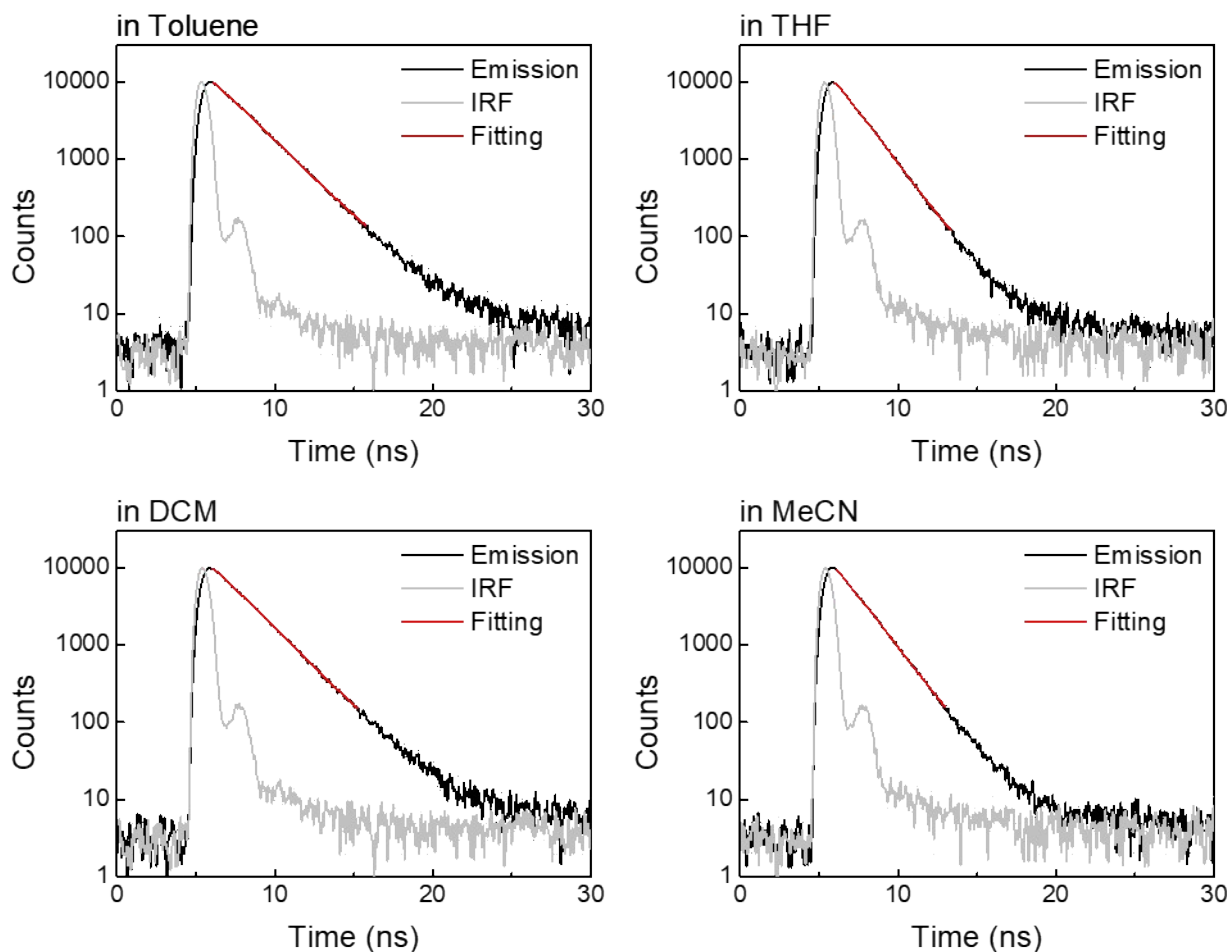
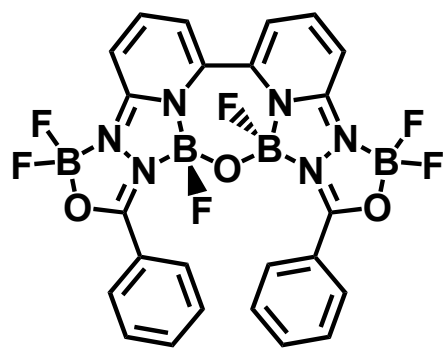


Figure S22. Emission decay curves (black line), fits (red line), and instrument response function (IRF) (gray line) of **1d** in various solvents. Excited at 405 nm and emission wavelength at $\lambda_{\text{em}}^{\text{max}}$.



2a

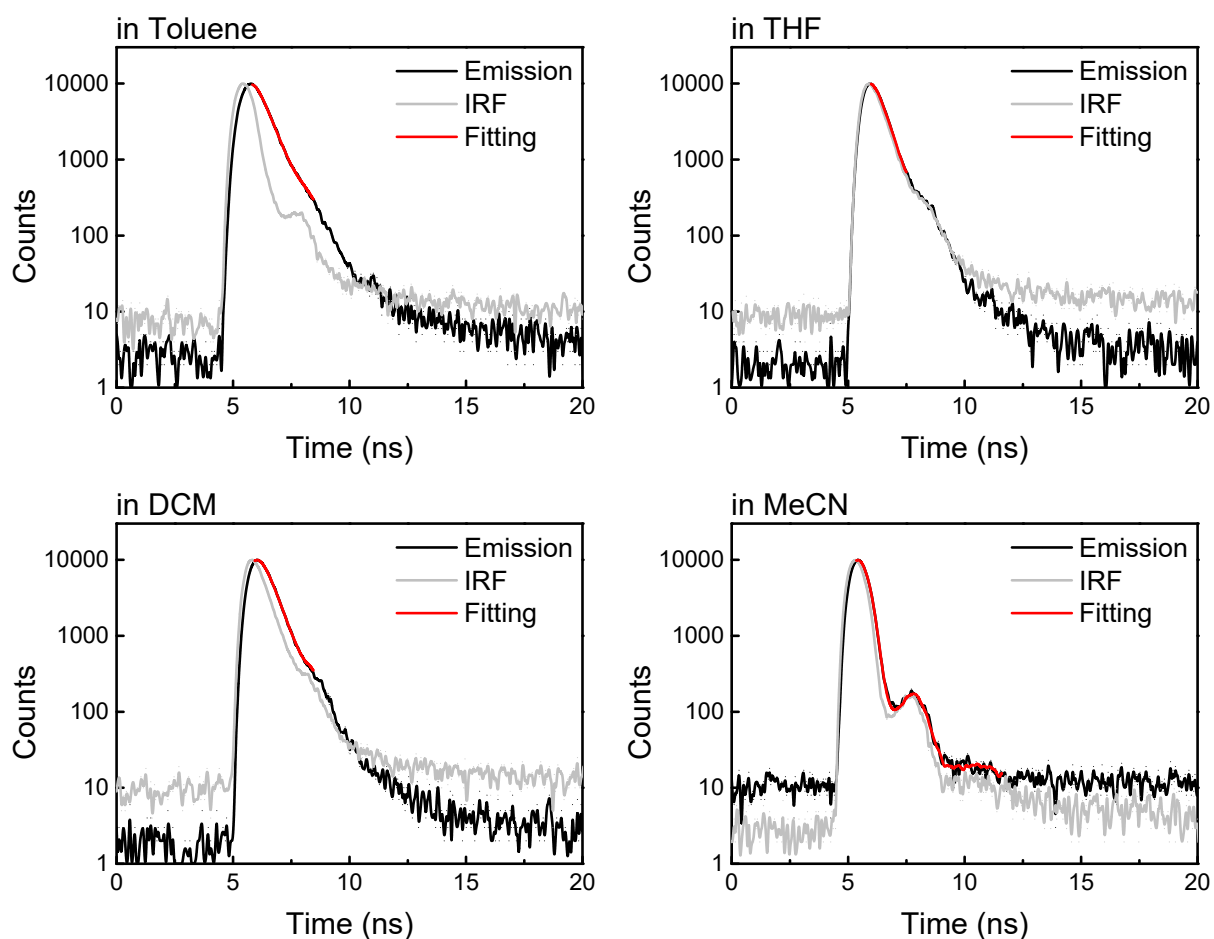
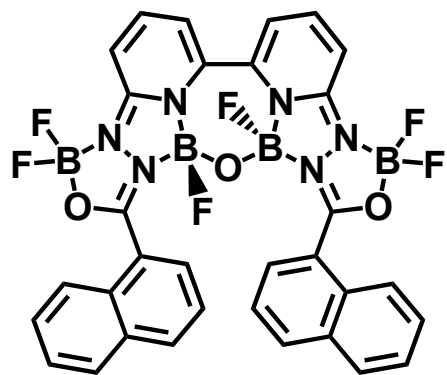


Figure S23. Emission decay curves (black line), fits (red line), and instrument response function (IRF) (gray line) of **2a** in various solvents.



2b

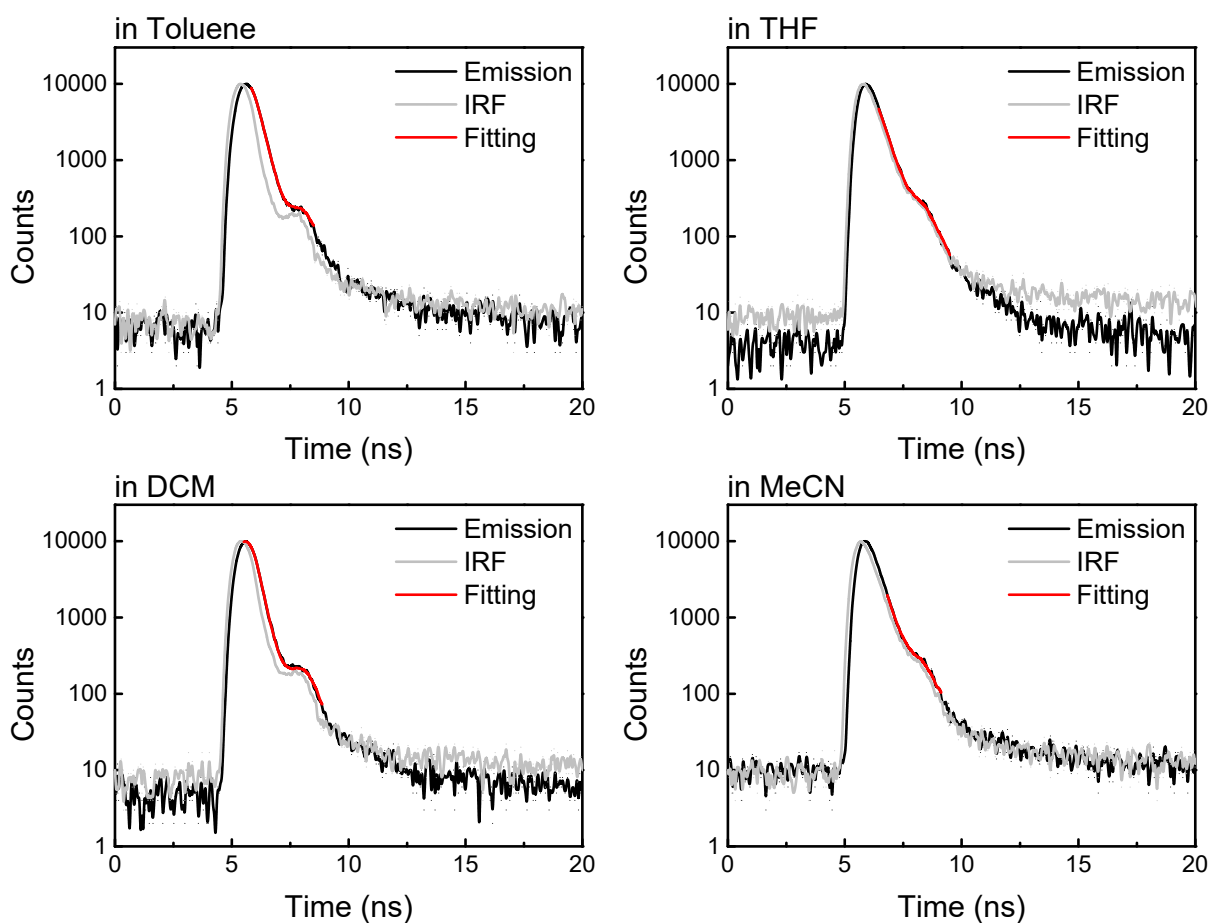
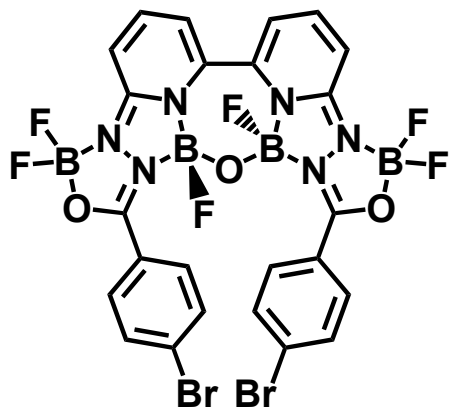


Figure S24. Emission decay curves (black line), fits (red line), and instrument response function (IRF) (gray line) of **2b** in various solvents. Excited at 340 or 365 nm and emission wavelength at $\lambda_{\text{em}}^{\text{max}}$.



2d

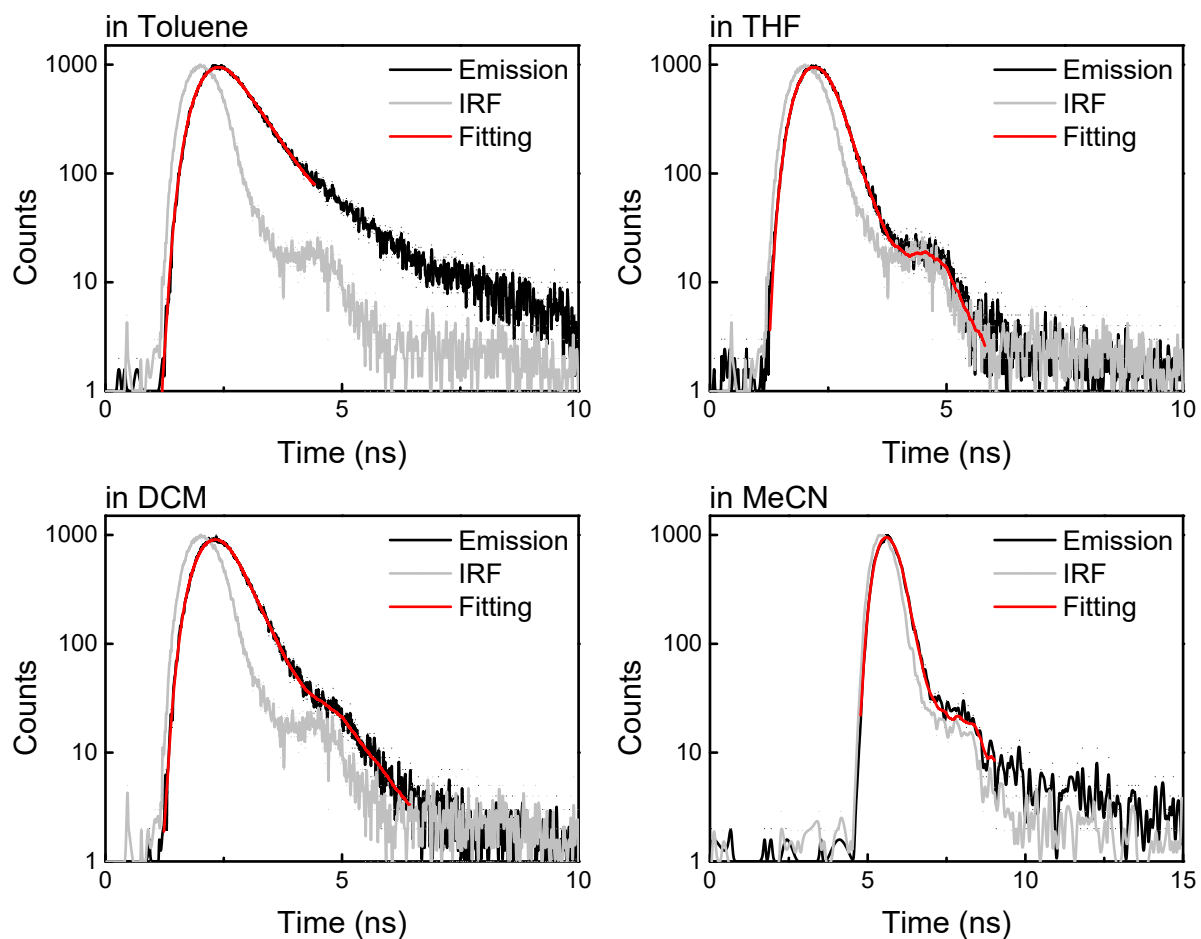


Figure S25. Emission decay curves (black line), fits (red line), and instrument response function (IRF) (gray line) of **2d** in various solvents. Excited at 365 nm and emission wavelength at $\lambda_{\text{em}}^{\text{max}}$.

Table S7. Summary of lifetime analyses for all compounds in various solvents. Emission lifetimes (τ), pre-exponential factor (A) and intensity average lifetime (τ_{av}).

Compd.	Solvent	λ_{ex} / nm ^[a]	λ_{em} / nm ^[b]	CHI	τ_{av} / ns	τ_1 / ns	τ_2 / ns	A ₁	A ₂
1a	Toluene	365	465	1.09	1.64	1.64	—	960.01	—
	THF	365	479	1.13	1.18	1.18	—	1068.65	—
	DCM	365	466	1.12	1.66	1.66	—	827.87	—
	MeCN	365	478	1.09	1.14	1.14	—	976.95	—
1c	Toluene	405	545	1.00	0.36	0.36	—	1869.93	—
	THF	405	585	1.14	0.16	0.072	1.52	7081.42	22.64
	DCM	405	570	1.10	0.13	0.12	0.79	4474.58	10.94
1d	Toluene	405	466	1.16	2.12	2.12	—	853.17	—
	THF	405	467	1.02	1.53	1.53	—	934.44	—
	DCM	405	479	1.07	2.06	2.06	—	828.32	—
	MeCN	405	478	1.13	1.57	1.57	—	898.91	—
2a	Toluene	365	530	1.12	0.50	0.50	—	1475.52	—
	THF	340	530	1.09	0.078	0.078	—	6553.13	—
	DCM	340	531	1.10	0.23	0.23	—	2521.77	—
	MeCN	405	531	1.08	0.12	0.12	—	4405.53	—
2b	Toluene	365	545	1.03	0.24	0.24	—	2571.82	—
	THF	340	539	1.05	0.094	0.094	—	5481.76	—
	DCM	365	545	1.08	0.17	0.17	—	3230.74	—
	MeCN	340	543	1.02	0.11	0.11	—	4783.96	—
2d	Toluene	365	531	1.02	0.59	0.59	—	28.49	—
	THF	365	534	1.00	0.21	0.21	—	59.81	—
	DCM	365	532	1.04	0.38	0.38	—	35.84	—
	MeCN	365	532	1.12	0.15	0.15	—	349.71	—

[a] Excitation wavelength. [b] Emission wavelength.

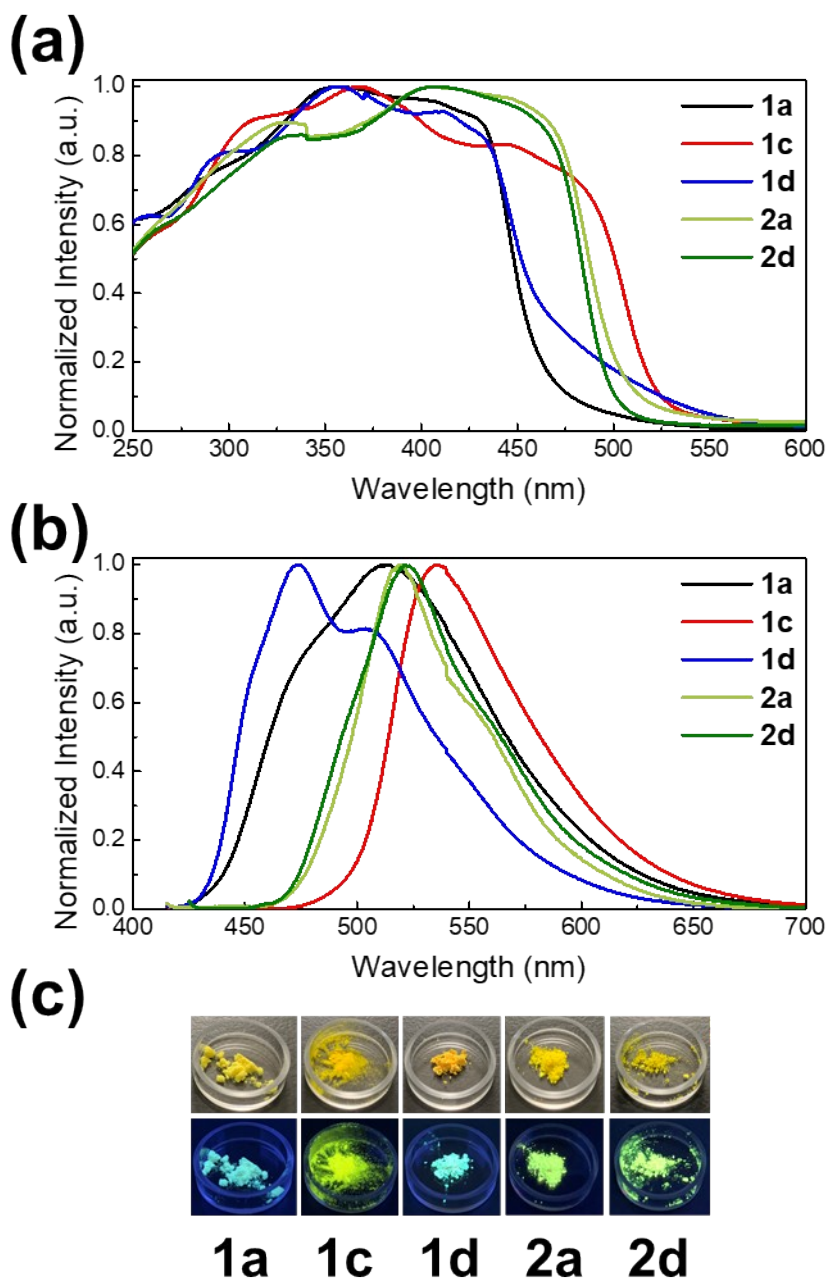


Figure S26-1. Normalized (a) UV-vis diffuse reflectance spectra, (b) emission spectra and (c) photographs under daylight (upper row) and 365 nm UV light irradiation of **1a**, **1c**, **1d**, **2a**, and **2d** in the solid powders.

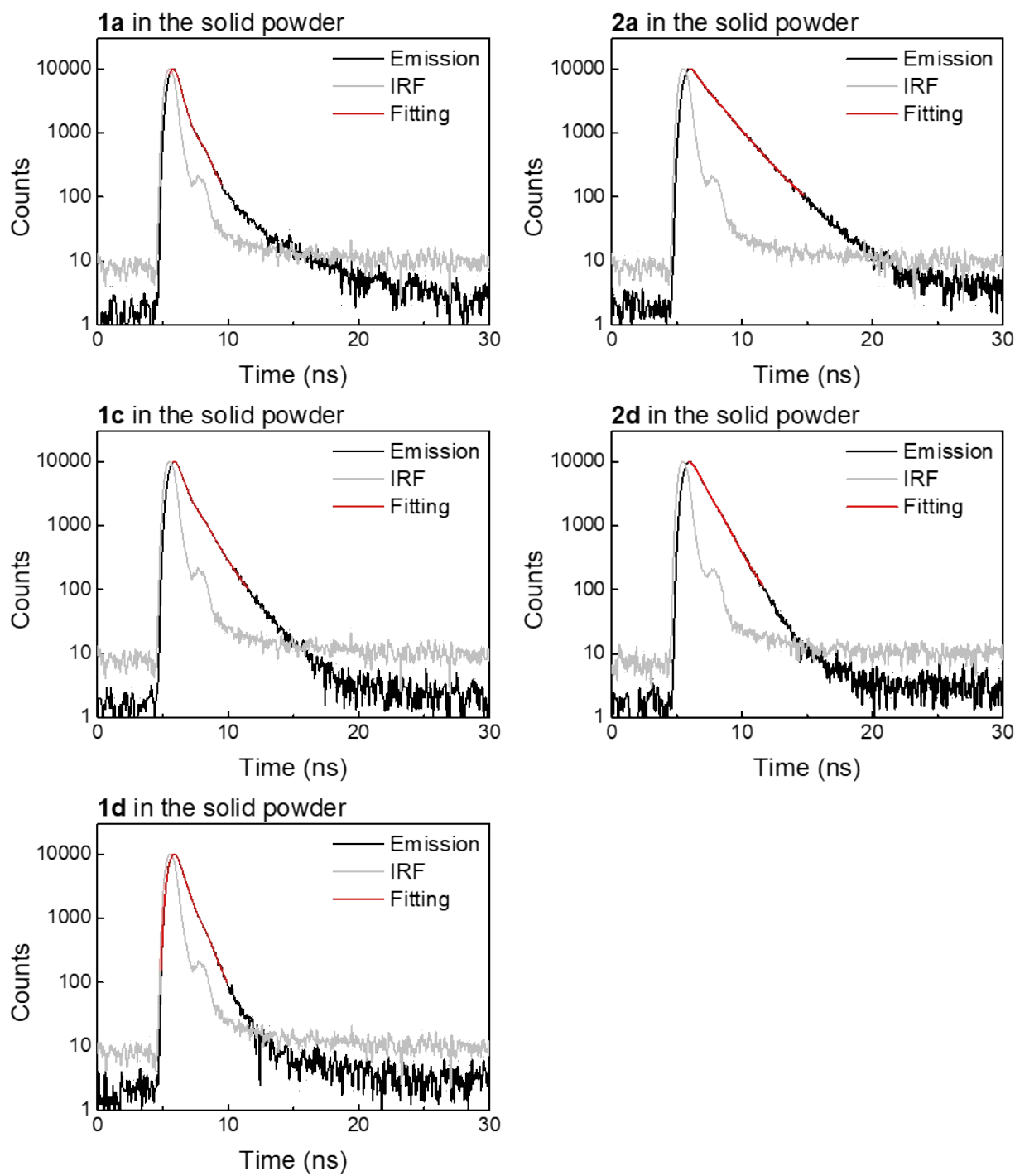


Figure S26-2. Emission decay curves (black line), fits (red line), and instrument response function (IRF) (gray line) of **1a**, **1c**, **1d**, **2a**, and **2d** in the solid powders. Excited at 365 nm and emission wavelength at $\lambda_{\text{em}}^{\text{max}}$.

Table S8. Summary of lifetime analyses for **1a**, **1c**, **1d**, **2a**, and **2d** in the solid powders. Emission lifetimes (τ), pre-exponential factor (A) and intensity average lifetime (τ_{av}).

Compd.	λ_{ex} / nm ^[a]	λ_{em} / nm ^[b]	CHI	τ_{av} / ns	τ_1 / ns	τ_2 / ns	A ₁	A ₂
1a	365	513	1.00	0.50	0.25	0.91	1773.52	307.57
1c	365	535	1.02	0.84	0.36	1.21	1094.28	418.75
1d	365	474	1.02	0.57	0.22	0.70	988.43	813.22
2a	365	519	1.14	1.56	0.51	1.75	404.78	637.74
2d	365	521	1.03	1.04	1.04	—	1038.79	—

[a] Excitation wavelength. [b] Emission wavelength.

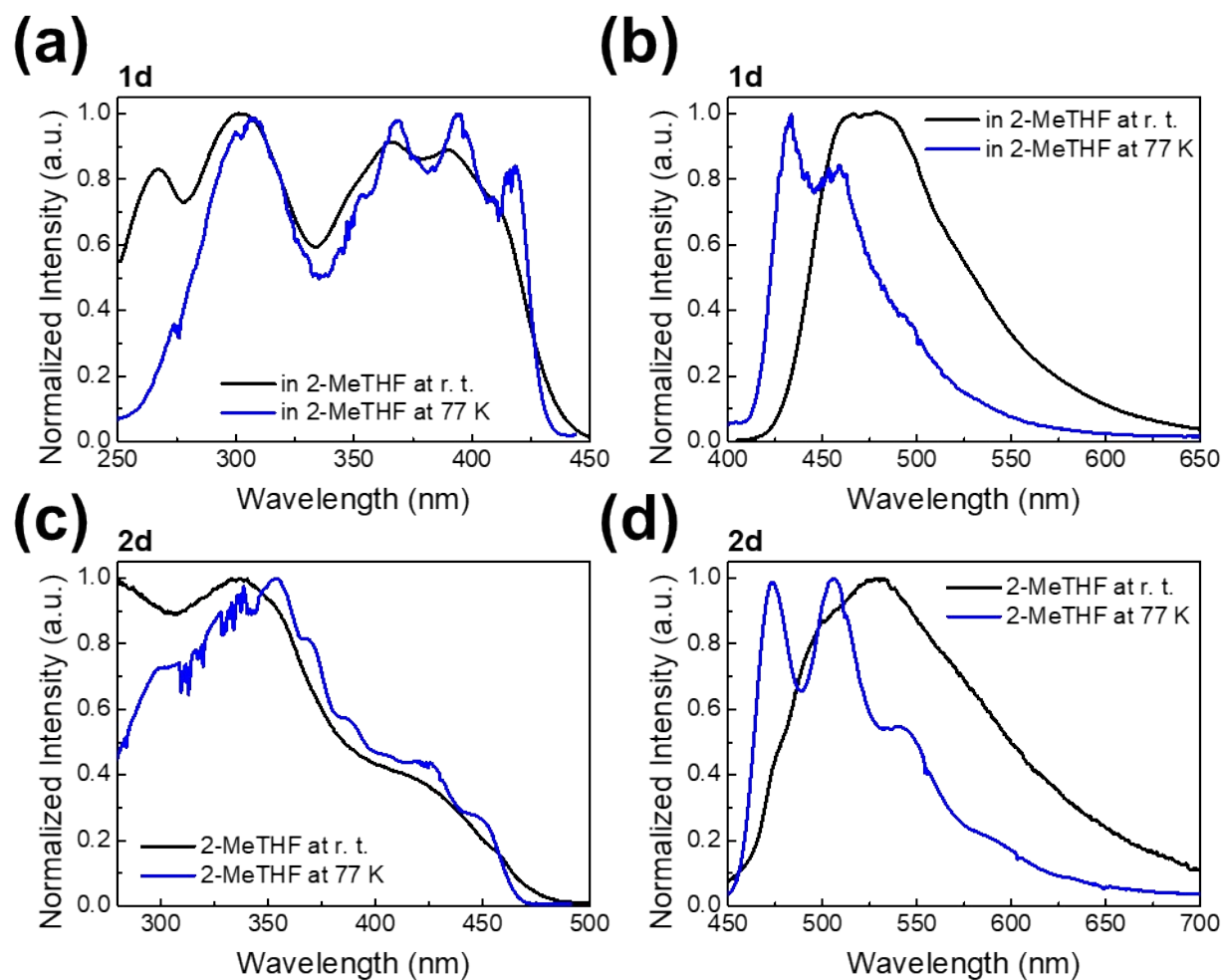


Figure S27-1. Normalized (a, c) excitation spectra and (b, d) emission spectra of **1d** and **2d** in 2-MeTHF ($c = 10^{-6}$ M) at room temperature (r.t.) and 77 K.

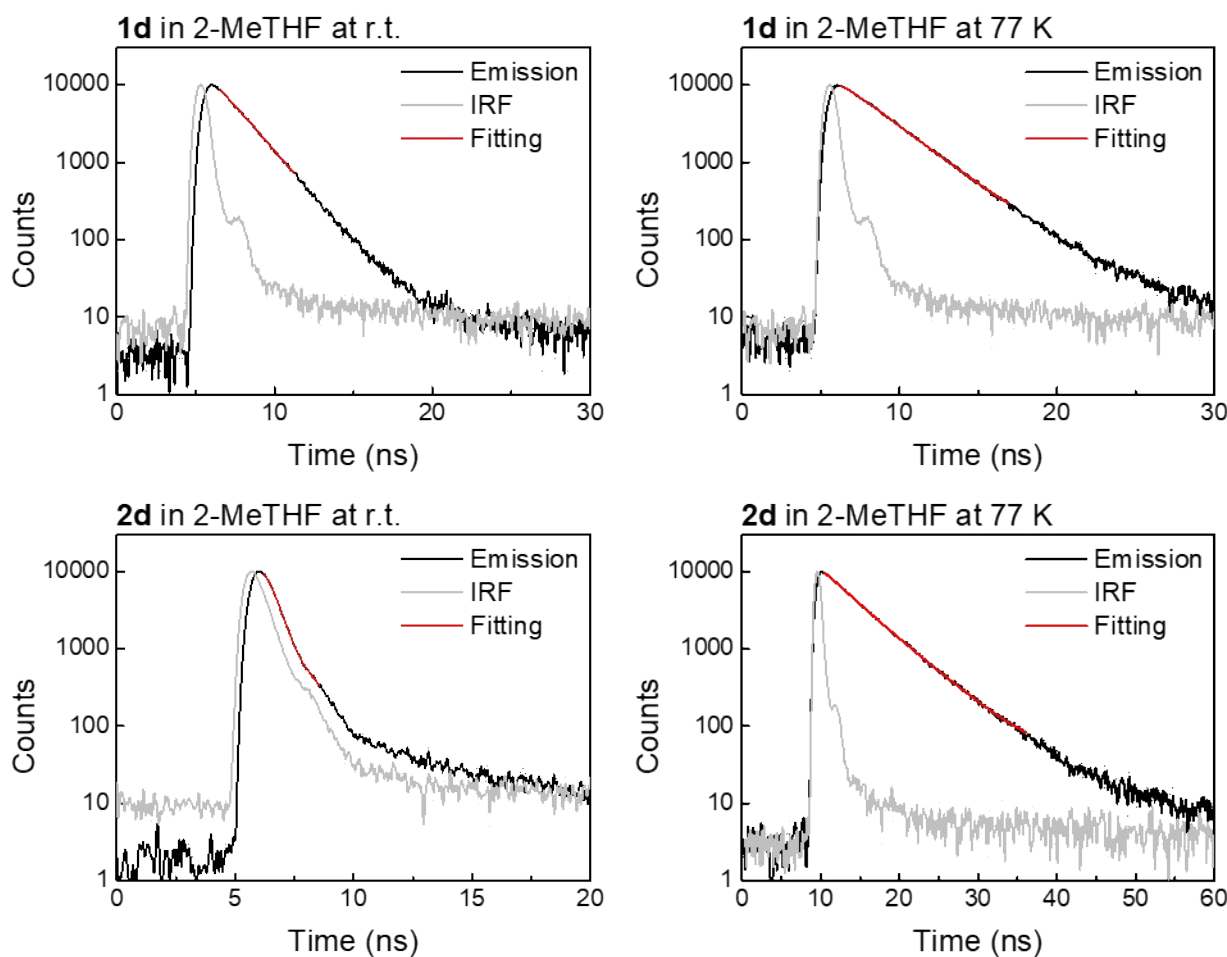


Figure S27-2. Emission decay curves (black line), fits (red line), and instrument response function (IRF) (gray line) of **1d** and **2d** in 2-MeTHF at room temperature (r.t.) and 77 K.

Table S9. Summary of lifetime analyses for **1d** and **2d** in 2-MeTHF at room temperature (r.t.) and 77 K. Emission lifetimes (τ), pre-exponential factor (A) and intensity average lifetime (τ_{av}).

Compd.	Solvent	λ_{ex} / nm ^[a]	λ_{em} / nm ^[b]	CHI	τ_{av} / ns	τ_1 / ns	τ_2 / ns	A ₁	A ₂
1d	2-MeTHF at r.t.	365	473	1.16	1.74	1.74	—	959.67	—
	2-MeTHF at 77 K	365	459	1.15	2.77	2.77	—	746.96	—
2d	2-MeTHF at r.t.	340	530	1.03	0.28	0.28	—	2563.06	—
	2-MeTHF at 77 K	365	474	1.03	4.71	2.16	4.96	241.61	1075.68

[a] Excitation wavelength. [b] Emission wavelength.

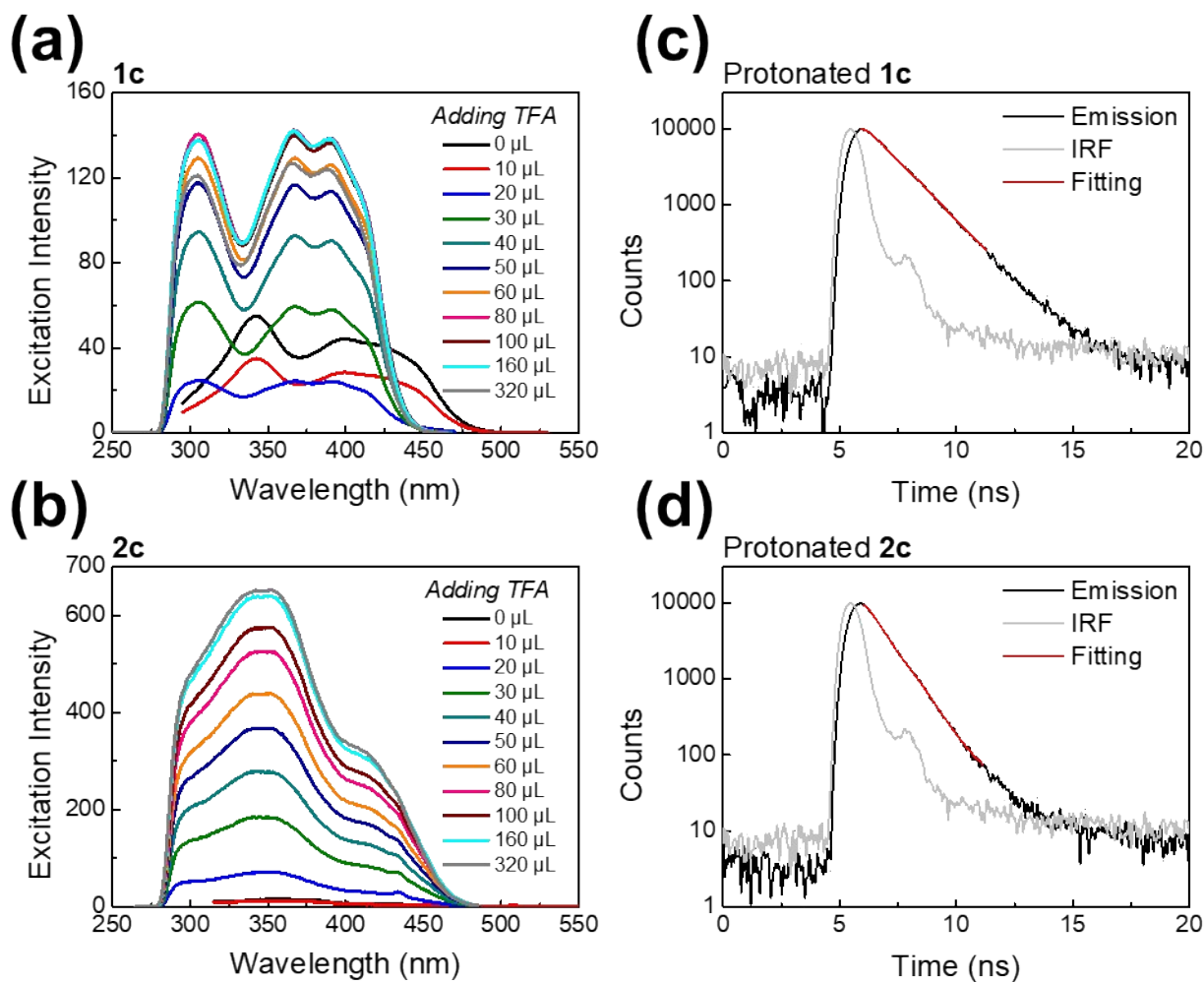


Figure S28. (a, b) Excitation spectra of **1c** and **2c** in toluene (3 mL, 10^{-6} M) upon protonation by adding various amounts of TFA, emission wavelength at λ_{em}^{max} for **1c** and 500 nm for **2c**. (c, d) Emission decay curves (black line), fits (red line), and instrument response function (IRF) (gray line) of protonated **1c** and **2c** in toluene. Excited at 365 nm and emission wavelength at λ_{em}^{max} .

Table S10. Summary of lifetime analyses for protonated **1c** and **2c** in toluene upon protonation. Emission lifetimes (τ), pre-exponential factor (A) and intensity average lifetime (τ_{av}).

Compd.	λ_{ex} / nm ^[a]	λ_{em} / nm ^[b]	CHI	τ_{av} / ns	τ_1 / ns	τ_2 / ns	A ₁	A ₂
protonated 1c	365	457	1.10	1.25	1.25	—	967.24	—
protonated 2c	365	515	1.09	0.83	0.83	—	1123.97	—

[a] Excitation wavelength. [b] Emission wavelength.

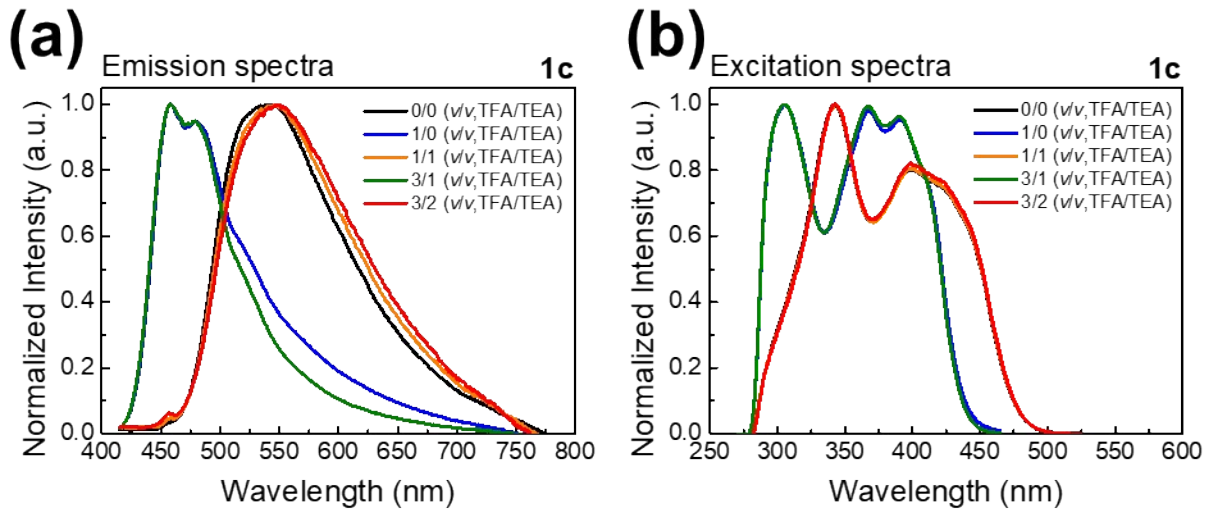
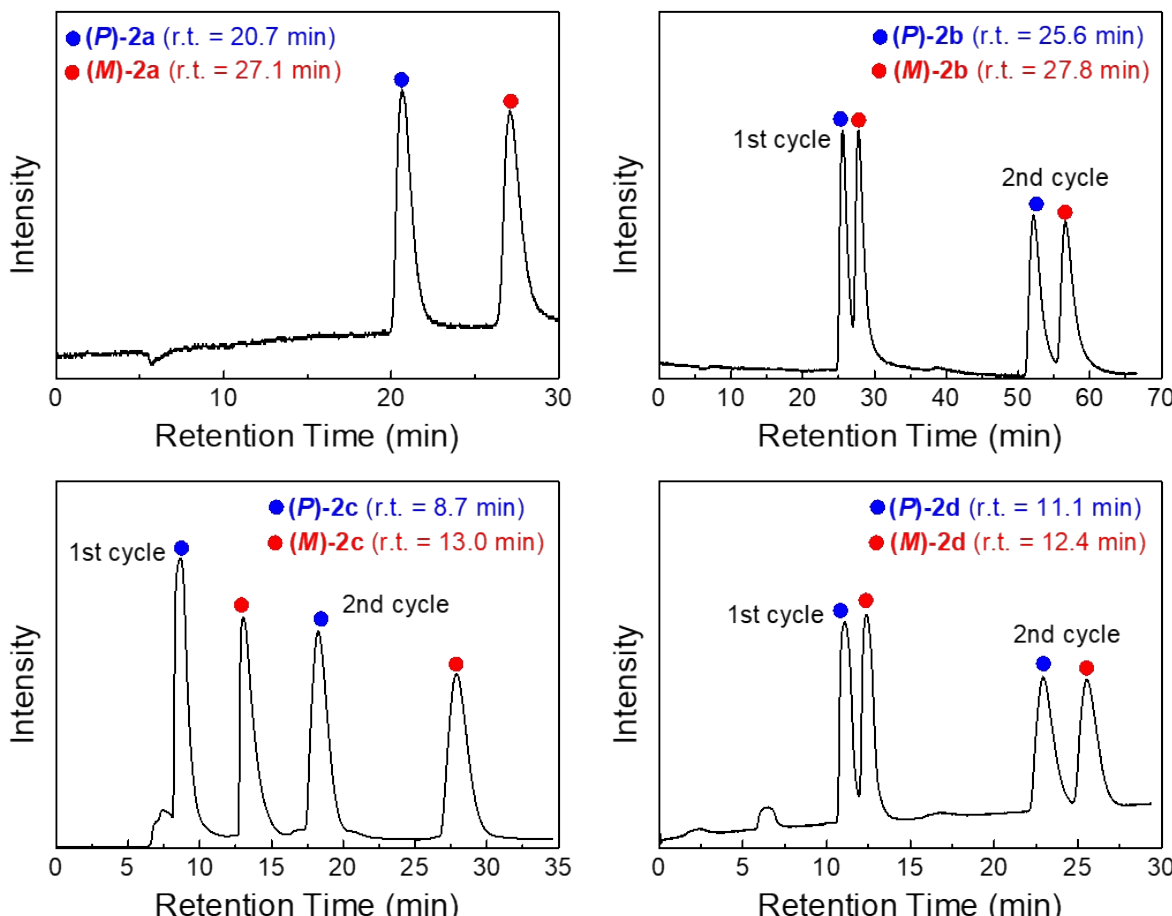


Figure S29. Normalized (a) emission spectra (excited at 400 nm) and (b) excitation spectra (emission wavelength at λ_{em}^{max}) of **1c** in toluene (3 mL, $c = 10^{-6}$ M) upon protonation by TFA and deprotonation by TEA. The added 1/1 (v/v) of TFA/TEA denoted as 20 μ L/20 μ L.

Optical resolution by Recycling Preparative Chiral HPLC

Optical resolution was performed using LaboACE LC-5060 instrument with UV detector (UV-4ch 400 LA) by Japan Analytical Industry Co., Ltd. equipped with a CHIRALPAK® ID (Particle Size:



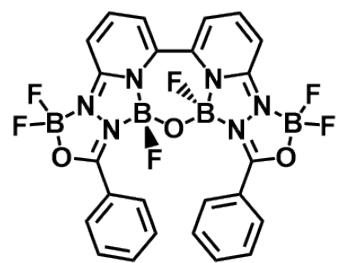
5 μ m; Dimensions: 20mm Ø × 250mm L).

Figure S30. Chiral HPLC profile for the separation of enantiomers of **2a–2d**. Frac.1 (blue) = (**P**)-enantiomer, Frac. 2 (red) = (**P**)-enantiomer.

Table S11. Chiral HPLC conditions for the separation of enantiomers of **2a–2d**.

Compd.	Chiral column ^[a]	Eluent (v / v)	Flow rate / mL min ⁻¹	λ / nm of UV detection
2a	CHIRALPAK® ID	ethyl acetate / hexane (3 / 7)	10	400
2b	CHIRALPAK® ID	ethyl acetate / hexane (3 / 7)	10	400
2c	CHIRALPAK® ID	CH ₂ Cl ₂ / hexane (9 / 1)	10	400
2d	CHIRALPAK® ID	CH ₂ Cl ₂ / hexane (8 / 2)	10	400

[a] For CHIRALPAK® ID: Particle Size: 5 μ m; Dimensions: 20mm Ø × 250mm L



2a

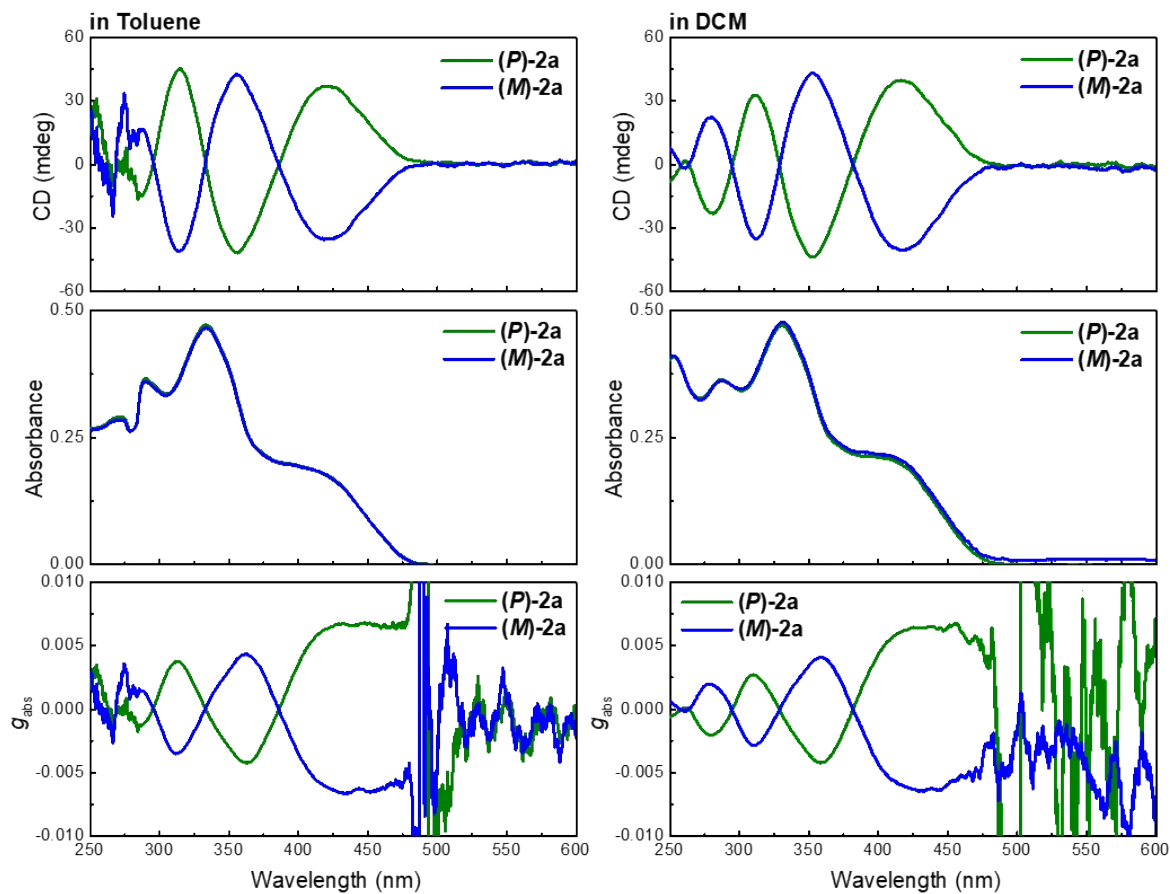
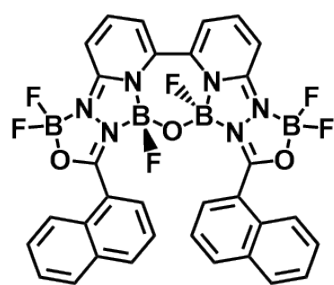


Figure S31. CD, absorption, and g_{abs} spectra of **(P)-2a** (green) and **(M)-2a** (blue) in toluene (left) and DCM (right) ($c = 10^{-6}$ M).



2b

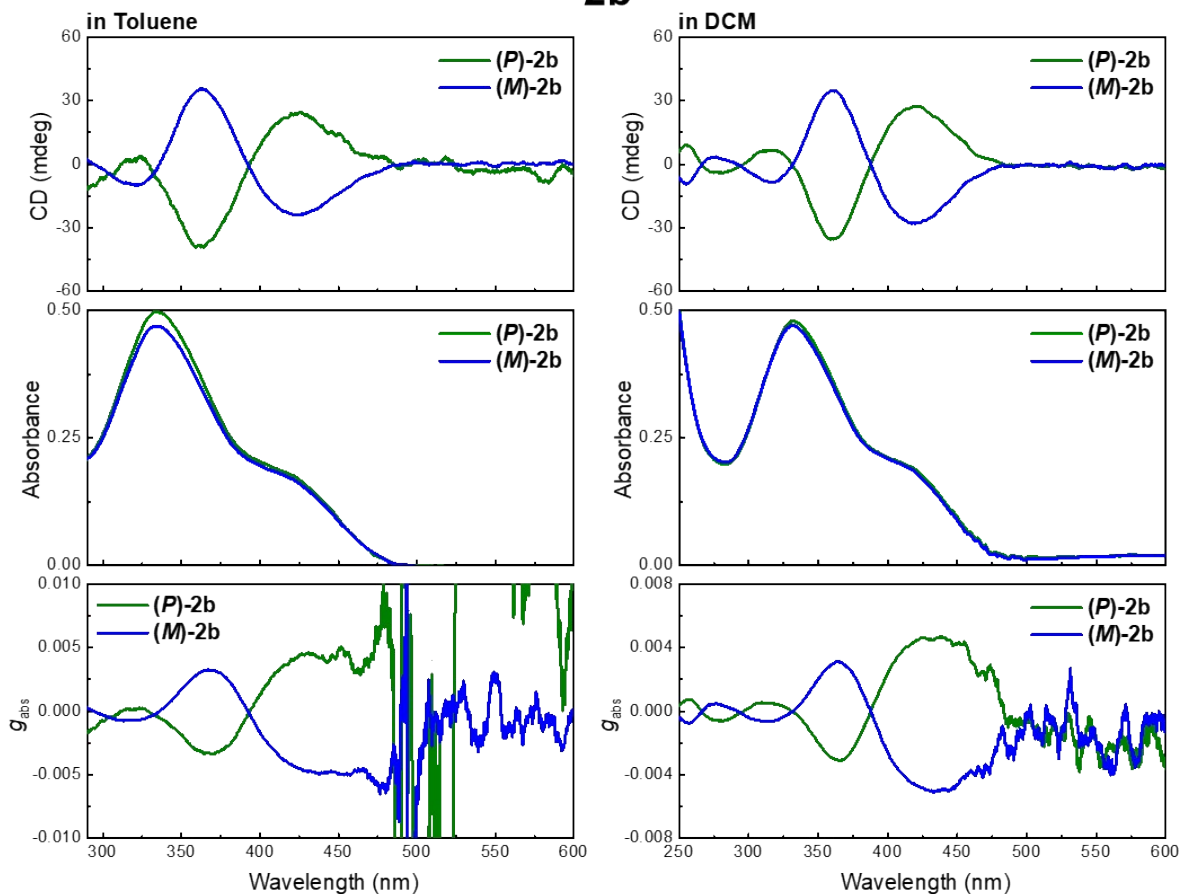


Figure S32. CD, absorption, and g_{abs} spectra of **(P)-2b** (green) and **(M)-2b** (blue) in toluene (left) and DCM (right) ($c = 10^{-6}$ M).

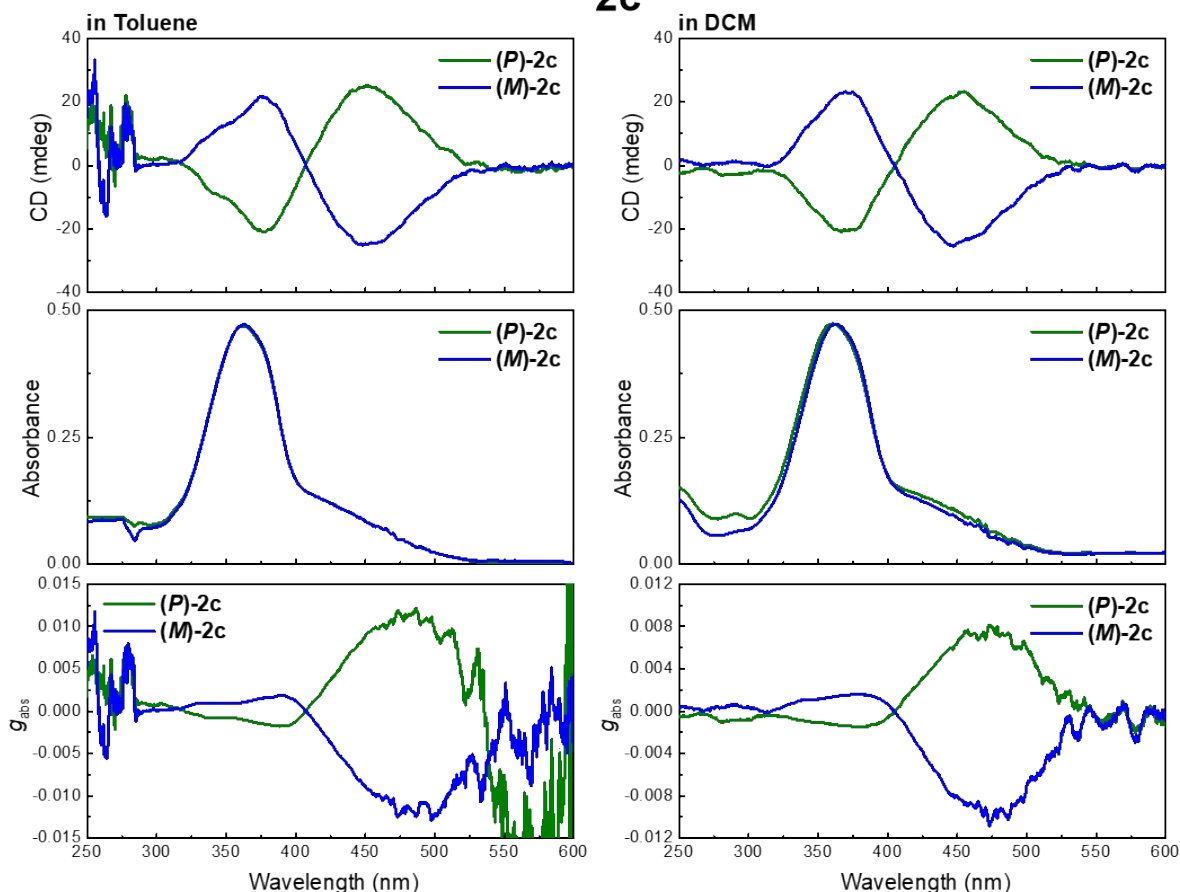
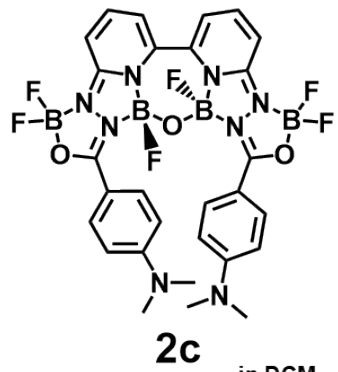
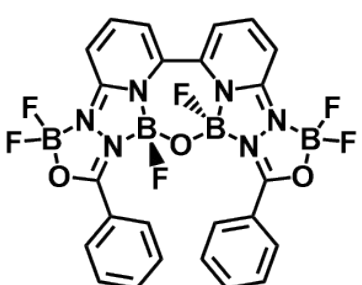
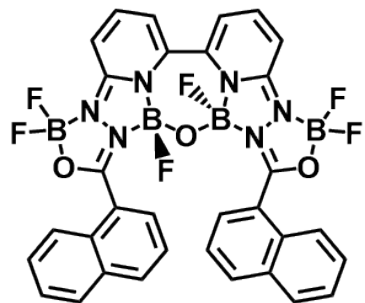


Figure S33. CD, absorption, and g_{abs} spectra of **(P)-2c** (green) and **(M)-2c** (blue) in toluene (left) and DCM (right) ($c = 10^{-6}$ M).



2a



2b

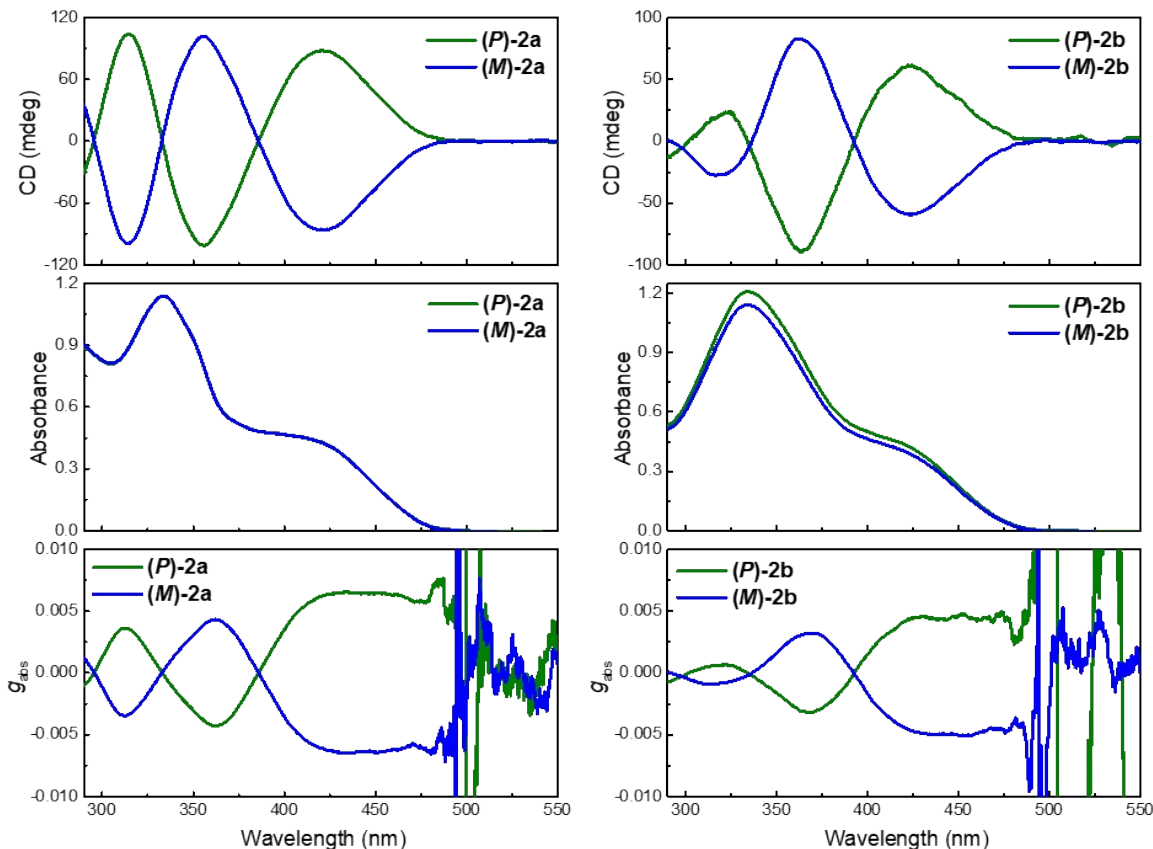


Figure S34-1. (Left) CD, absorption, and g_{abs} spectra of (P) -2a (green) and (M) -2a (blue) in toluene ($c = 10^{-5}$ M). (Right) CD, absorption, and g_{abs} spectra of (P) -2b (green) and (M) -2b (blue) in toluene ($c = 10^{-5}$ M).

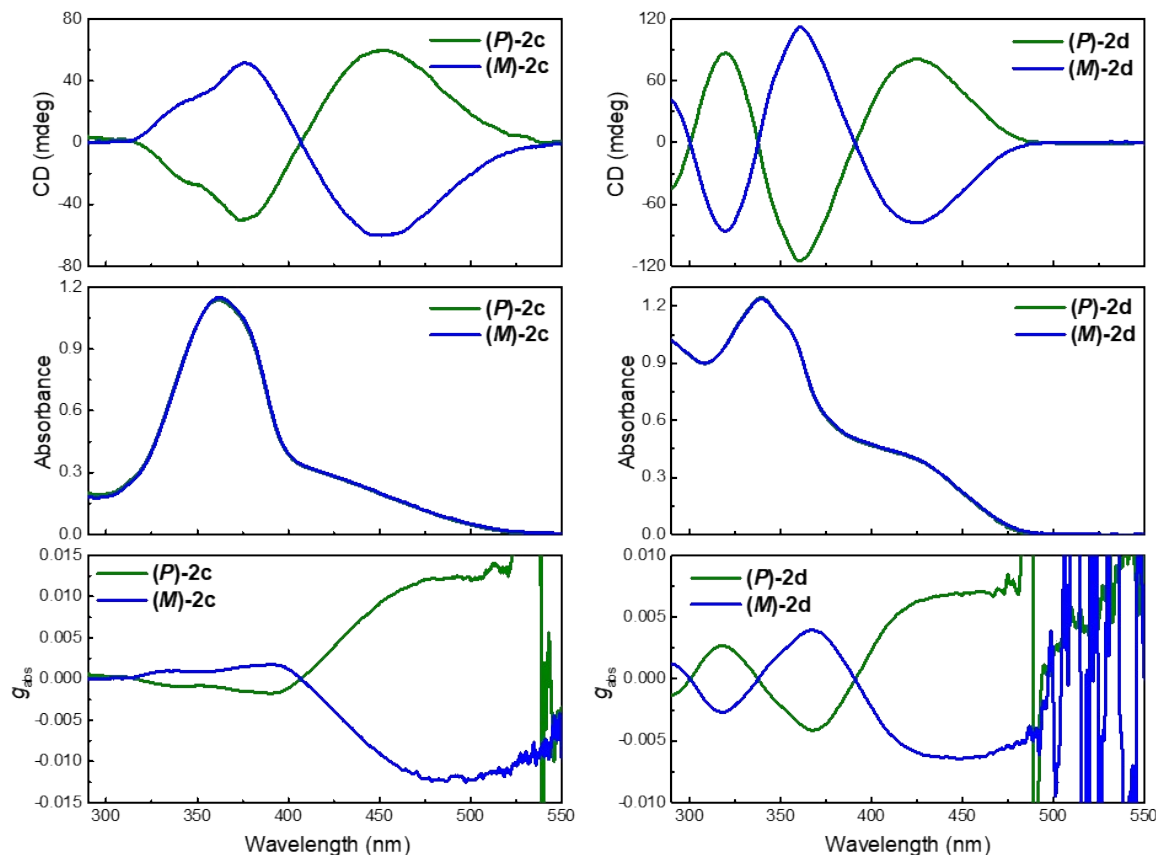
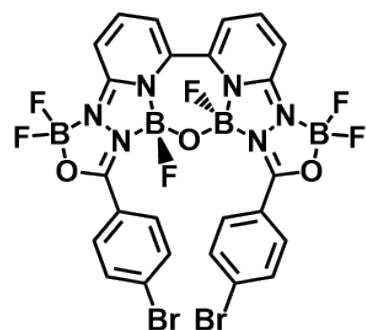
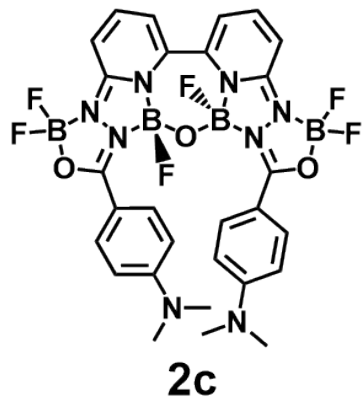


Figure S34-2. (Left) CD, absorption, and g_{abs} spectra of **(P)-2c** (green) and **(M)-2c** (blue) in toluene ($c = 10^{-5}$ M). (Right) CD, absorption, and g_{abs} spectra of **(P)-2d** (green) and **(M)-2d** (blue) in toluene ($c = 10^{-5}$ M).

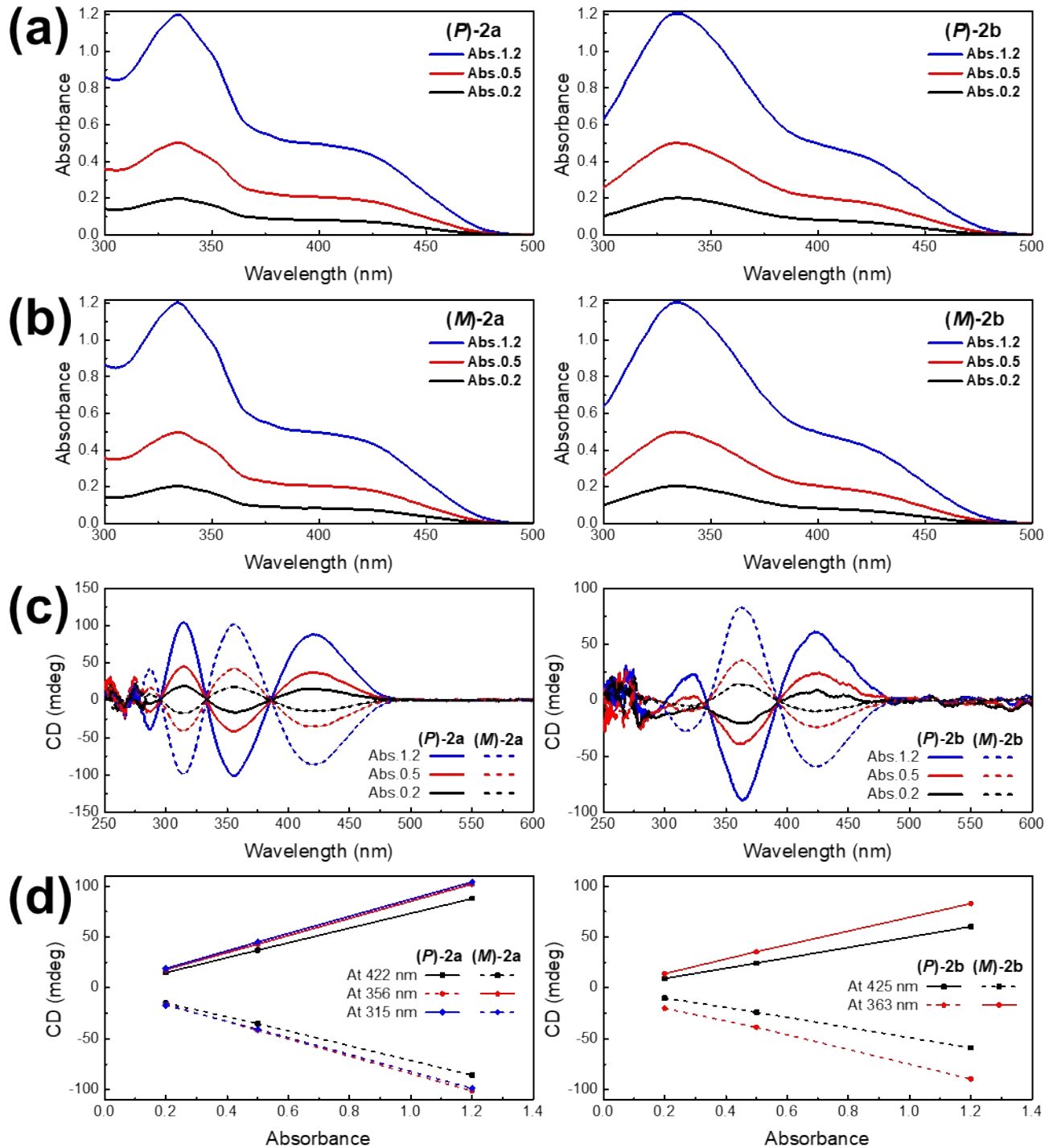


Figure S35-1. Concentration-dependent UV-vis absorption and CD spectra of **(P)/(M)-2a** and **(P)/(M)-2b** in toluene at 25 °C. (a, b) UV-vis absorption spectra at maximum absorbance of 0.2, 0.5, 1.2, and their (c) CD spectra. (d) A linear correlation between absorbance and ellipticity at different wavelengths in toluene. The optical path length of CD cell is 1 cm.

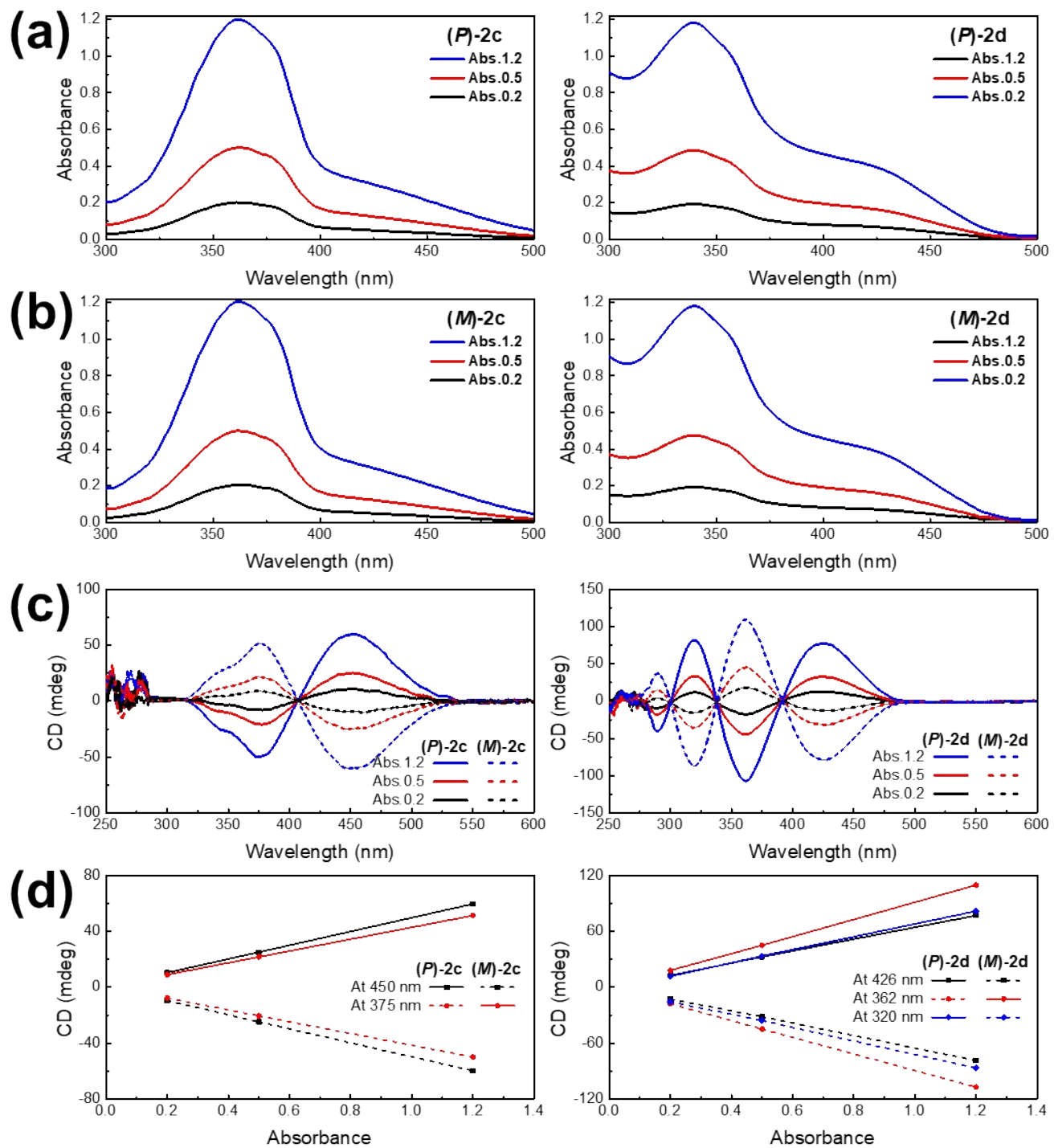


Figure S35-2. Concentration-dependent UV-vis absorption and CD spectra of **(P)/(M)-2c** and **(P)/(M)-2d** in toluene at 25 °C. (a, b) UV-vis absorption spectra at maximum absorbance of 0.2, 0.5, 1.2, and their (c) CD spectra. (d) A linear correlation between absorbance and ellipticity at different wavelengths in toluene. The optical path length of CD cell is 1 cm.

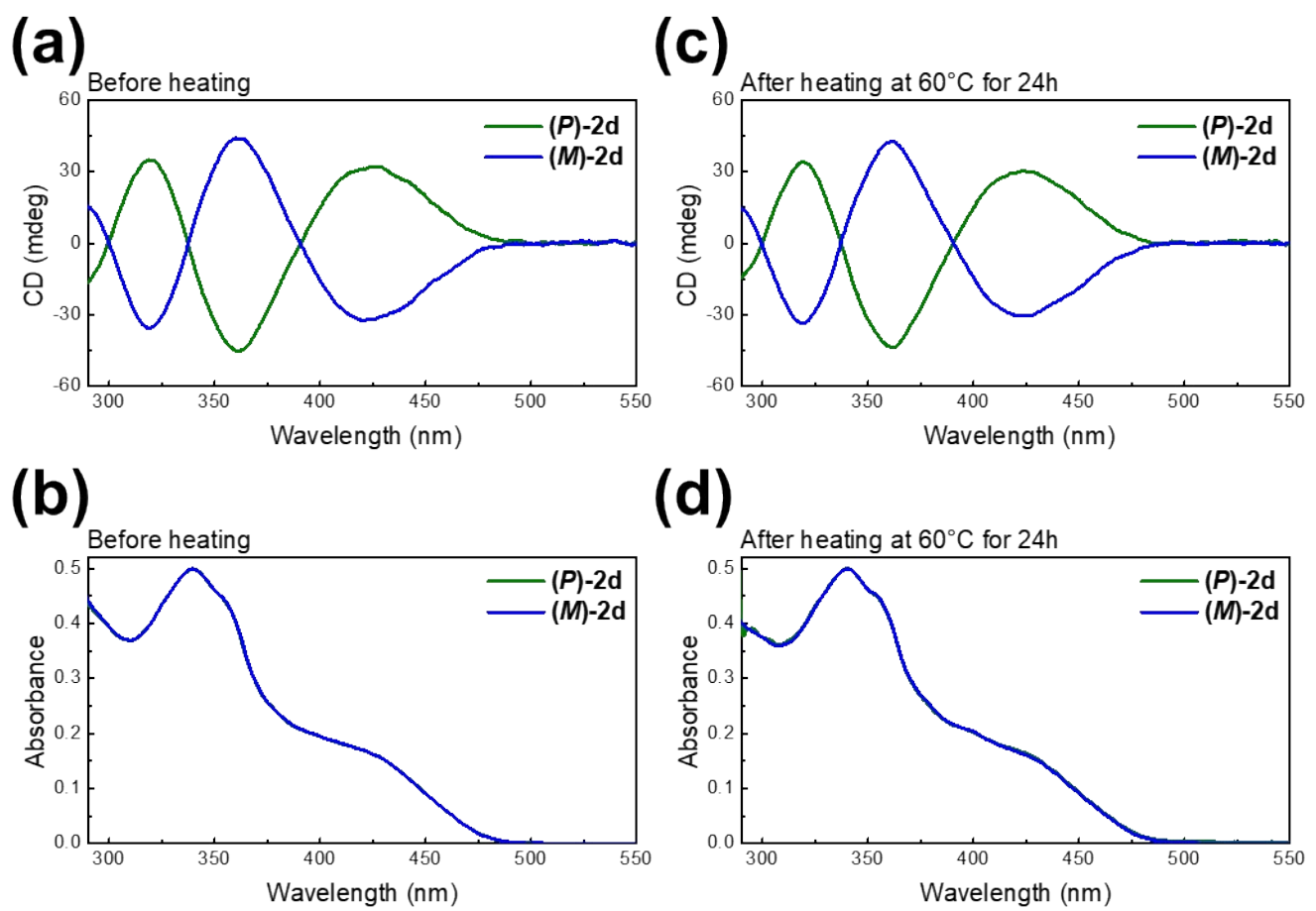


Figure S36. (a) CD and (b) UV-vis absorption spectra of **(P)-2d** and **(M)-2d** in toluene at 25 °C. (c) CD and (d) UV-vis absorption spectra of **(P)-2d** and **(M)-2d** after heating at 60°C for 24 h in toluene.

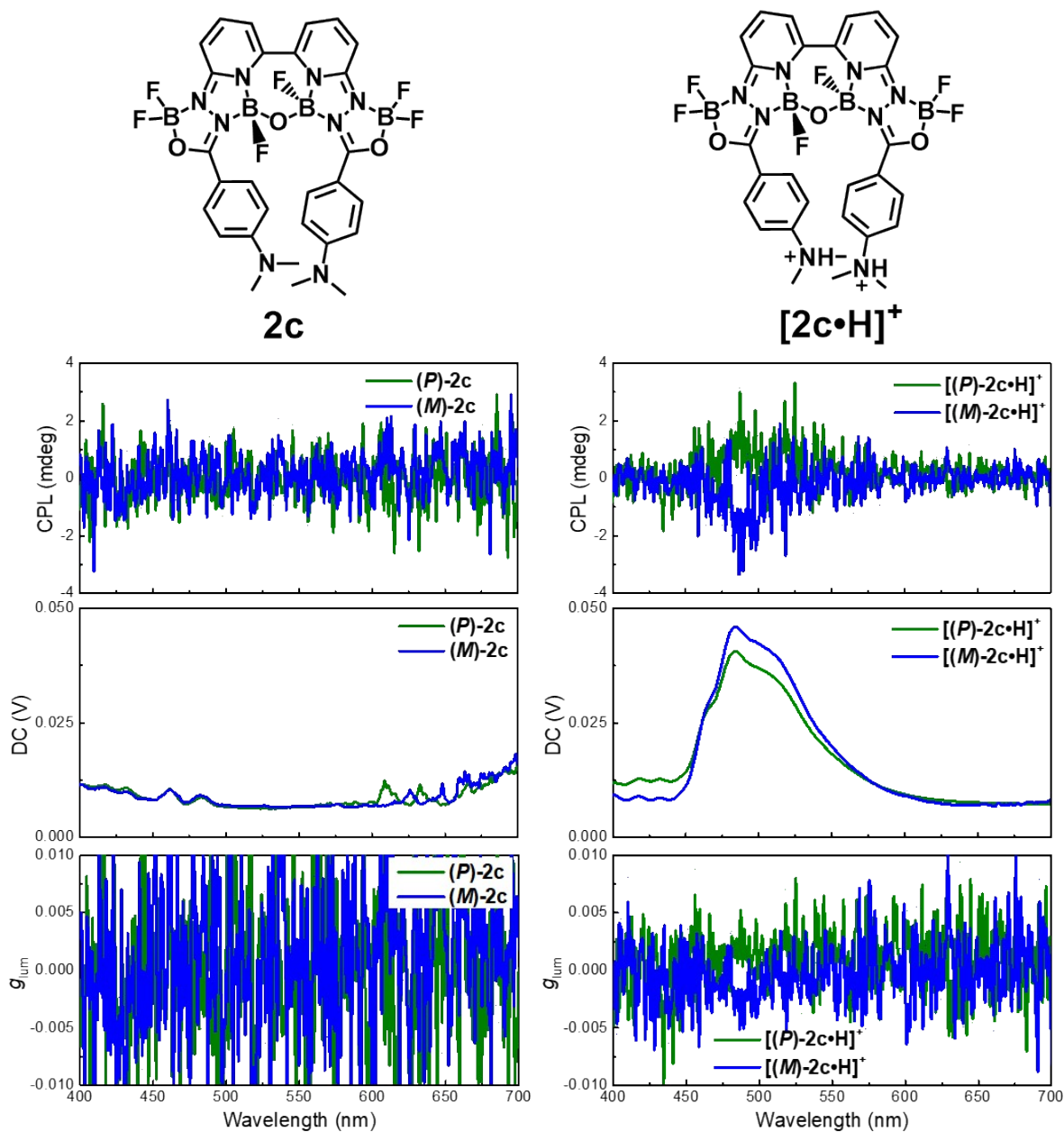
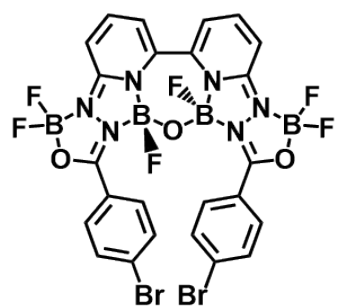


Figure S37. (Left) CPL, DC (nonpolarized fluorescence) and g_{lum} spectra of **(P)-2c** (green) and **(M)-2c** (blue) in toluene ($c = 10^{-6}$ M). (Right) CPL, DC (nonpolarized fluorescence) and g_{lum} spectra of $[(P)\text{-}2\text{c}\cdot\text{H}]^+$ (green) and $[(M)\text{-}2\text{c}\cdot\text{H}]^+$ (blue) in toluene (3 mL, 10^{-6} M) upon protonation by adding 100 μ L TFA. Excited at 330 nm.



2d

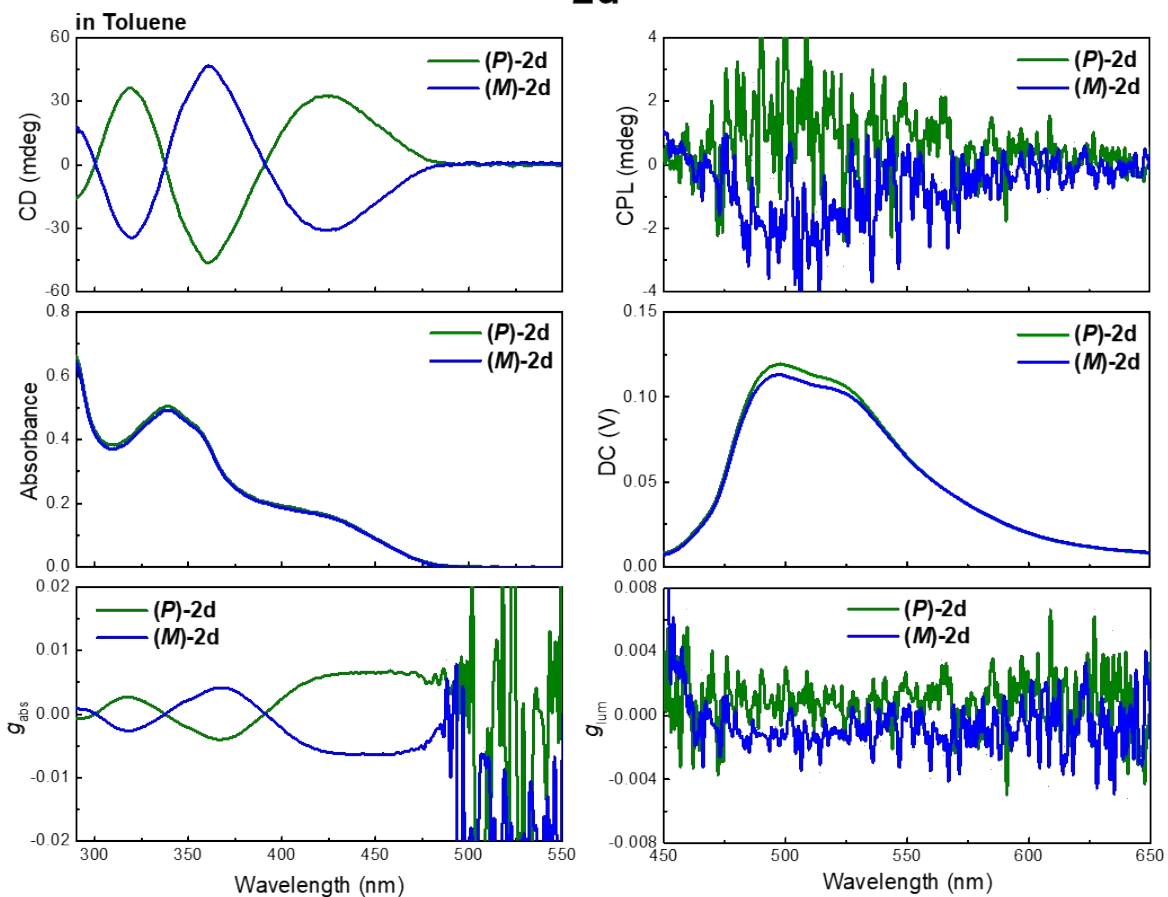


Figure S38. (Left) CD, absorption, and g_{abs} spectra of **(P)-2d** (green) and **(M)-2d** (blue) in toluene ($c = 10^{-6}$ M). (Right) CPL, DC (nonpolarized fluorescence) and g_{lum} spectra of **(P)-2d** (green) and **(M)-2d** (blue) in toluene ($c = 10^{-6}$ M). Excited at 330 nm.

Preparation of **1b**-doped polymer films

The **1b**-doped polymer films were prepared using poly (methyl methacrylate) (PMMA, SigmaAldrich, Mw ~120,000) as the inert matrix. 300 μ L of toluene solution of (*P*)/(*M*)-**1b** adjusted to a maximum absorbance of 1.2 ($c = 4.15 \times 10^{-5}$ mol/L) was mixed with 300 μ L of toluene solution of PMMA (0.1 g/mL). A 100 μ L of the mixture was cast onto a quartz substrate (1 cm \times 1 cm), air-dried, and vacuumed for 3 hours to obtain the hybrid PMMA films.

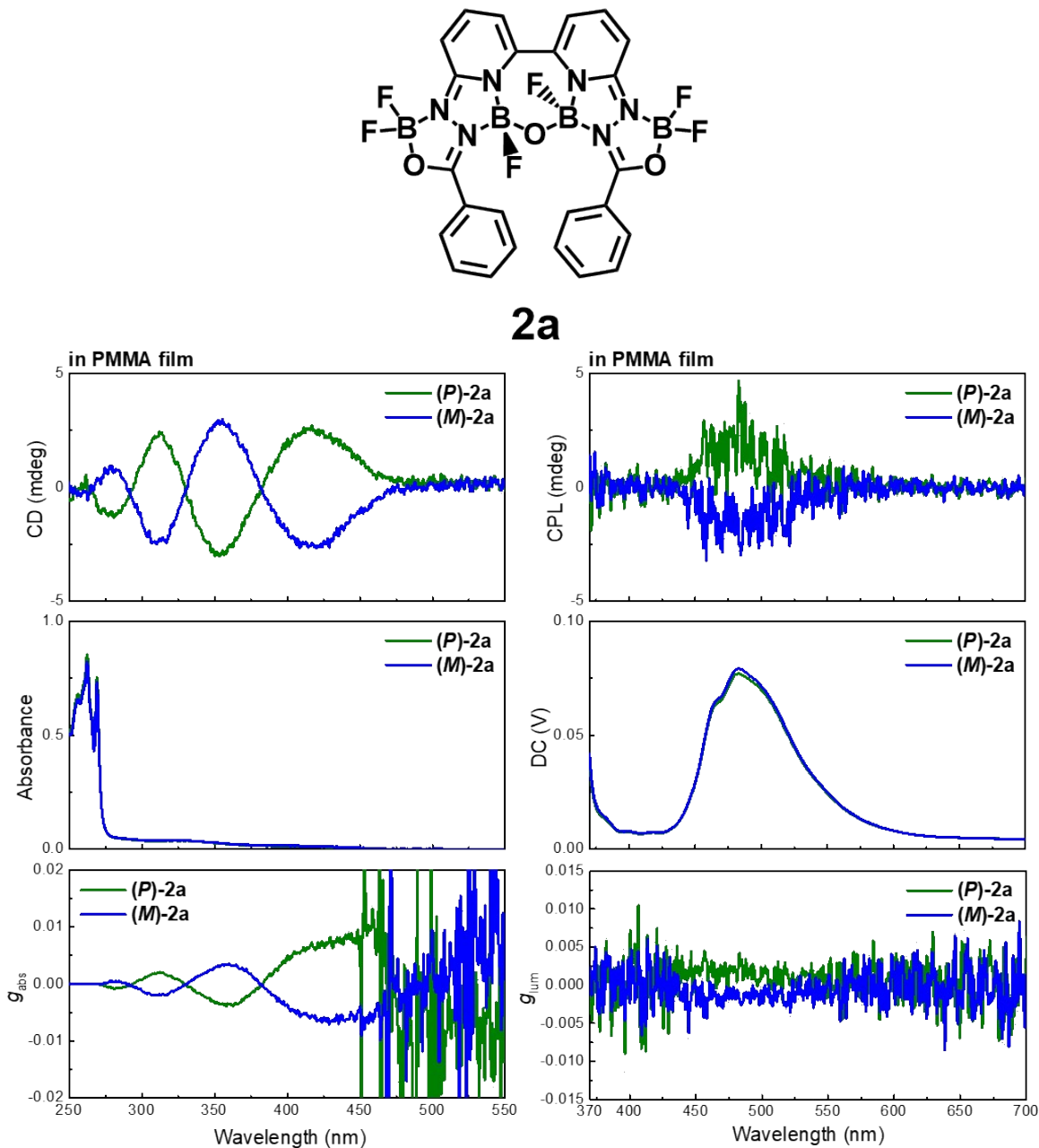


Figure S39. (Left) CD, absorption, and g_{abs} spectra of (*P*)-**2a** (green) and (*M*)-**2a** (blue) in PMMA film. (Right) CPL, DC (nonpolarized fluorescence) and g_{lum} spectra of (*P*)-**2a** (green) and (*M*)-**2a** (blue) in PMMA film. Excited at 330 nm.

Density-Functional Theory Calculations.

Theoretical calculations were performed using Gaussian 16, revision A.03. Ground state (S_0) geometries were optimized by density-functional theory (DFT) level with the B3LYP/6-31G(d,p) level. Equilibrium geometries were verified via frequency calculation, where no imaginary frequency was found. TD-DFT calculations were performed using TD-cam-B3LYP/6-31G(d,p) level for the first 30 singlet–singlet transitions with an additional keyword of IOP(9/40=2). First singlet excited state (S_1) geometries were optimized using cam-B3LYP/6-31G(d,p) level. DFT data were visualized and analyzed with Chemcraft or GaussView 6.0.

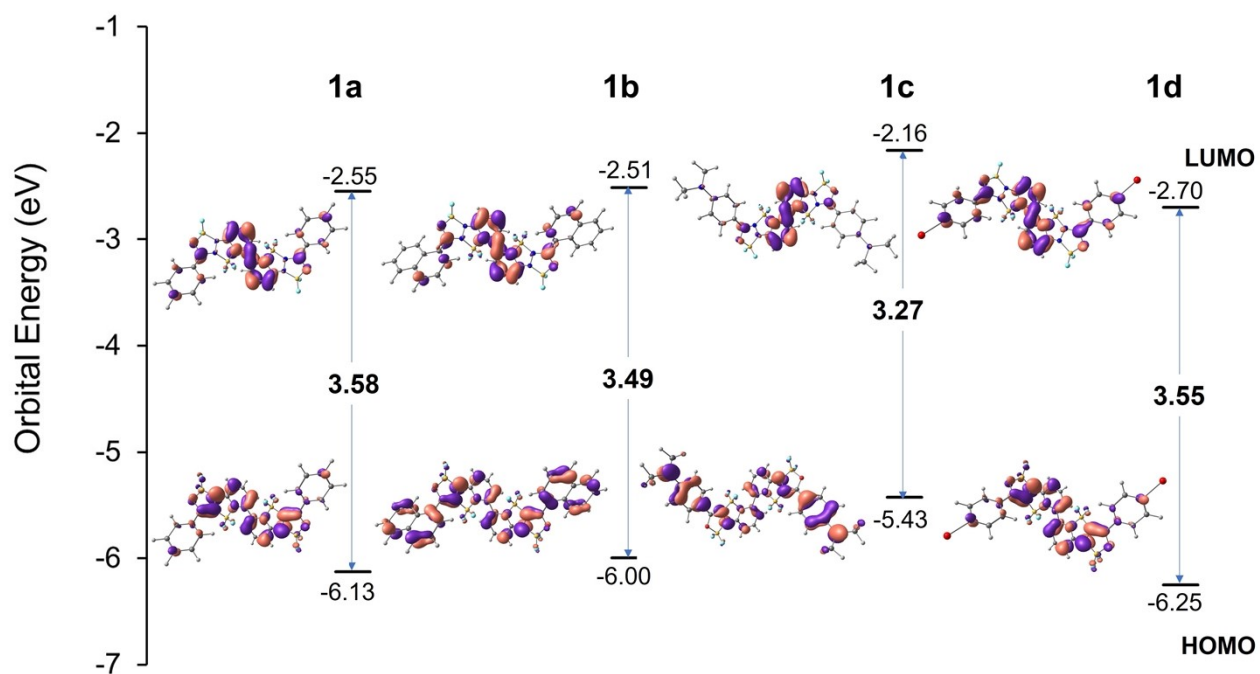


Figure S40-1. Frontier molecular orbitals of **1a–1d**.

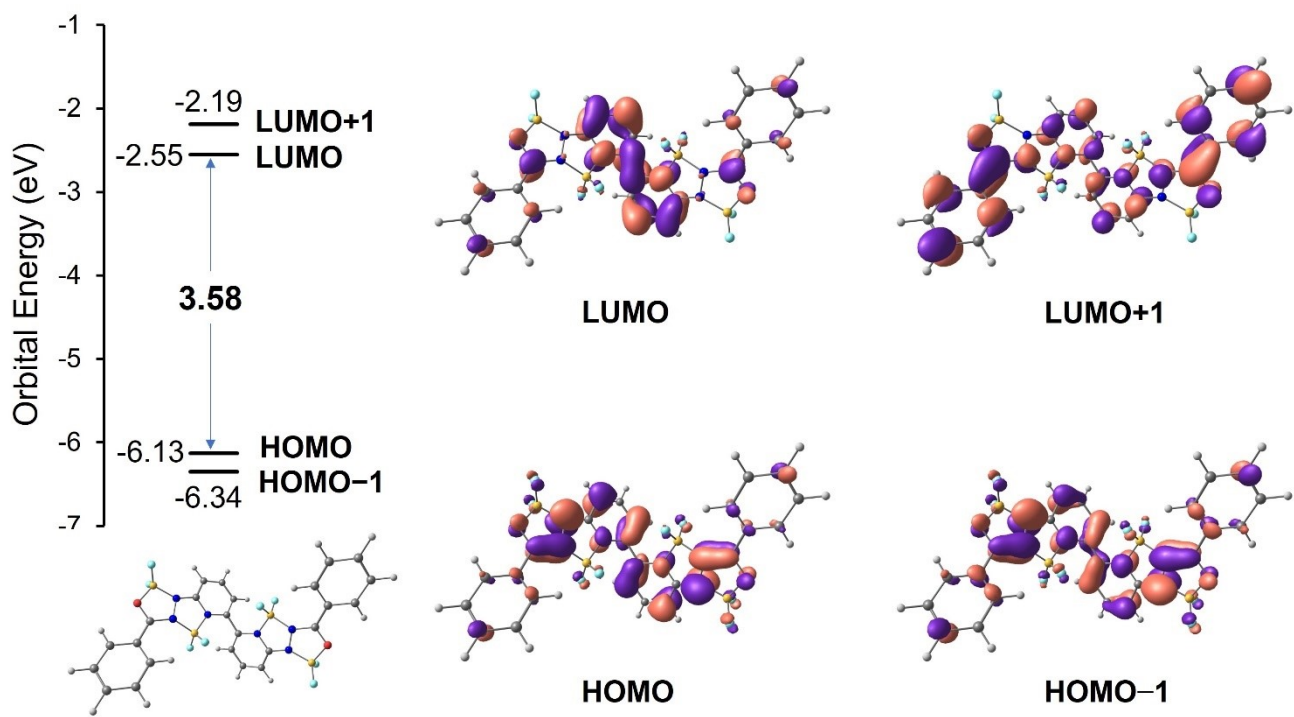


Figure S40-2. Frontier molecular orbitals of **1a**.

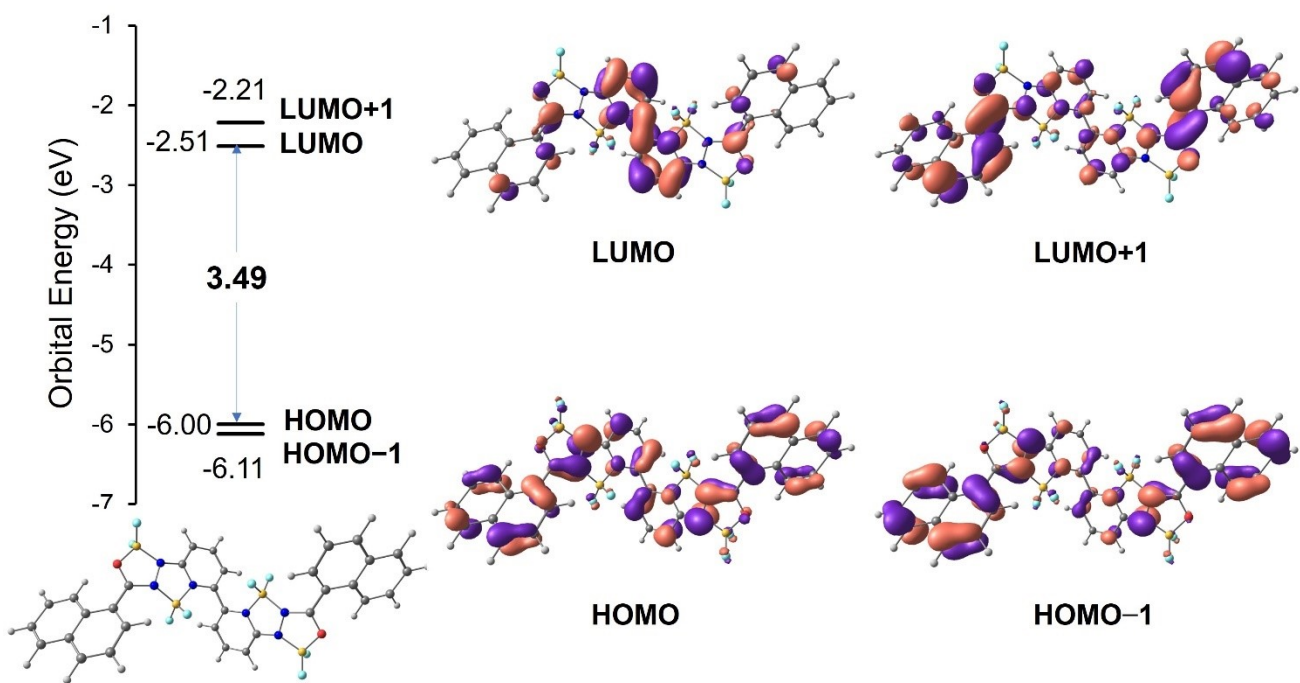


Figure S40-3. Frontier molecular orbitals of **1b**.

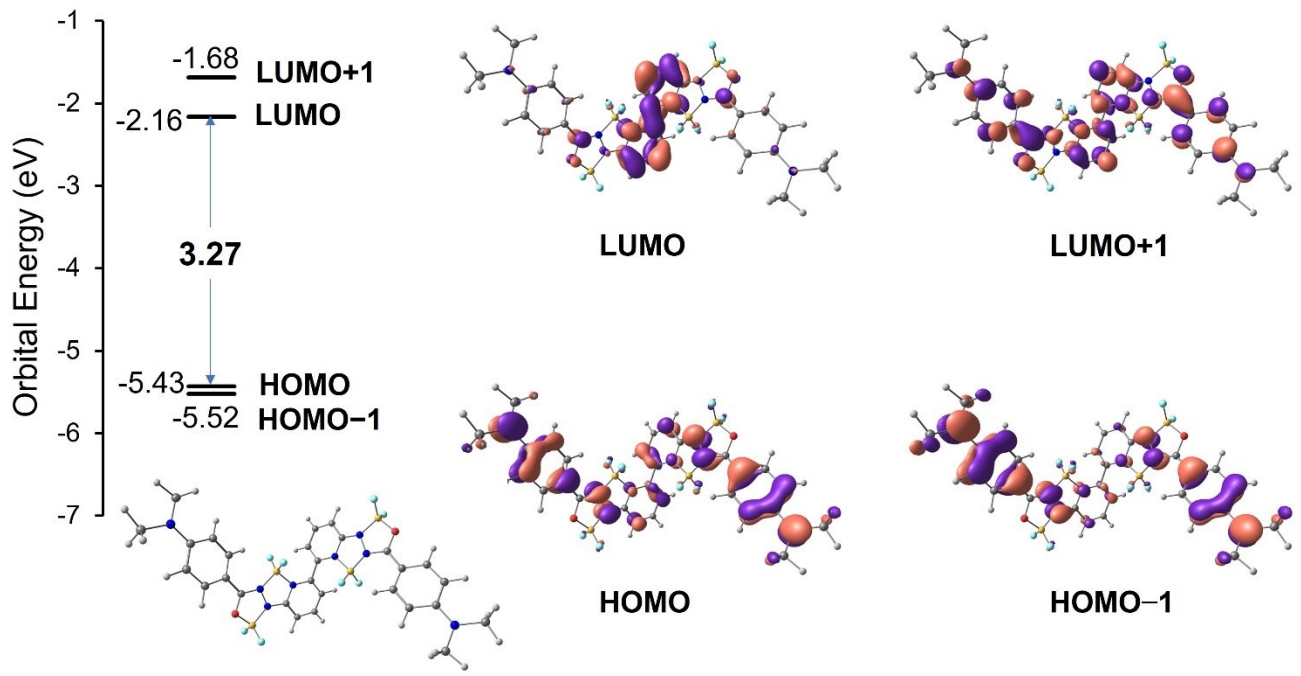


Figure S40-4. Frontier molecular orbitals of **1c**.

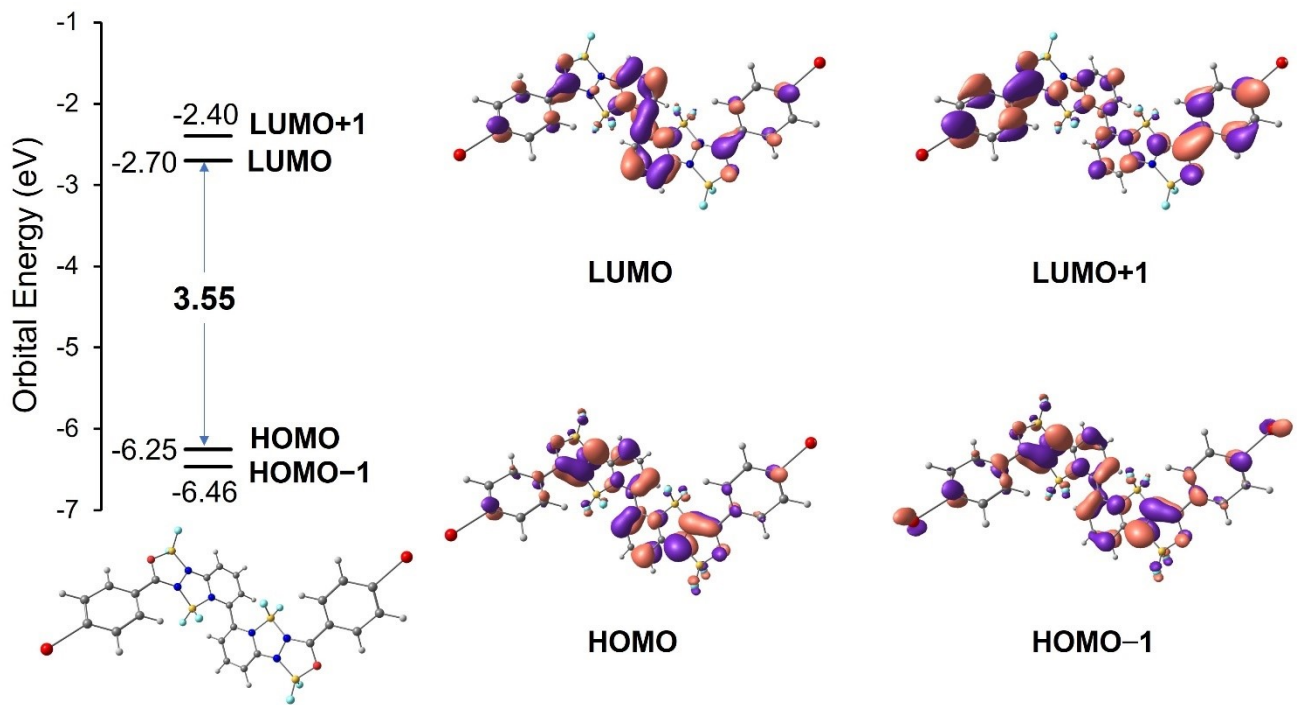


Figure S40-5. Frontier molecular orbitals of **1d**.

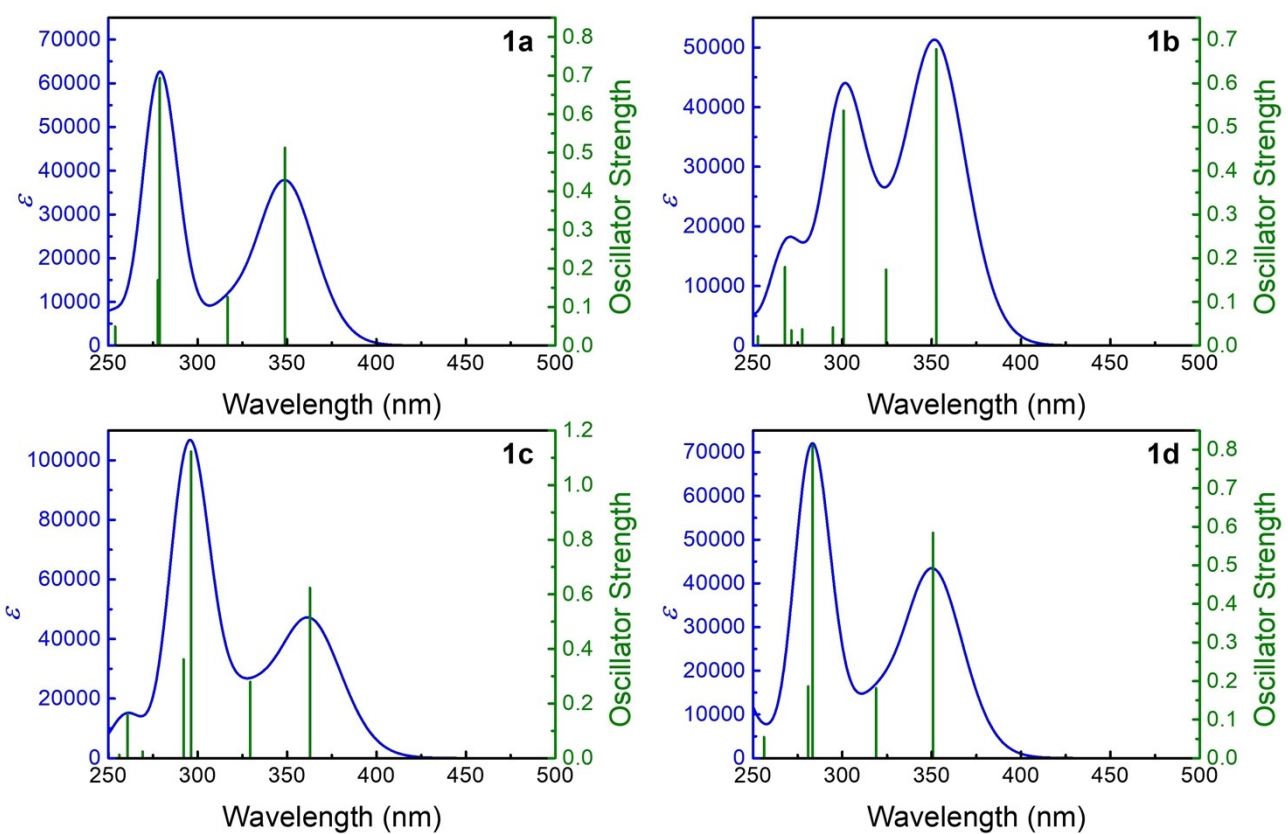


Figure S41. Calculated UV-vis absorption spectra of **1a–1d** by TD-DFT method.

Table S12. Calculated photophysical property data of the ground state for **1a–1d** at the cam-B3LYP/6-31G(d,p) level.

	Electronic Transition	TD//cam-B3LYP/6-31G(d,p)			
		Energy/eV ^a	f ^b	Major contributions	
1a	S ₀ →S ₁	3.5537 eV	348.88 nm	0.5130	H-1->L+1 (15%), HOMO->LUMO (79%)
	S ₀ →S ₂	3.9143 eV	316.75 nm	0.1263	H-1->LUMO (62%), HOMO->L+1 (30%)
	S ₀ →S ₃	4.4461 eV	278.86 nm	0.6939	H-1->L+1 (30%), HOMO->L+2 (57%)
	S ₀ →S ₄	4.4626 eV	277.83 nm	0.1702	H-1->LUMO (14%), H-1->L+2 (41%), HOMO->L+1 (37%)
1b	S ₀ →S ₁	3.5167 eV	352.56 nm	0.6782	H-1->L+1 (16%), HOMO->LUMO (64%)
	S ₀ →S ₂	3.8207 eV	324.51 nm	0.1737	H-1->LUMO (44%), HOMO->L+1 (36%)
	S ₀ →S ₃	4.1232 eV	300.70 nm	0.5374	H-2->LUMO (18%), H-1->L+1 (29%), HOMO->L+2 (39%)
	S ₀ →S ₄	4.2058 eV	294.79 nm	0.0416	H-3->LUMO (26%), H-2->L+1 (11%), H-1->L+2 (36%), HOMO->L+1 (10%)
1c	S ₀ →S ₁	3.4176 eV	362.79 nm	0.6241	H-2->LUMO (18%), H-1->L+1 (14%), HOMO->LUMO (59%)
	S ₀ →S ₂	3.7636 eV	329.43 nm	0.2798	H-3->LUMO (16%), H-1->LUMO (46%), HOMO->L+1 (28%)
	S ₀ →S ₃	4.1847 eV	296.28 nm	1.1234	H-2->LUMO (11%), H-1->L+1 (27%), HOMO->L+2 (44%)
	S ₀ →S ₄	4.2439 eV	292.15 nm	0.3620	H-3->LUMO (16%), H-1->L+2 (35%), HOMO->L+1 (23%)
1d	S ₀ →S ₁	3.5346 eV	350.77 nm	0.5845	H-1->L+1 (16%), HOMO->LUMO (76%)
	S ₀ →S ₂	3.8887 eV	318.83 nm	0.1821	H-1->LUMO (58%), HOMO->L+1 (33%)
	S ₀ →S ₃	4.3751 eV	283.38 nm	0.8106	H-1->L+1 (29%), HOMO->L+2 (59%)
	S ₀ →S ₄	4.4144 eV	280.86 nm	0.1865	H-1->LUMO (12%), H-1->L+2 (45%), HOMO->L+1 (31%)

^aOnly the selected low-lying excited states are presented. ^bOscillator strength.

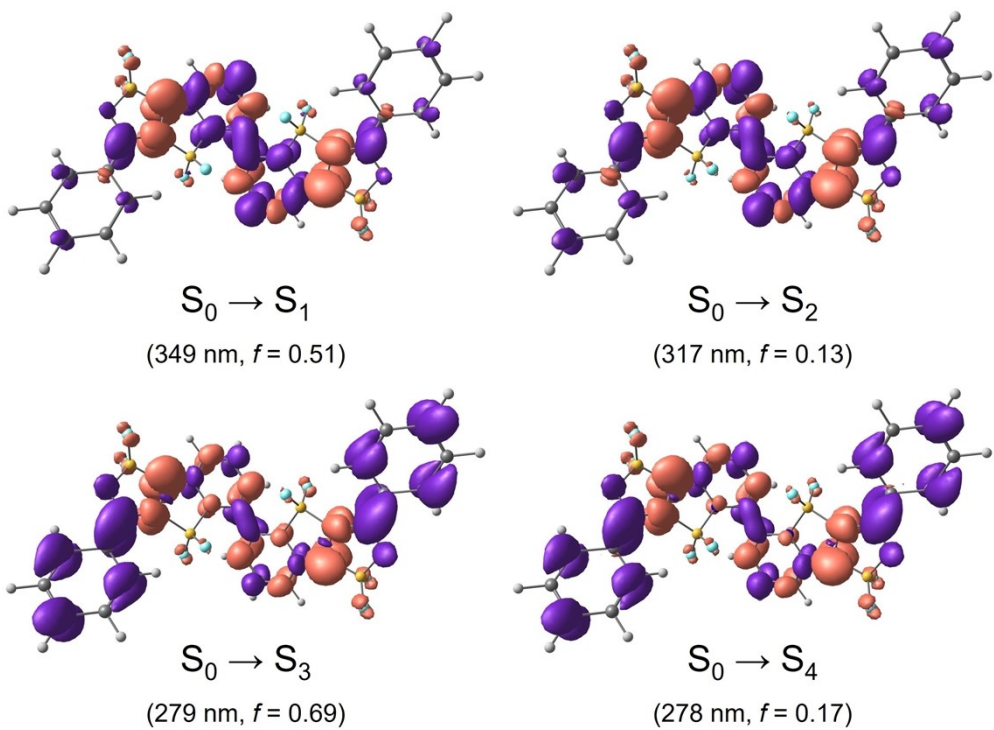


Figure S42-1. TD-DFT-calculated $S_0 \rightarrow S_1$, $S_0 \rightarrow S_2$, $S_0 \rightarrow S_3$, and $S_0 \rightarrow S_4$ transitions of **1a**.

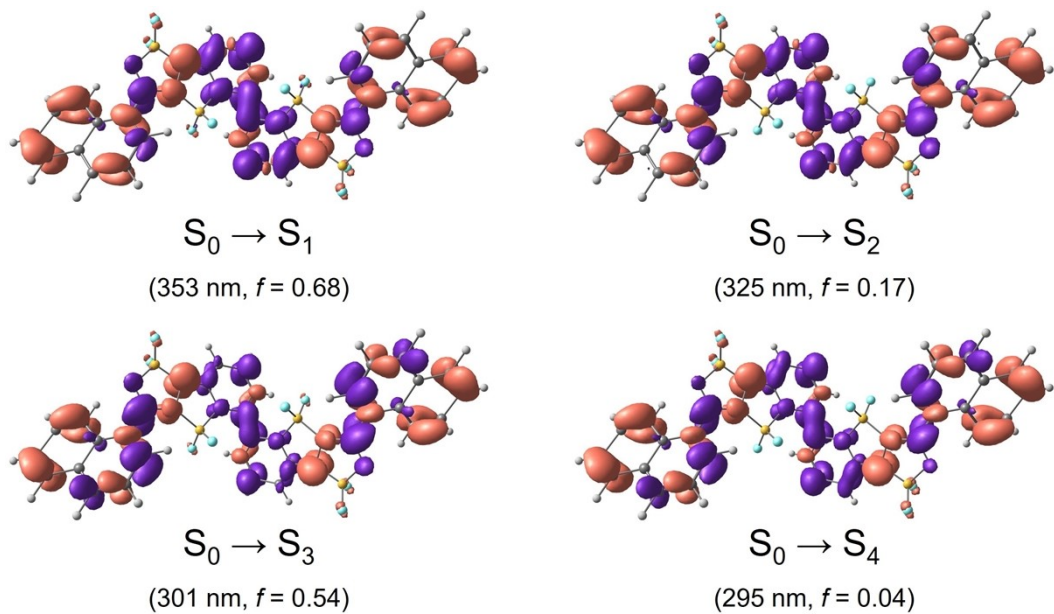


Figure S42-2. TD-DFT-calculated $S_0 \rightarrow S_1$, $S_0 \rightarrow S_2$, $S_0 \rightarrow S_3$, and $S_0 \rightarrow S_4$ transitions of **1b**.

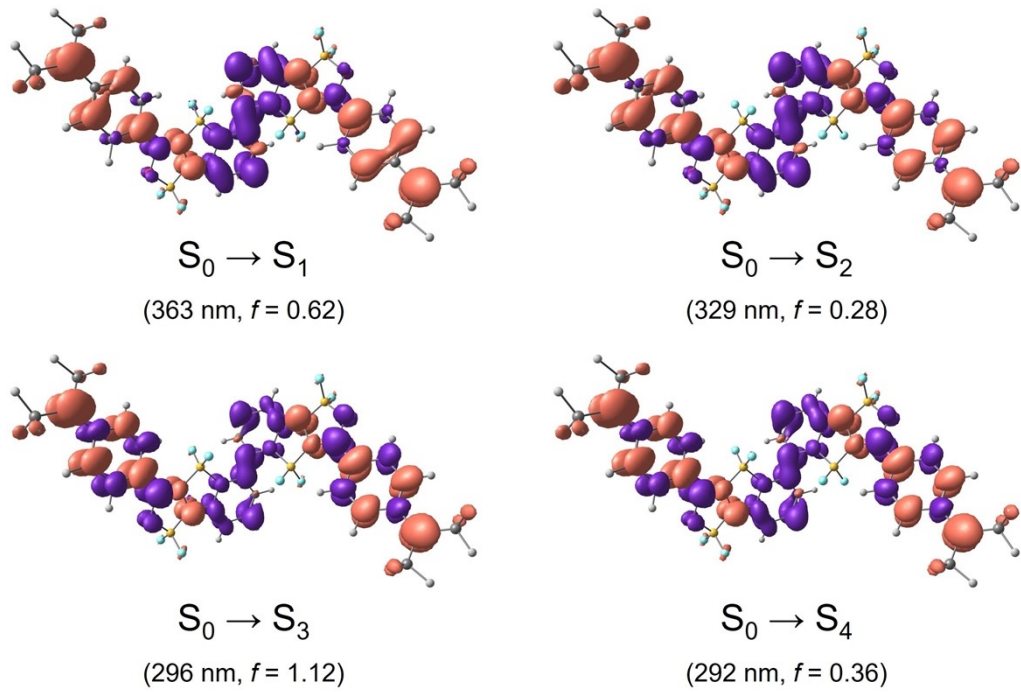


Figure S42-3. TD-DFT-calculated $S_0 \rightarrow S_1$, $S_0 \rightarrow S_2$, $S_0 \rightarrow S_3$, and $S_0 \rightarrow S_4$ transitions of **1c**.

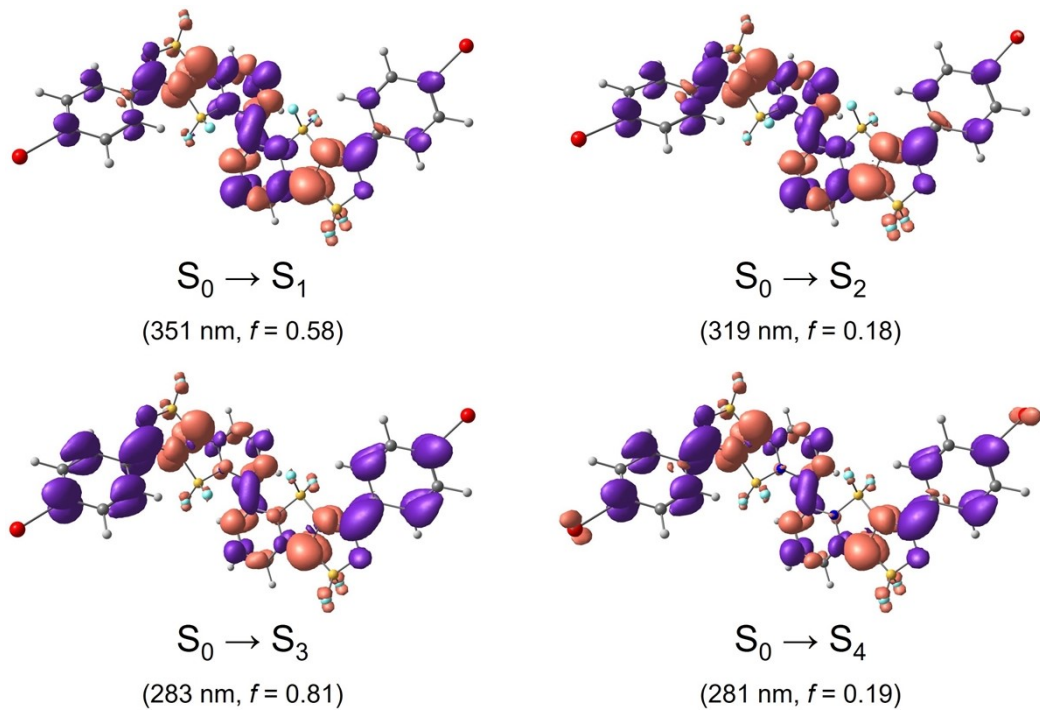


Figure S42-4. TD-DFT-calculated $S_0 \rightarrow S_1$, $S_0 \rightarrow S_2$, $S_0 \rightarrow S_3$, and $S_0 \rightarrow S_4$ transitions of **1d**.

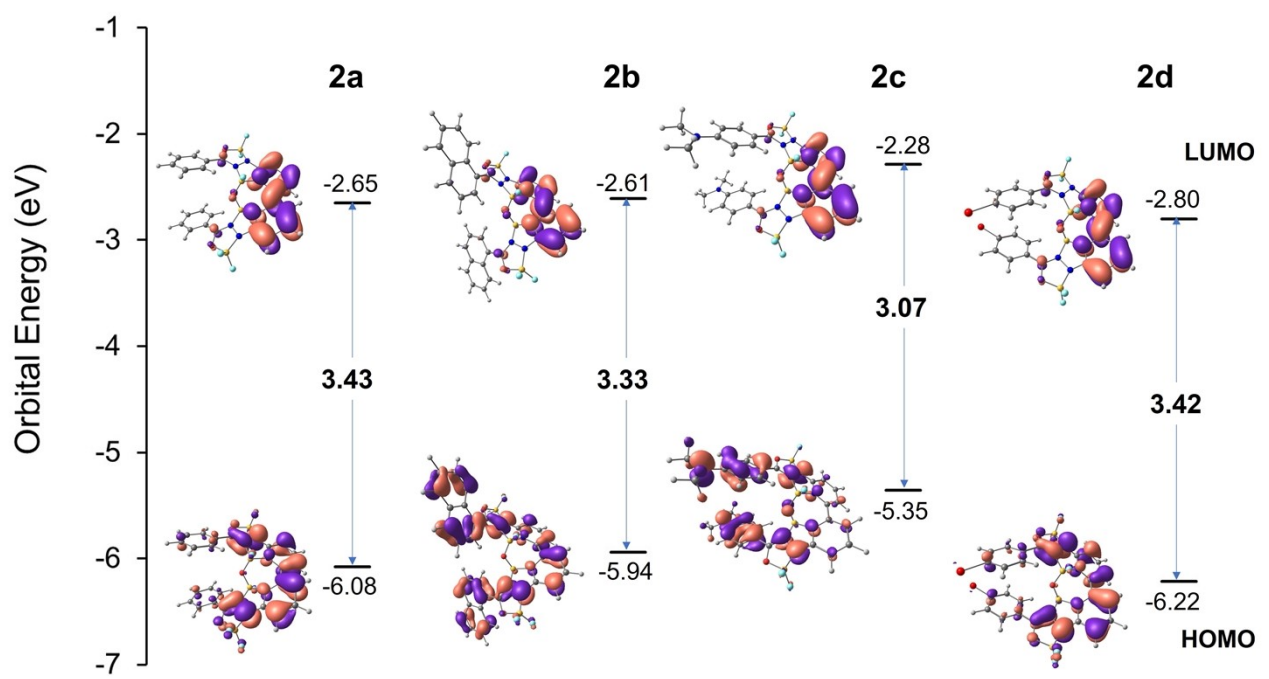


Figure S43. Frontier molecular orbitals of **2a**–**2d**.

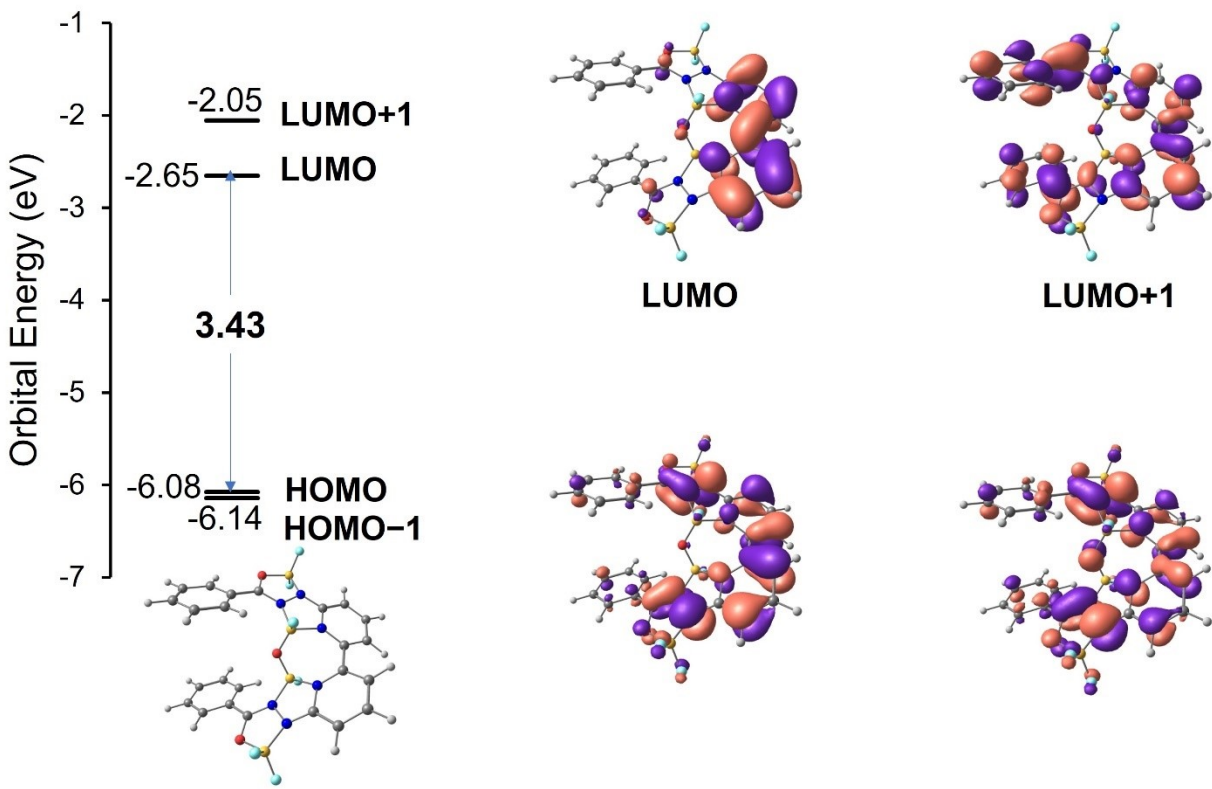


Figure S44-1. Frontier molecular orbitals of (*P*)-2a.

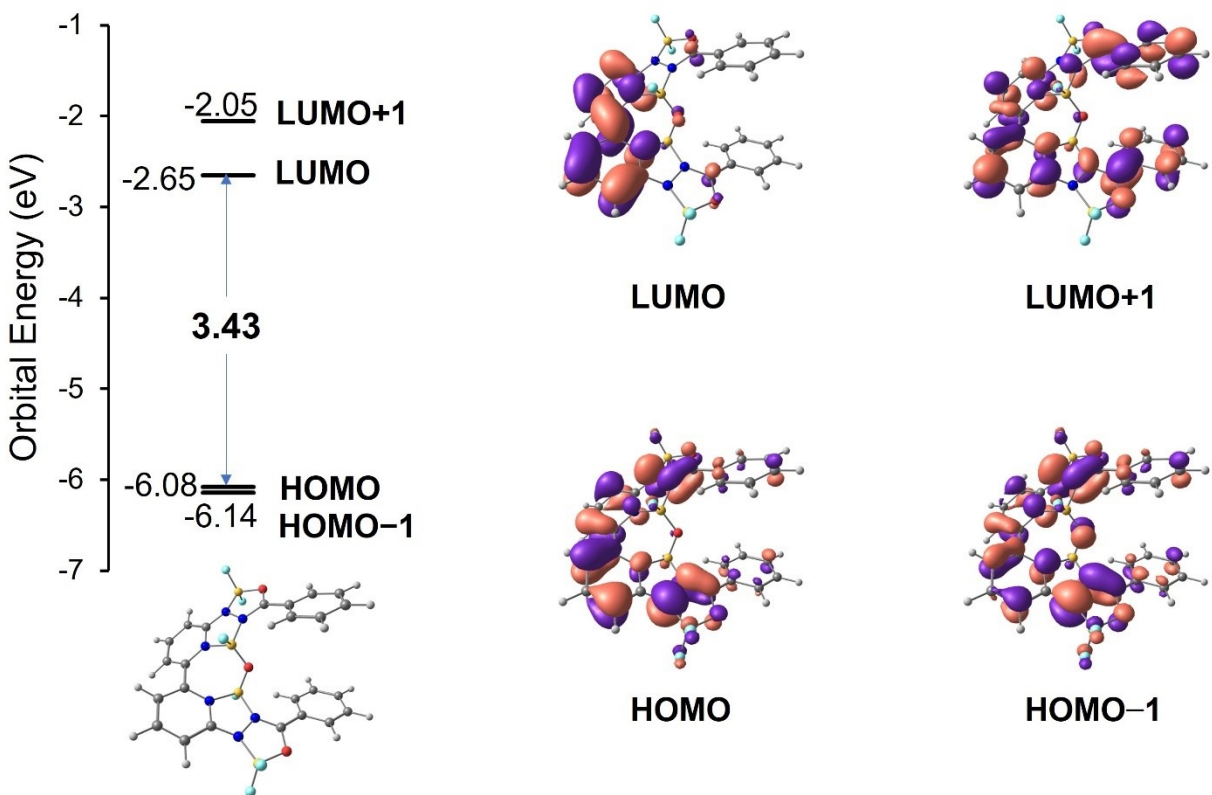


Figure S44-2. Frontier molecular orbitals of (*M*)-2a.

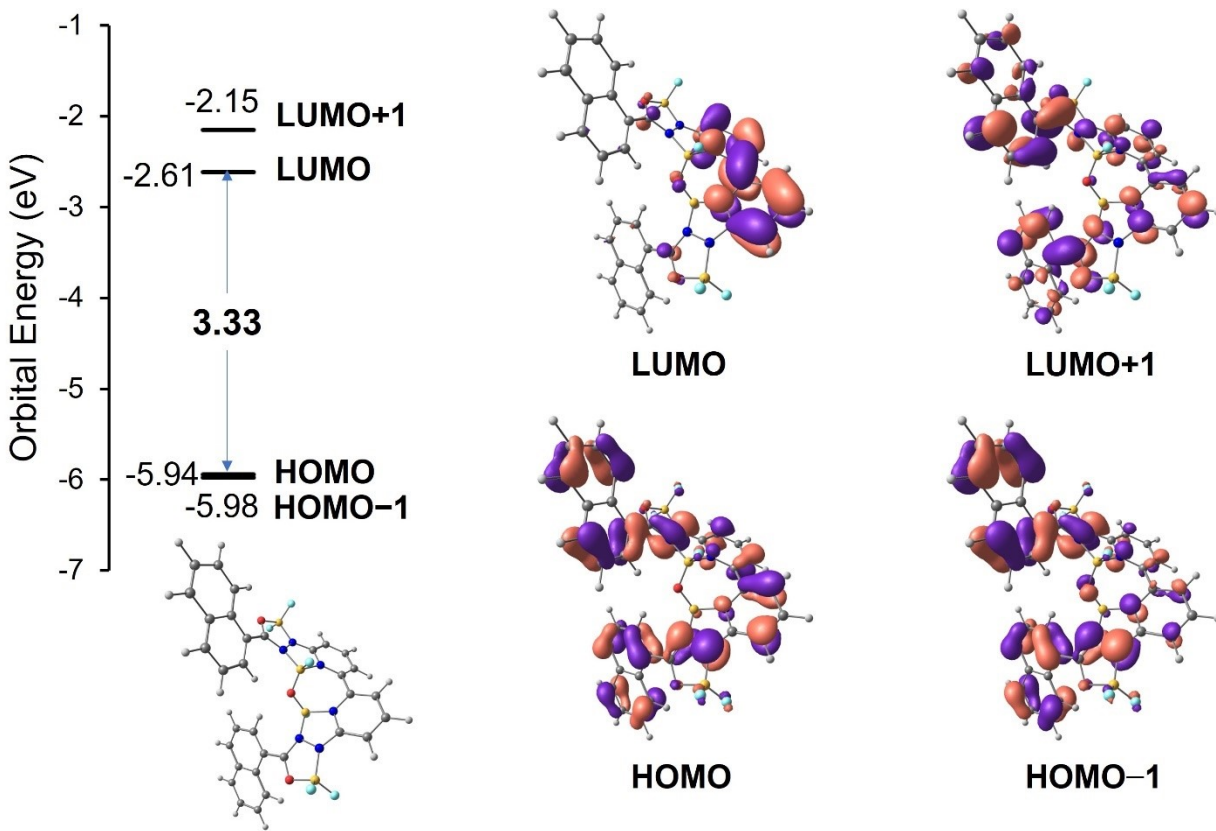


Figure S45-1. Frontier molecular orbitals of **(P)-2b**.

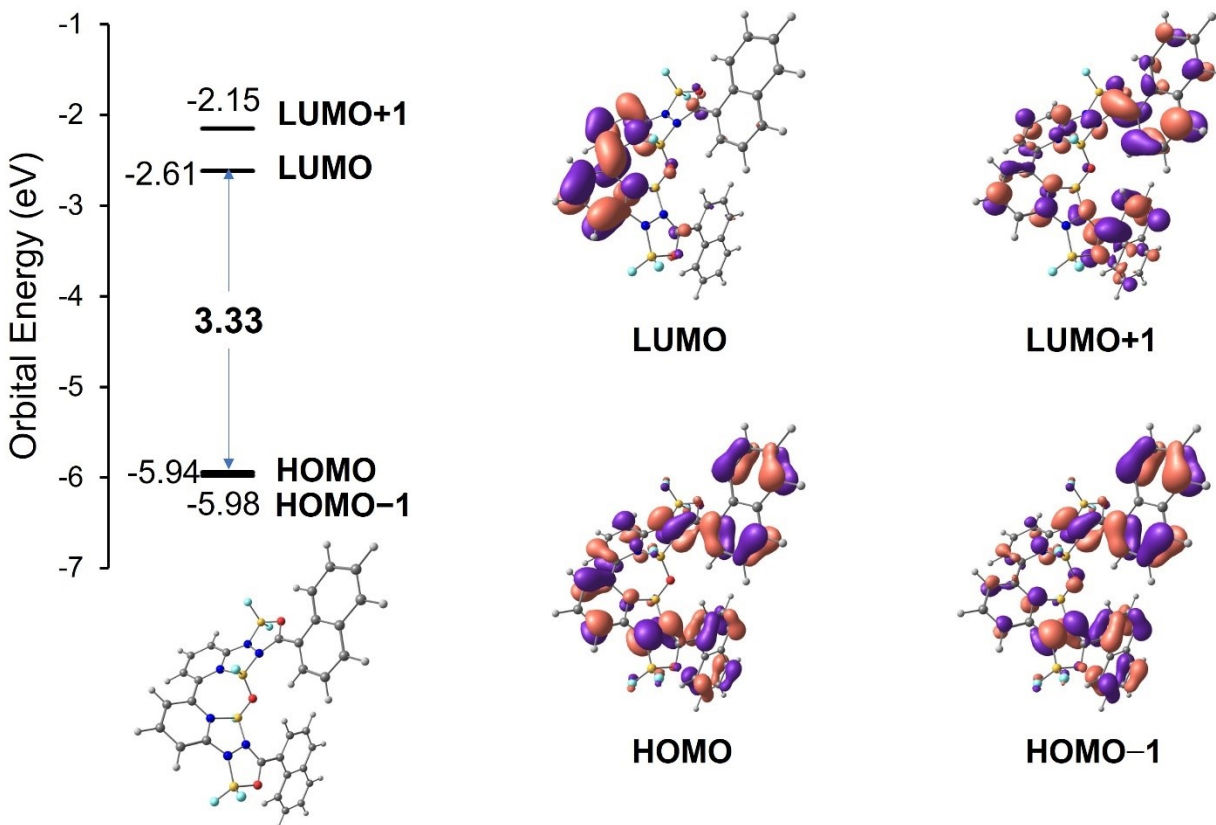


Figure S45-2. Frontier molecular orbitals of **(M)-2b**.

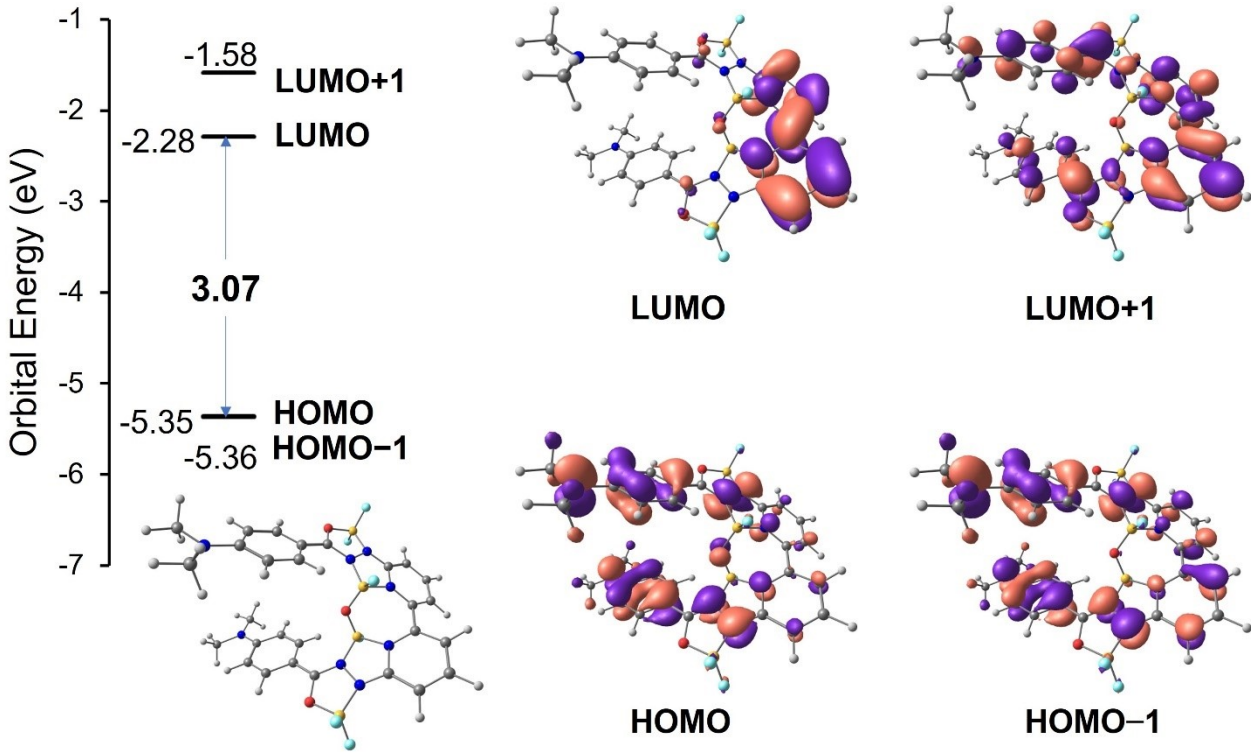


Figure S46-1. Frontier molecular orbitals of (*P*)-2c.

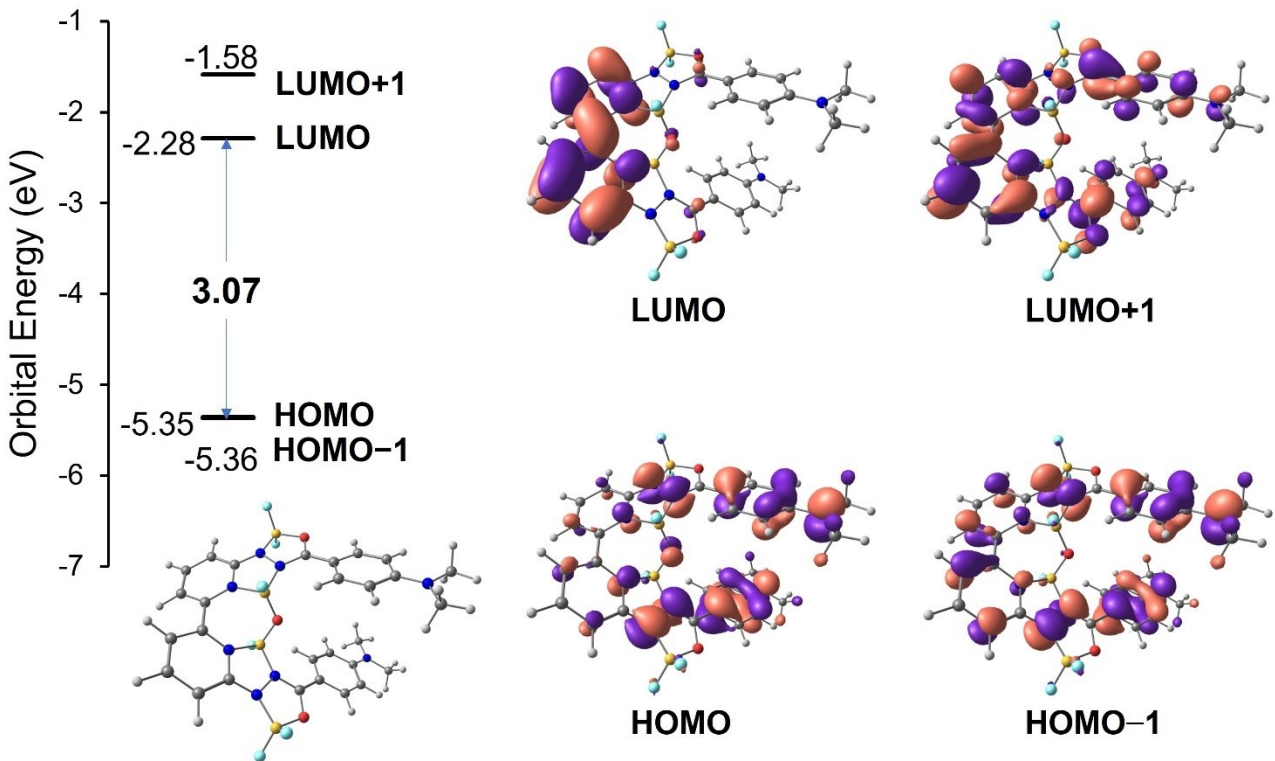


Figure S46-2. Frontier molecular orbitals of (*M*)-2c.

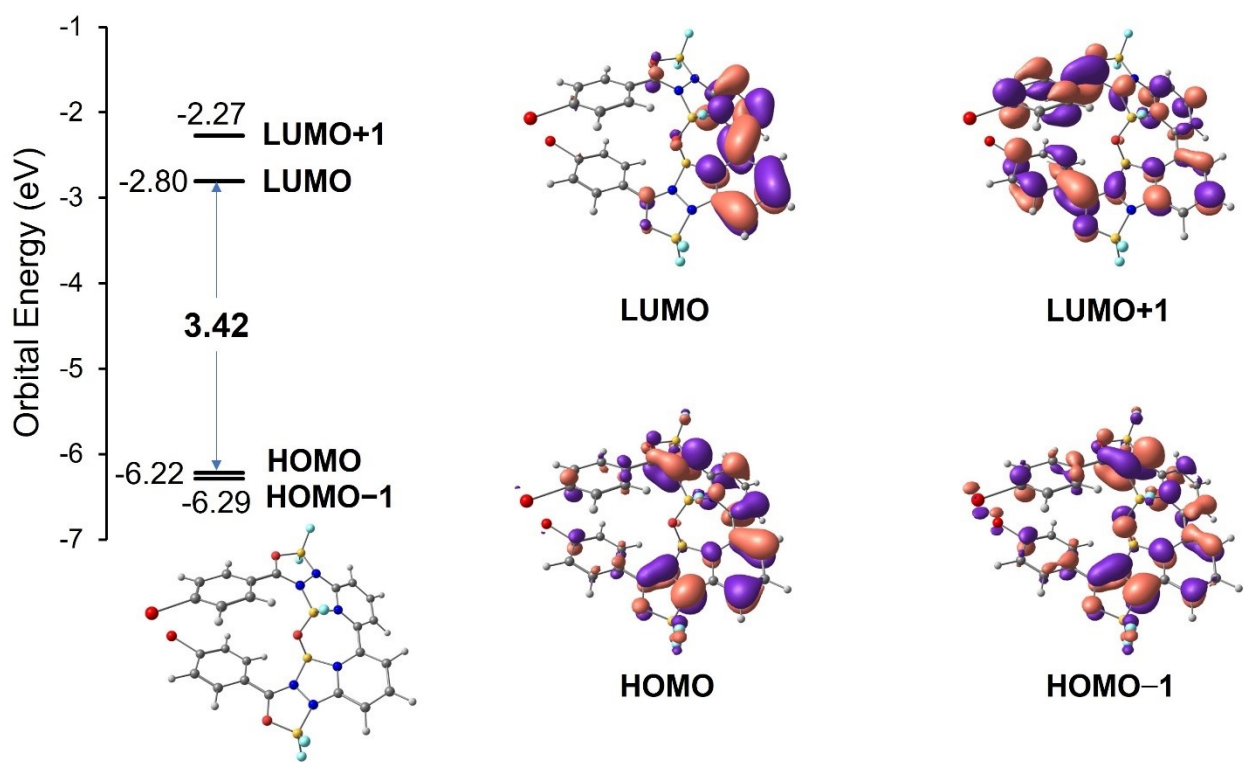


Figure S47-1. Frontier molecular orbitals of (*P*)-2d.

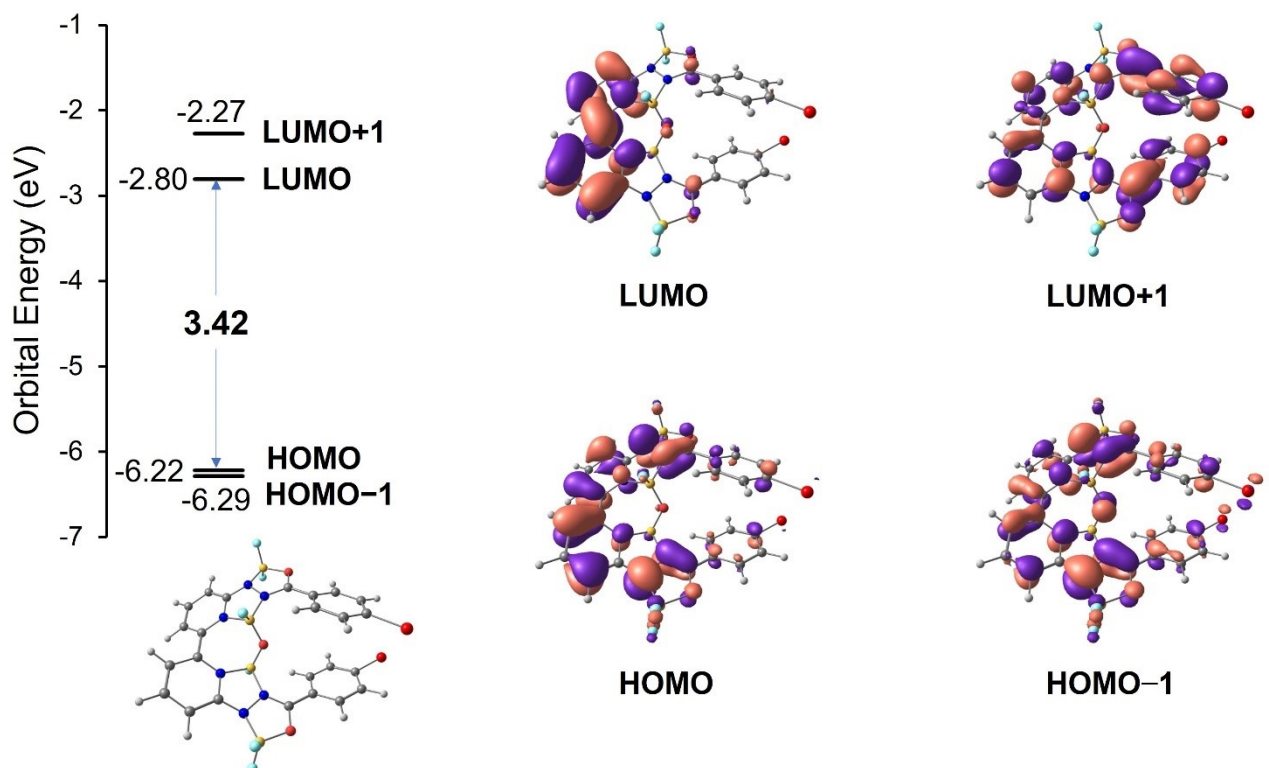


Figure S47-2. Frontier molecular orbitals of (*M*)-2d.

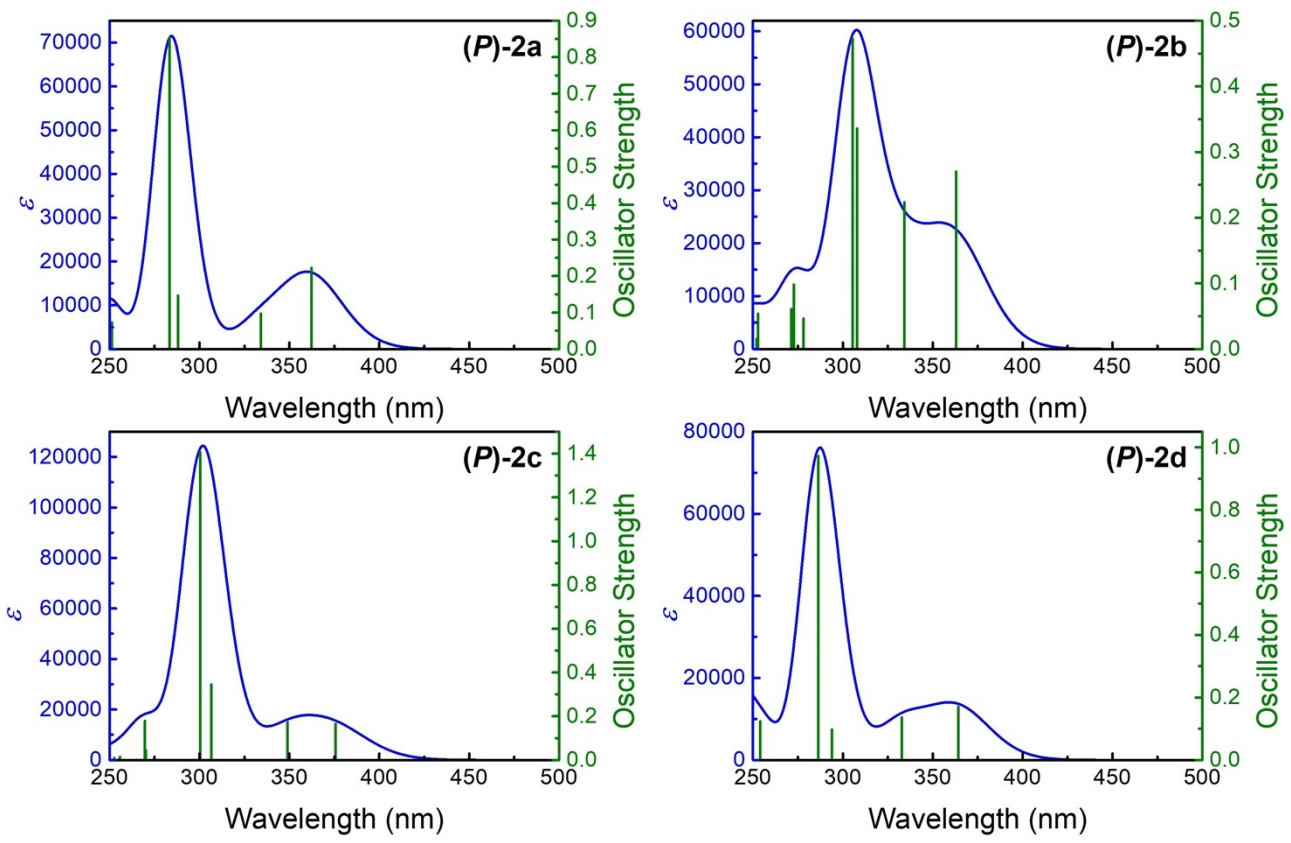


Figure S48-1. Calculated UV-vis absorption spectra of (P)-enantiomers of **2a–2d** by TD-DFT method.

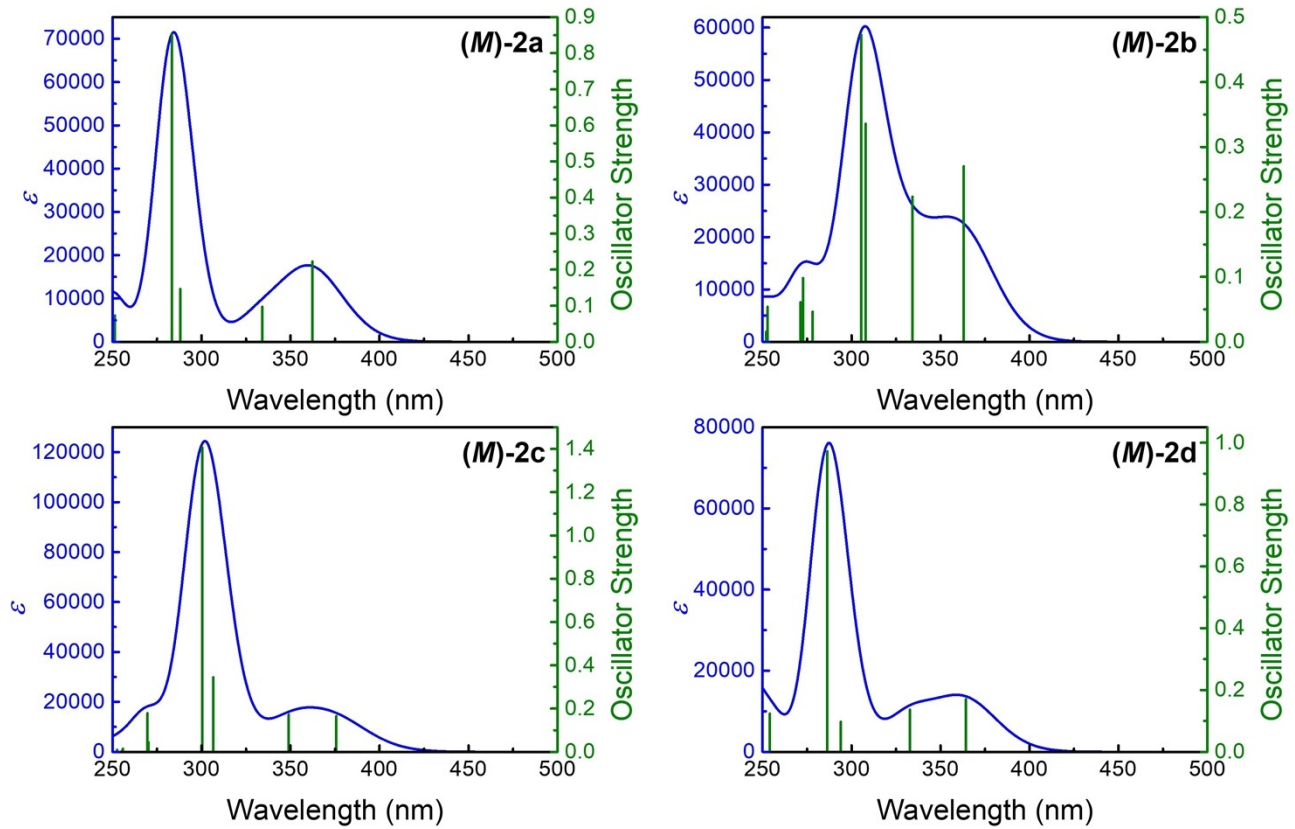


Figure S48-2. Calculated UV-vis absorption spectra of (*M*)-enantiomers of **2a–2d** by TD-DFT method.

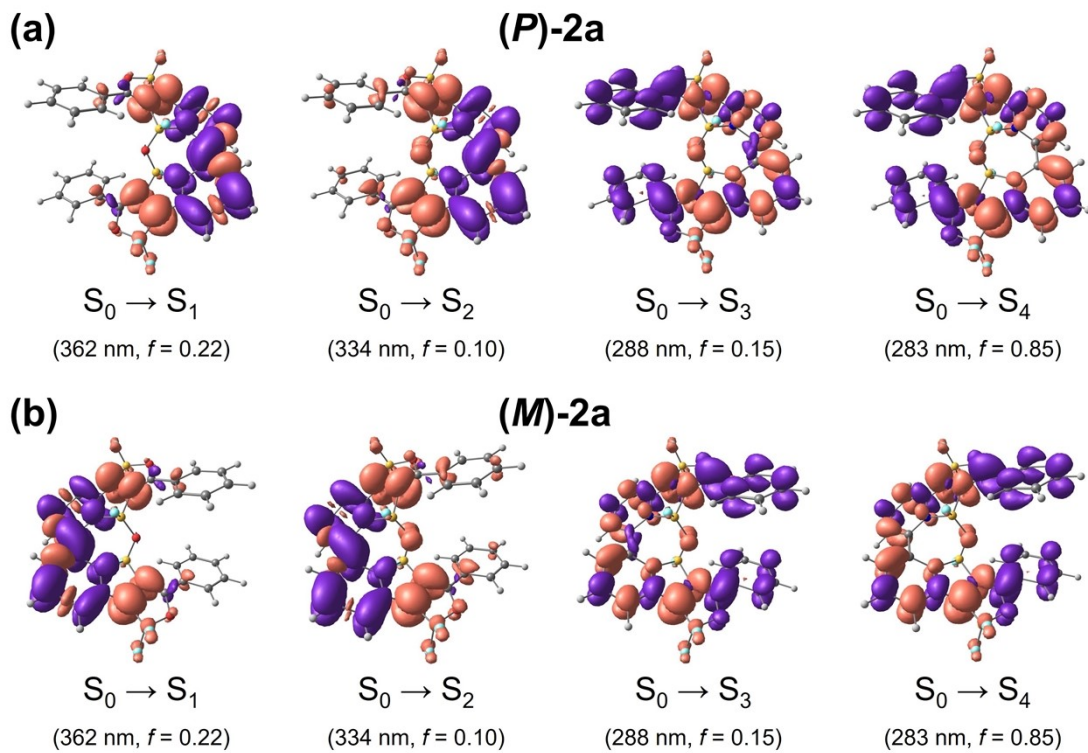


Figure S49-1. TD-DFT-calculated $S_0 \rightarrow S_1$, $S_0 \rightarrow S_2$, $S_0 \rightarrow S_3$, and $S_0 \rightarrow S_4$ transitions of (a) (*P*)-**2a** and (b) (*M*)-**2a**.

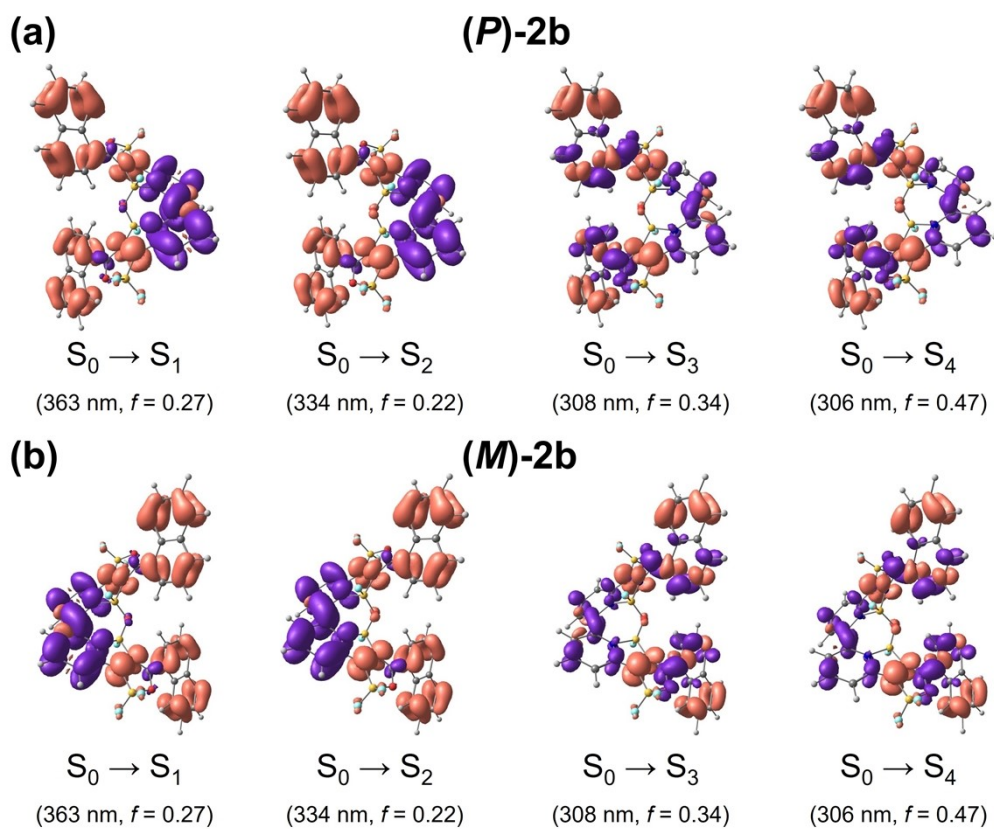


Figure S49-2. TD-DFT-calculated $S_0 \rightarrow S_1$, $S_0 \rightarrow S_2$, $S_0 \rightarrow S_3$, and $S_0 \rightarrow S_4$ transitions of (a) (*P*)-2b and (b) (*M*)-2b.

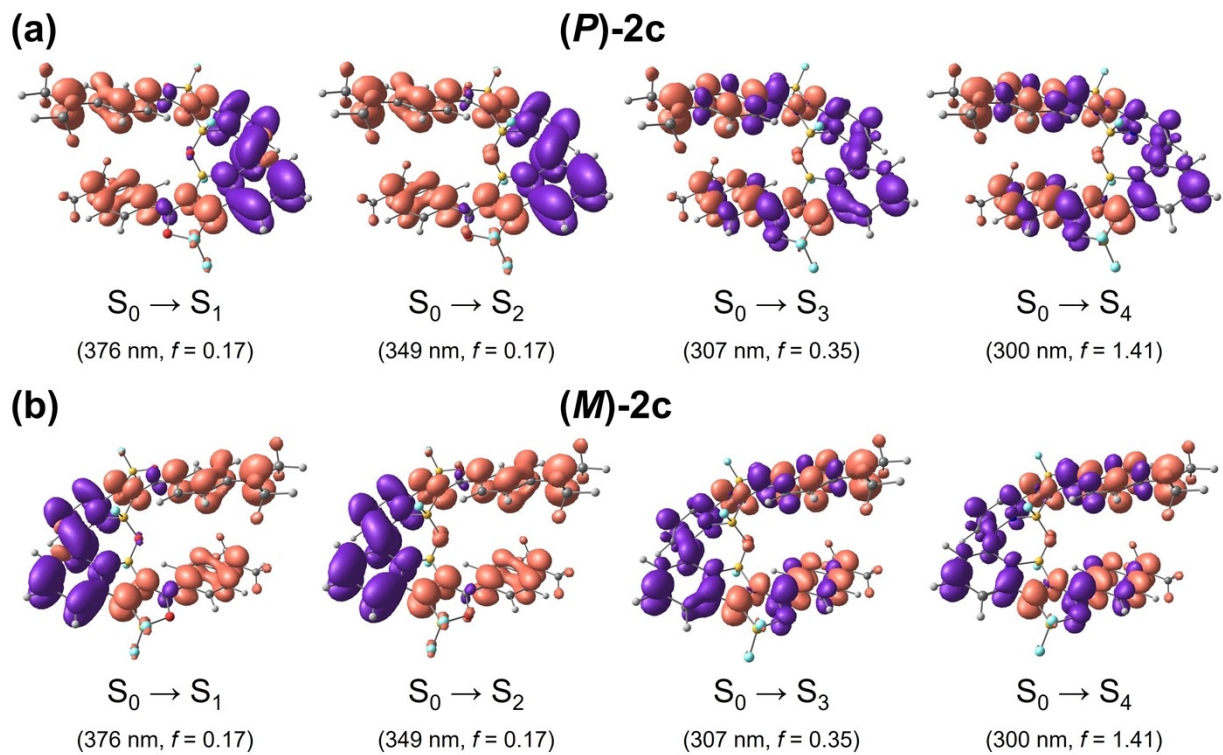


Figure S49-3. TD-DFT-calculated $S_0 \rightarrow S_1$, $S_0 \rightarrow S_2$, $S_0 \rightarrow S_3$, and $S_0 \rightarrow S_4$ transitions of (a) (*P*)-2c and (b) (*M*)-2c.

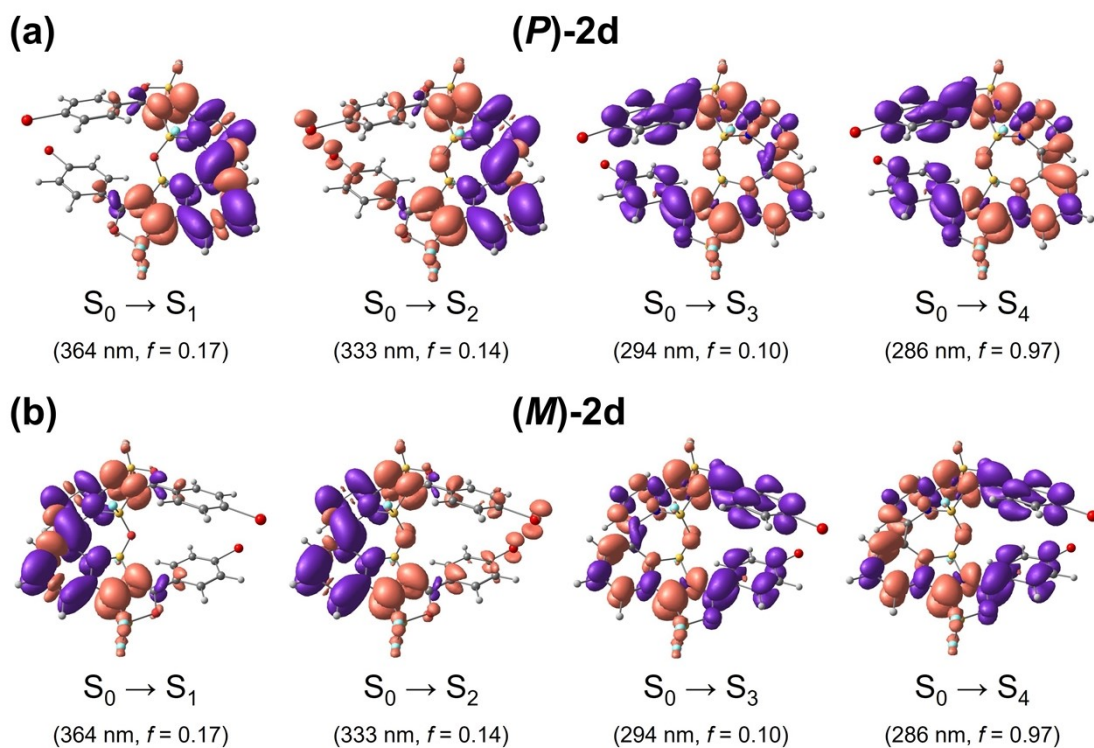


Figure S49-4. TD-DFT-calculated $S_0 \rightarrow S_1$, $S_0 \rightarrow S_2$, $S_0 \rightarrow S_3$, and $S_0 \rightarrow S_4$ transitions of (a) (*P*)-**2d** and (b) (*M*)-**2d**.

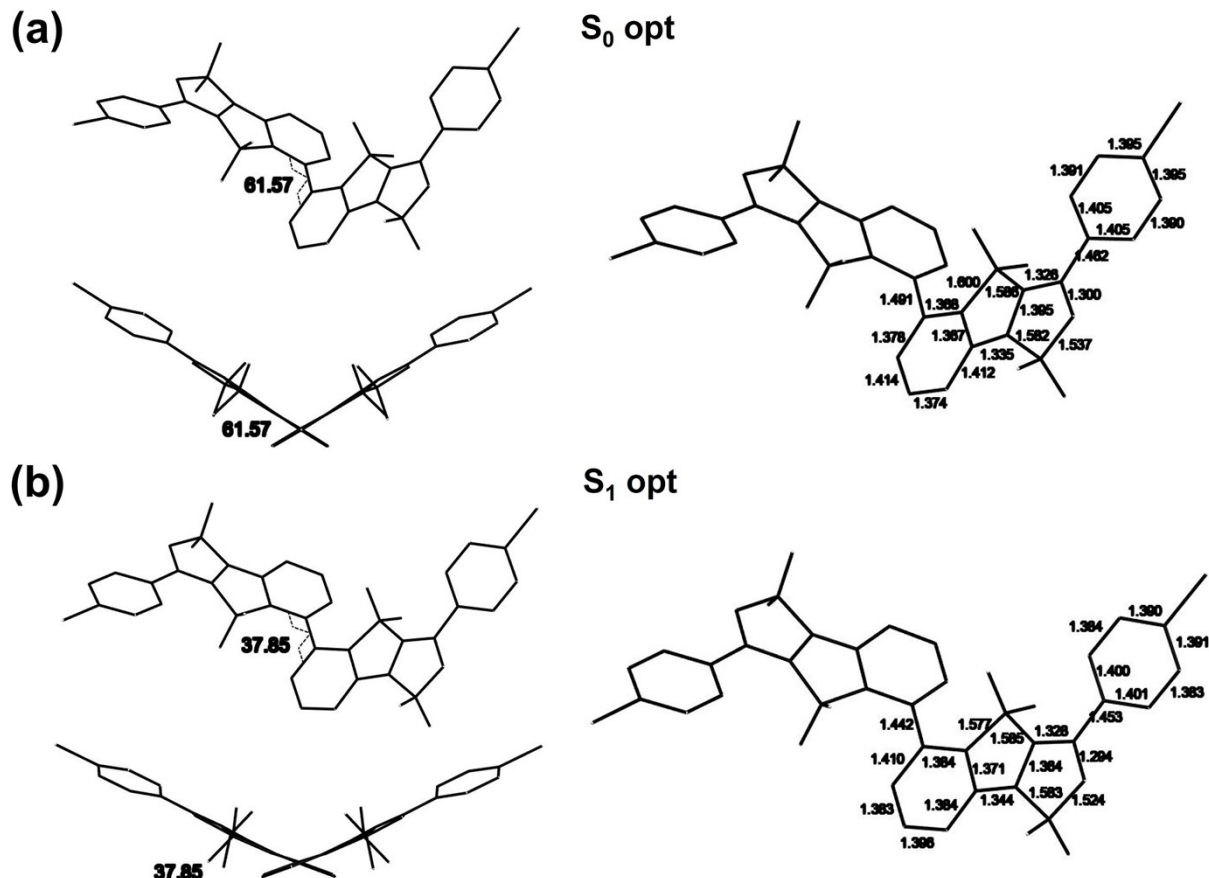


Figure S50-1. Optimized geometries of **1d** in (a) S_0 and (b) S_1 showing representative bond length (Å). The bond length between the carbon atoms of bipyridine is 1.491 Å in S_0 , but it is shortened to 1.442 Å in S_1 . The torsion angle is 61.57 degree for S_0 , while it is 37.85 degree in the S_1 state, suggesting that the compound is more planar conformation in the S_1 state than in the S_0 state.

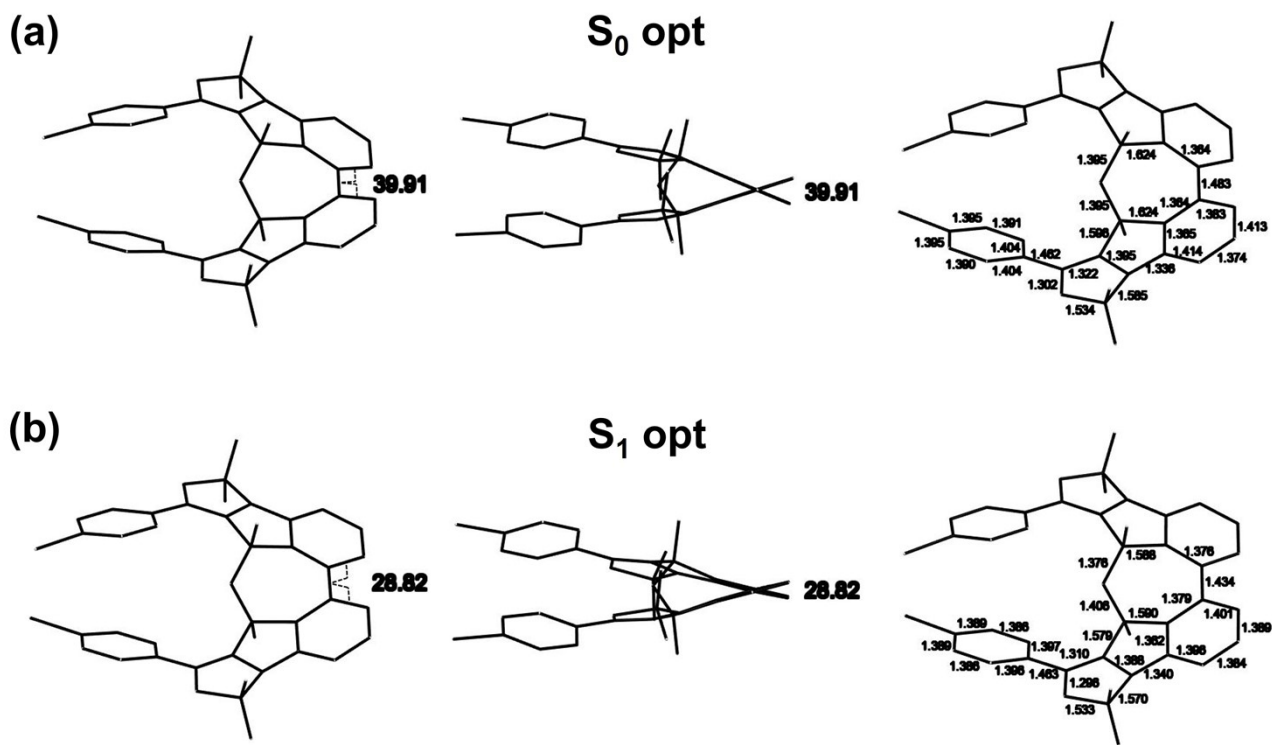


Figure S50-2. Optimized geometries of **2d** in (a) S_0 and (b) S_1 showing representative bond length (\AA). The bond length between the carbon atoms of bipyridine is 1.483 \AA in S_0 , but it is shortened to 1.434 \AA in S_1 . The torsion angle is 39.91 degree for S_0 , while it is 28.82 degree in the S_1 state, suggesting that the compound is more planar conformation in the S_1 state than in the S_0 state.

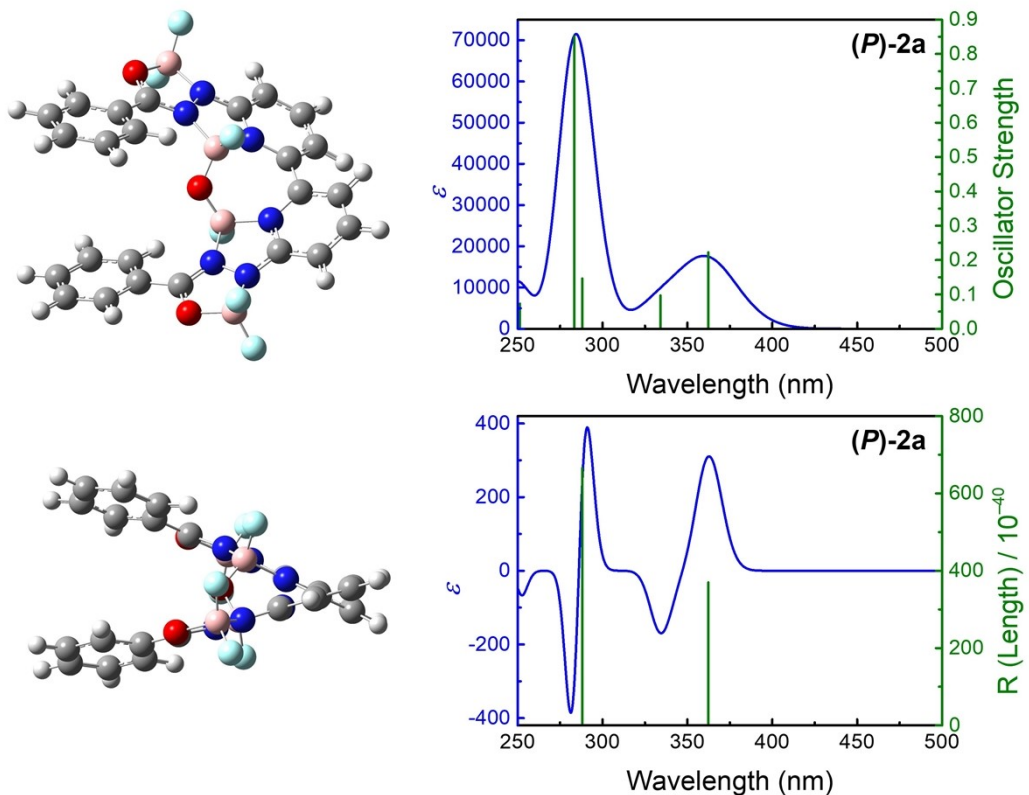


Figure S51-1. Calculated UV-vis and ECD spectra of **(P)-2a** by TD-DFT method [cam-B3LYP/6-31G(d,p)].

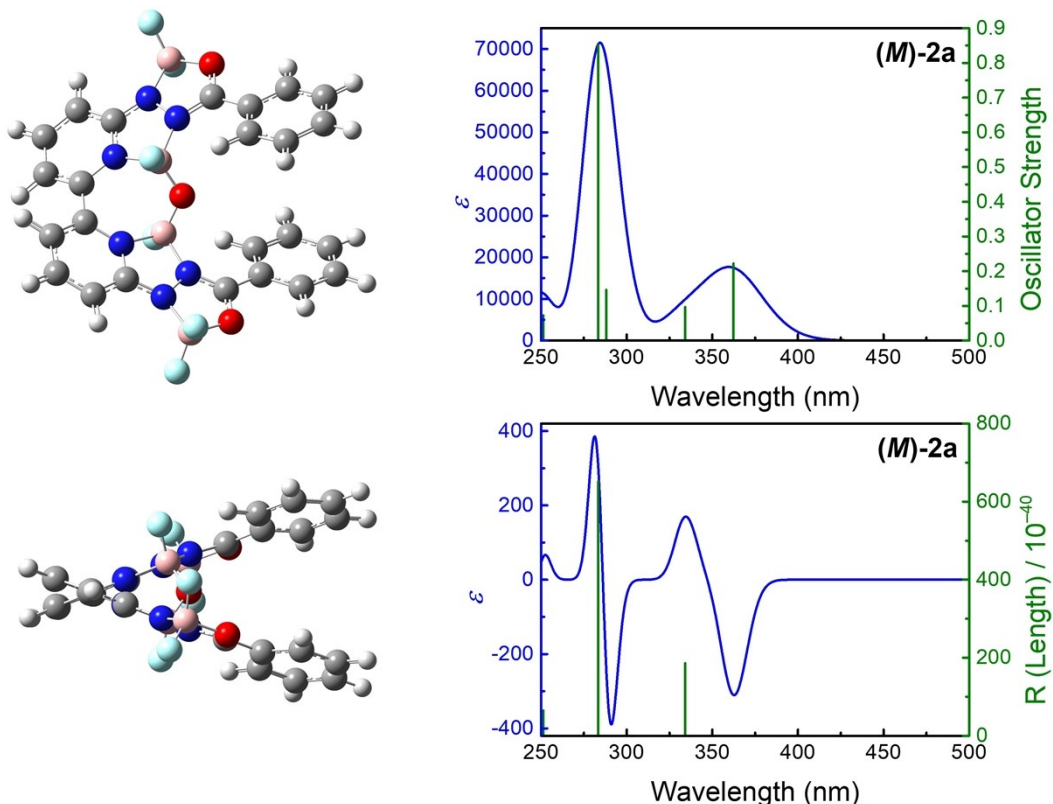


Figure S51-2. Calculated UV-vis and ECD spectra of **(M)-2a** by TD-DFT method [cam-B3LYP/6-31G(d,p)].

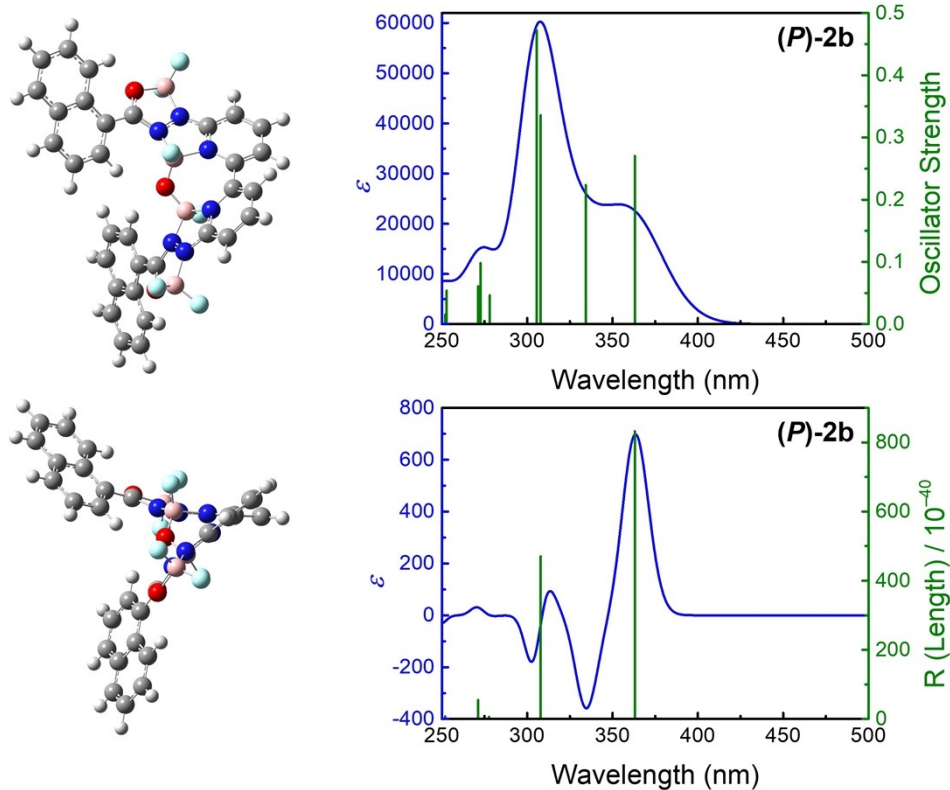


Figure S52-1. Calculated UV-vis and ECD spectra of **(P)-2b** by TD-DFT method [cam-B3LYP/6-31G(d,p)].

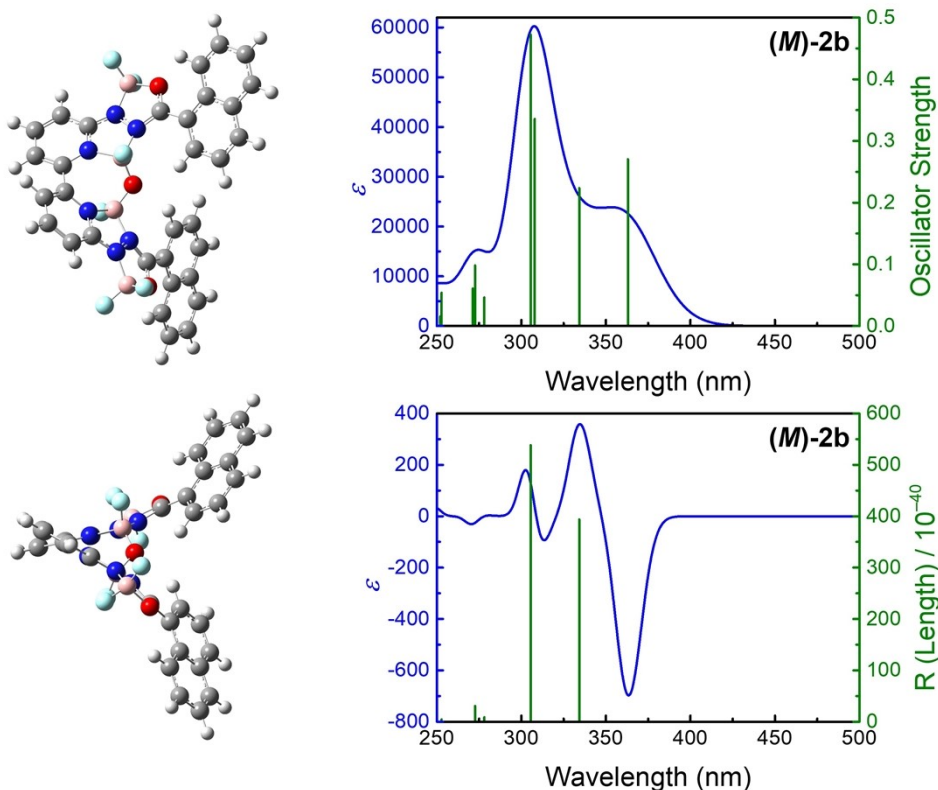


Figure S52-2. Calculated UV-vis and ECD spectra of **(M)-2b** by TD-DFT method [cam-B3LYP/6-31G(d,p)].

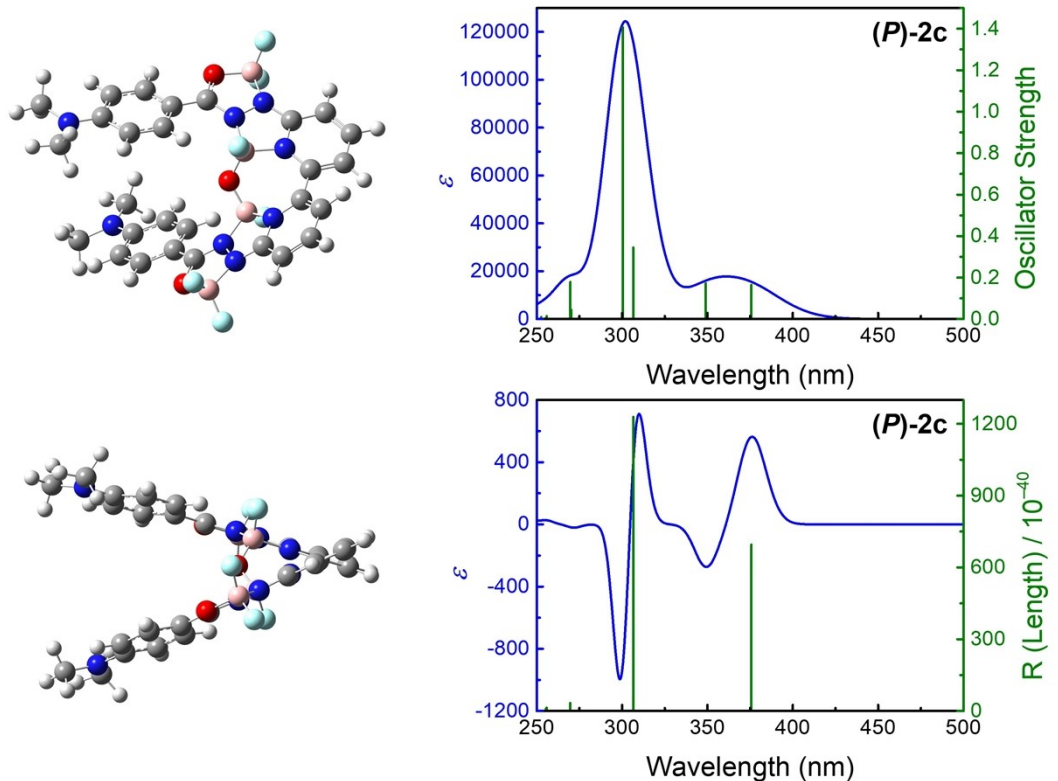


Figure S53-1. Calculated UV-vis and ECD spectra of **(P)-2c** by TD-DFT method [cam-B3LYP/6-31G(d,p)].

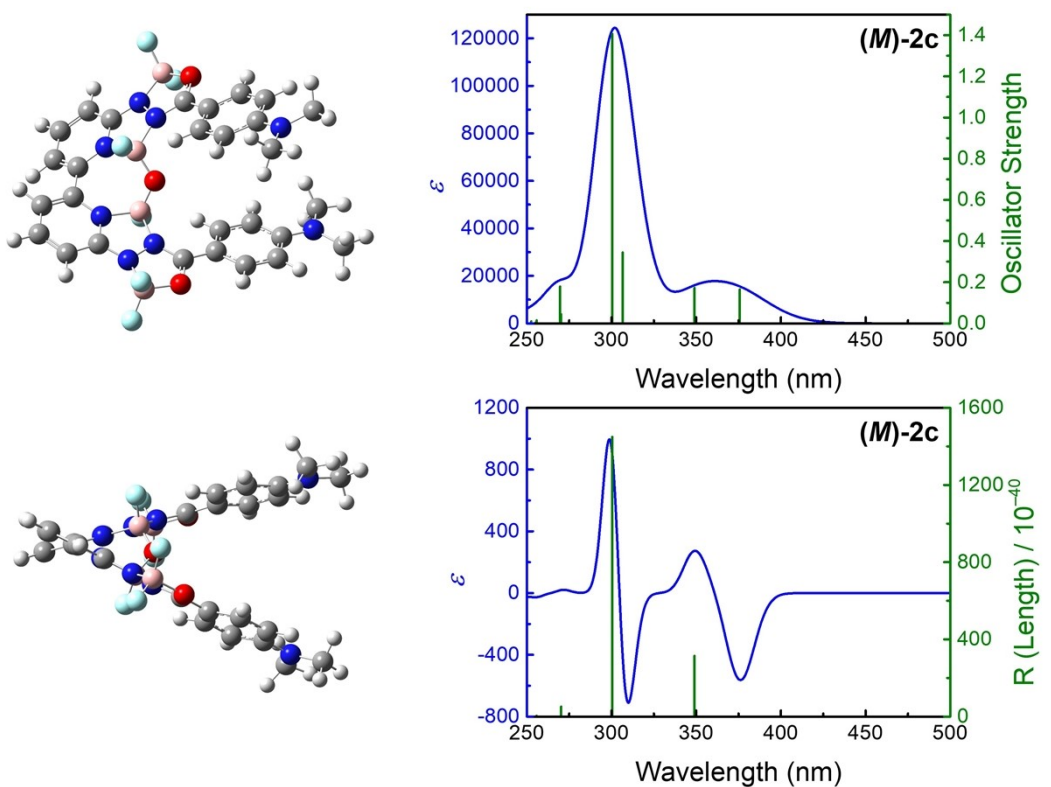


Figure S53-2. Calculated UV-vis and ECD spectra of **(M)-2c** by TD-DFT method [cam-B3LYP/6-31G(d,p)].

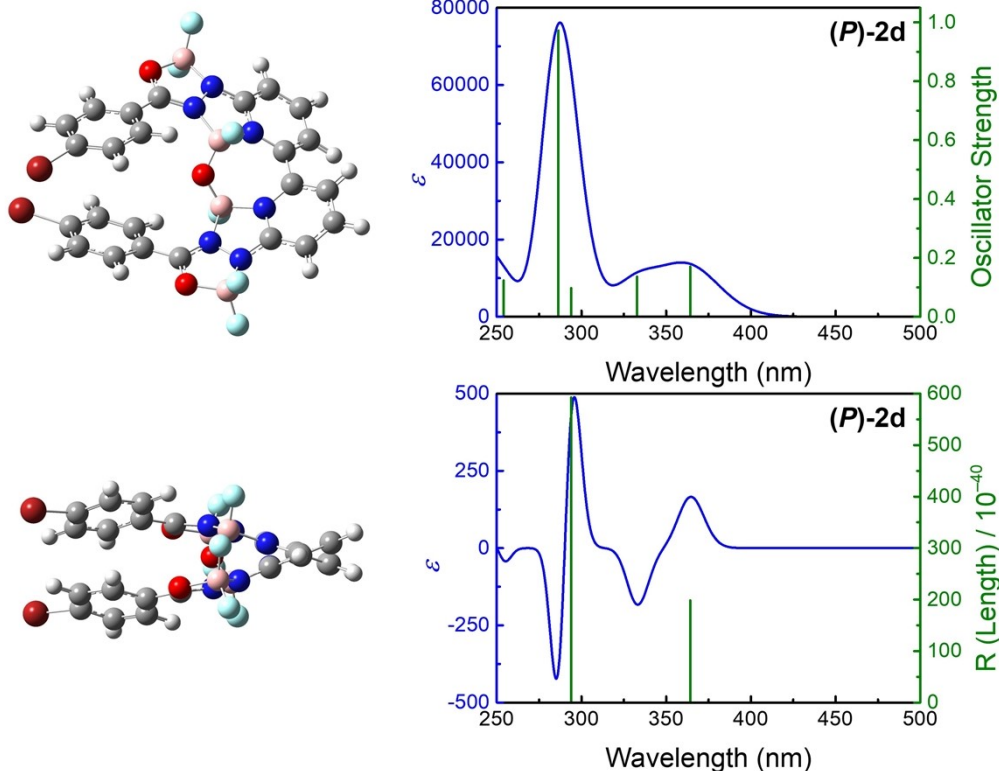


Figure S54-1. Calculated UV-vis and ECD spectra of **(P)-2d** by TD-DFT method [cam-B3LYP/6-31G(d,p)].

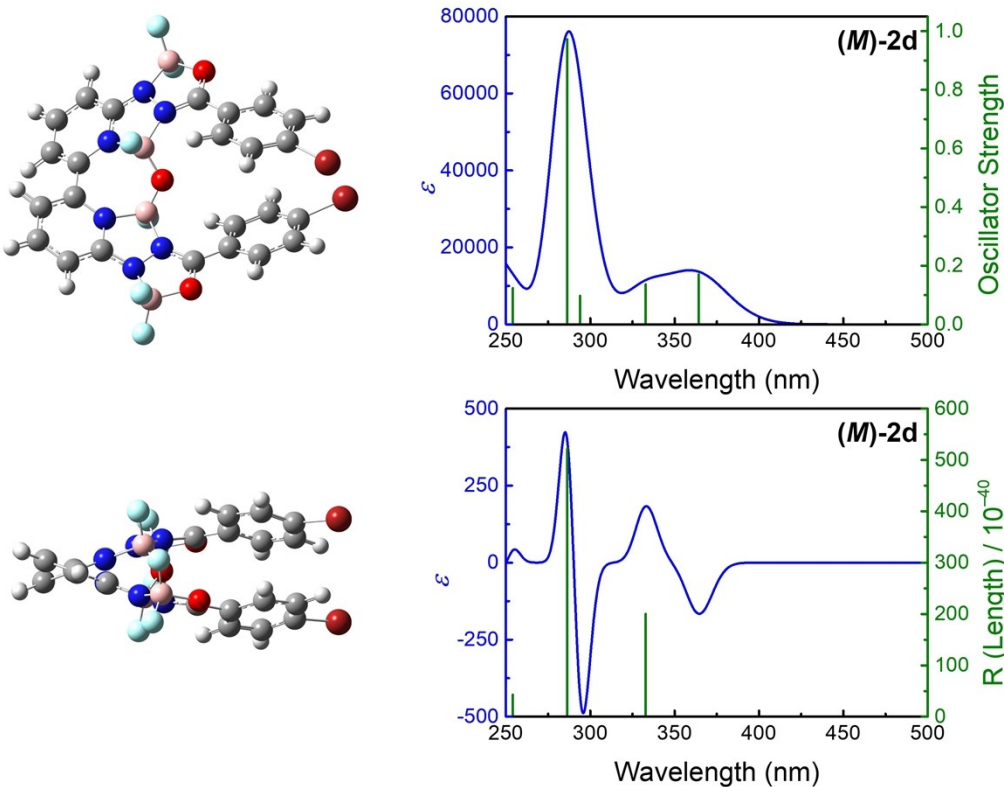


Figure S54-2. Calculated UV-vis and ECD spectra of **(M)-2d** by TD-DFT method [cam-B3LYP/6-31G(d,p)].

Table S13. Calculated photophysical property data of the ground state for **2a–2d** at the cam-B3LYP/6-31G(d,p) level.

	Electronic Transition	TD//cam-B3LYP/6-31G(d,p)			
		Energy/eV ^a		f ^b	Major contributions
2a	S ₀ →S ₁	3.4216 eV	362.36 nm	0.2226	H-1->L+1 (11%), HOMO->LUMO (83%)
	S ₀ →S ₂	3.7104 eV	334.15 nm	0.0972	H-1->LUMO (85%) HOMO->L+1 (9%), HOMO->L+3 (3%)
	S ₀ →S ₃	4.3042 eV	288.05 nm	0.1468	H-1->L+1 (46%), HOMO->L+2 (39%)
	S ₀ →S ₄	4.3740 eV	283.46 nm	0.8521	H-1->L+2 (35%), HOMO->L+1 (55%)
2b	S ₀ →S ₁	3.4151 eV	363.05 nm	0.2704	H-2->LUMO (17%), H-1->L+1 (12%), HOMO->LUMO (62%)
	S ₀ →S ₂	3.7092 eV	334.26 nm	0.2236	H-3->LUMO (20%), H-1->LUMO (57%), HOMO->L+1 (15%)
	S ₀ →S ₃	4.0266 eV	307.91 nm	0.3360	H-2->LUMO (10%), H-1->L+1 (40%), HOMO->L+2 (36%)
	S ₀ →S ₄	4.0582 eV	305.51 nm	0.4727	H-3->LUMO (12%), H-1->L+2 (39%), HOMO->L+1 (35%)
2c	S ₀ →S ₁	3.2996 eV	375.75 nm	0.1653	H-2->LUMO (24%), H-1->L+1 (11%), HOMO->LUMO (57%)
	S ₀ →S ₂	3.5525 eV	349.00 nm	0.1727	H-3->LUMO (24%), H-1->LUMO (64%)
	S ₀ →S ₃	4.0439 eV	306.59 nm	0.3451	H-1->L+1 (41%), HOMO->L+2 (33%)
	S ₀ →S ₄	4.1263 eV	300.48 nm	1.4066	H-1->L+2 (36%), HOMO->L+1 (47%)
2d	S ₀ →S ₁	3.4040 eV	364.23 nm	0.1709	H-1->L+1 (12%), HOMO->LUMO (80%)
	S ₀ →S ₂	3.7252 eV	332.82 nm	0.1369	H-1->LUMO (82%)
	S ₀ →S ₃	4.2186 eV	293.90 nm	0.0979	H-1->L+1 (46%), HOMO->LUMO (10%), HOMO->L+2 (36%)
	S ₀ →S ₄	4.3293 eV	286.38 nm	0.9724	H-1->L+2 (34%), HOMO->L+1 (55%)

^aOnly the selected low-lying excited states are presented. ^bOscillator strength.

Table S14. Coordinates of electric transition dipole moment (μ) and magnetic transition dipole moments (m) of the ground state of **2a–2d** at the cam-B3LYP/6-31G(d,p) level.

Electronic Transition		μ [a.u.]			m [a.u.]		
		x	y	z	x	y	z
2a	$S_0 \rightarrow S_1$	1.6242	0.0002	0.1287	-0.6809	-0.0003	-3.6047
	$S_0 \rightarrow S_2$	-0.0002	1.0342	0.0001	0.0002	0.7644	-0.0005
	$S_0 \rightarrow S_3$	0.0520	0.0043	1.1789	0.3273	0.0018	-2.4114
	$S_0 \rightarrow S_4$	-0.0012	2.8198	-0.0018	-0.0007	0.9816	0.0031
2b	$S_0 \rightarrow S_1$	-1.791	-0.0001	-0.1540	2.2284	-0.0004	-2.9776
	$S_0 \rightarrow S_2$	-0.0000	1.5688	-0.0002	0.0003	1.0655	-0.0004
	$S_0 \rightarrow S_3$	0.6243	0.0027	-1.7368	0.0505	0.0013	1.1673
	$S_0 \rightarrow S_4$	-0.0007	2.1804	0.0022	0.0001	1.0478	-0.0016
2c	$S_0 \rightarrow S_1$	-0.0005	1.3713	-0.4058	0.0010	-0.9436	4.0883
	$S_0 \rightarrow S_2$	1.4087	0.0003	-0.0000	0.9486	0.0008	-0.0005
	$S_0 \rightarrow S_3$	-0.0024	0.3569	1.8318	-0.0010	-0.5586	-2.7384
	$S_0 \rightarrow S_4$	-3.7302	-0.0014	-0.0011	-1.6484	-0.0008	0.0013
2d	$S_0 \rightarrow S_1$	-0.0005	-1.4258	-0.1300	-0.0003	0.1875	4.4231
	$S_0 \rightarrow S_2$	-1.2247	0.0003	-0.0000	-0.6937	-0.0001	-0.0012
	$S_0 \rightarrow S_3$	-0.0009	0.5518	-0.8015	-0.0003	-0.9992	2.4490
	$S_0 \rightarrow S_4$	-3.0278	-0.0002	0.0002	-0.7315	0.0003	-0.0007

Table S15. Calculated transition dipole moments (μ , m , and θ) and g_{abs} values of (*P*)-enantiomers of **2a–2d**.

	Electronic Transition	Energy [nm]	$ \mu $ [10^{-20} esu cm]	$ m $ [10^{-20} erg G $^{-1}$]	θ [°]	$\cos \theta$	$ g_{abs} ^{cal}$
2a	$S_0 \rightarrow S_1$	362.36	414.12	3.40	105.23	-0.26	8.63×10^{-3}
	$S_0 \rightarrow S_2$	334.15	262.87	0.71	0.05	1.00	1.08×10^{-2}
	$S_0 \rightarrow S_3$	288.05	299.94	2.26	169.74	-0.98	2.96×10^{-2}
	$S_0 \rightarrow S_4$	283.46	716.72	0.91	0.22	1.00	5.08×10^{-3}
2b	$S_0 \rightarrow S_1$	363.05	456.91	3.45	121.90	-0.53	1.60×10^{-2}
	$S_0 \rightarrow S_2$	334.26	398.75	0.99	0.021	1.00	9.91×10^{-3}
	$S_0 \rightarrow S_3$	307.91	469.10	1.08	157.75	-0.93	8.55×10^{-3}
	$S_0 \rightarrow S_4$	305.51	554.20	0.97	0.15	1.00	7.01×10^{-3}
2c	$S_0 \rightarrow S_1$	375.75	363.49	3.89	119.48	-0.49	2.11×10^{-2}
	$S_0 \rightarrow S_2$	349.00	358.06	0.88	0.047	1.00	9.83×10^{-3}
	$S_0 \rightarrow S_3$	306.59	474.35	2.59	179.49	-1.00	2.19×10^{-2}
	$S_0 \rightarrow S_4$	300.48	948.12	1.53	0.06	1.00	6.45×10^{-3}
2d	$S_0 \rightarrow S_1$	364.23	363.91	4.11	97.64	-0.13	6.00×10^{-3}
	$S_0 \rightarrow S_2$	332.82	311.29	0.64	0.10	1.00	8.27×10^{-3}
	$S_0 \rightarrow S_3$	293.90	247.33	2.45	167.65	-0.98	3.87×10^{-2}
	$S_0 \rightarrow S_4$	286.38	769.59	0.68	0.065	1.00	3.53×10^{-3}

Table S16. Calculated photophysical property data of the S_1 excited state for all compounds at the cam-B3LYP/6-31G(d,p) level.

	Electronic Transition	TD//cam-B3LYP/6-31G(d,p)			
		Energy/eV ^a	f ^b	Major contributions	
1a	$S_1 \rightarrow S_0$	2.9036 eV	427.00 nm	0.4441	HOMO->LUMO (91%)
1b	$S_1 \rightarrow S_0$	2.7627 eV	448.78 nm	0.4191	HOMO->LUMO (83%)
1c	$S_1 \rightarrow S_0$	2.6151 eV	474.10 nm	0.3309	H-2->LUMO (11%), HOMO->LUMO (80%)
1d	$S_1 \rightarrow S_0$	2.9047 eV	426.84 nm	0.4810	HOMO->LUMO (90%)
2a	$S_1 \rightarrow S_0$	2.4628 eV	503.43 nm	0.1221	HOMO->LUMO (94%)
2b	$S_1 \rightarrow S_0$	2.4362 eV	508.93 nm	0.1396	HOMO->LUMO (87%)
2c	$S_1 \rightarrow S_0$	2.2683 eV	546.59 nm	0.0922	H-2->LUMO (11%), HOMO->LUMO (85%)
2d	$S_1 \rightarrow S_0$	2.4944 eV	497.06 nm	0.1209	HOMO->LUMO (93%)

^aOnly the selected low-lying excited states are presented. ^bOscillator strength.

Table S17. Coordinates of electric transition dipole moment (μ) and magnetic transition dipole moments (m) of the excited state of (P)-enantiomers of **2a–2d** at the cam-B3LYP/6-31G(d,p) level.

Electronic Transition		μ [a.u.]			m [a.u.]		
		x	y	z	x	y	z
2a	$S_1 \rightarrow S_0$	-1.3640	-0.4051	-0.0204	0.3668	-0.2160	2.2284
2b	$S_1 \rightarrow S_0$	1.4134	-0.5007	0.3002	-1.2166	-0.4952	1.9163
2c	$S_1 \rightarrow S_0$	-0.6225	-1.1218	-0.1115	-0.2810	0.4822	2.2386
2d	$S_1 \rightarrow S_0$	-0.5874	-1.2776	0.0306	-0.1178	0.1980	-2.7374

Table S18. Calculated transition dipole moments (μ , m , and θ) and g_{lum} values of (P)-enantiomers of **2a–2d**.

	Electronic Transition	Energy [nm]	$ \mu $ [10^{-20} esu cm]	$ m $ [10^{-20} erg G $^{-1}$]	θ [°]	$\cos \theta$	$ g_{lum} ^{\text{cal}}$
2a	$S_1 \rightarrow S_0$	503.43	361.70	2.10	98.16	-0.14	3.30×10^{-3}
2b	$S_1 \rightarrow S_0$	508.96	388.70	2.15	104.61	-0.25	5.59×10^{-3}
2c	$S_1 \rightarrow S_0$	546.59	327.32	2.14	101.96	-0.21	5.42×10^{-3}
2d	$S_1 \rightarrow S_0$	497.06	357.50	2.55	93.97	-0.069	1.97×10^{-3}

HPLC measurements for bulk purity

HPLC was performed using LaboACE LC-5060 instrument with UV detector (UV-4ch 400 LA) by Japan Analytical Industry Co., Ltd. equipped with a JAIGEL-2HR with a chloroform (CHCl_3) eluent.

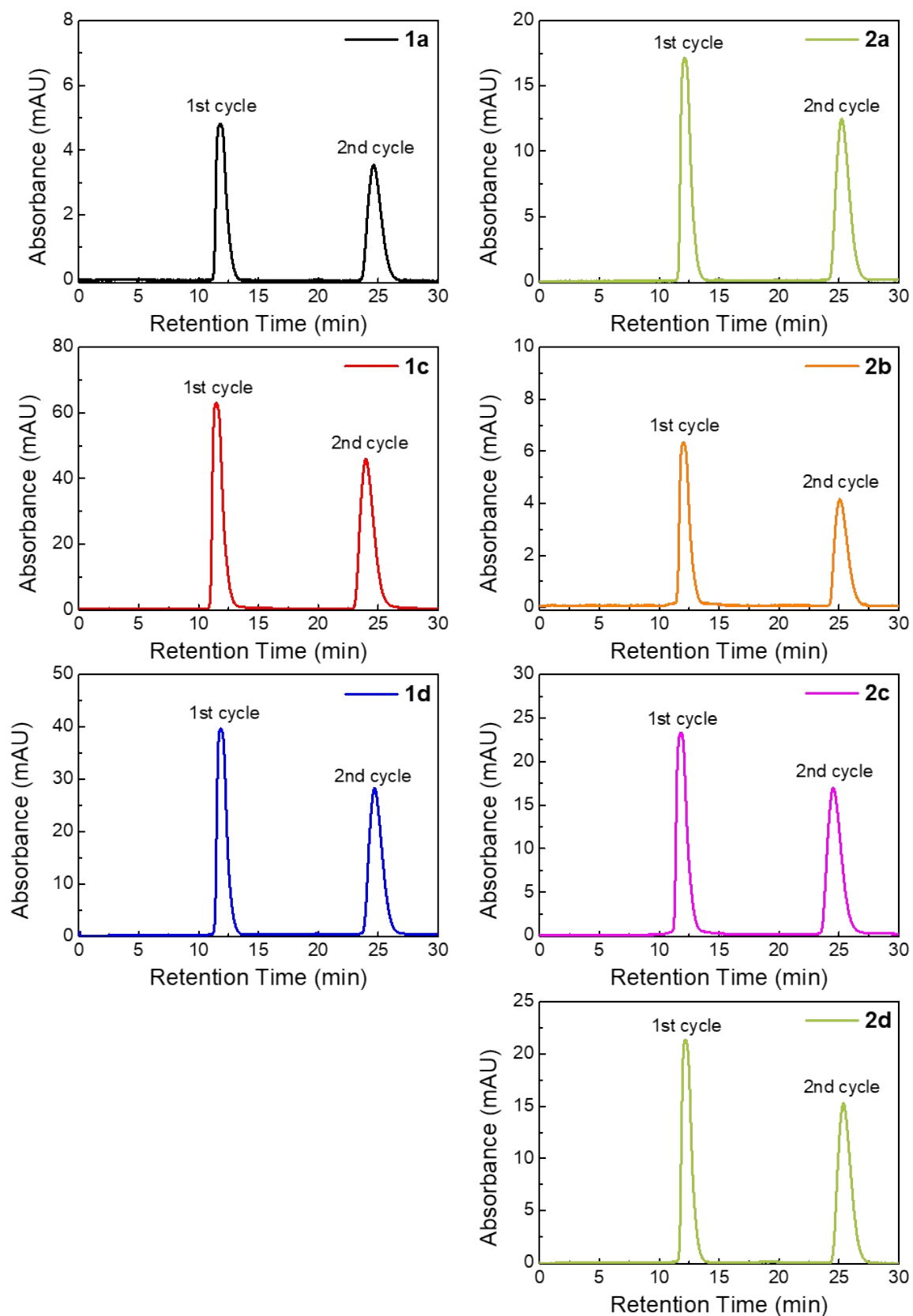


Figure S55. HPLC profiles of all compounds in CHCl_3 . The results show that all synthesized complexes are pure.

The ground states of 1a optimized at B3LYP/6-31G(d,p) level.

C	0.377021162	-0.643323692	-1.757350309
N	1.611559839	-0.663130156	-1.168352202
C	2.347600000	-1.814628825	-1.139507560
C	1.896843337	-2.992252075	-1.776504890
C	0.668031608	-2.952226616	-2.388582698
C	-0.112612758	-1.773140429	-2.376234458
C	-0.377027793	0.643366508	-1.757329782
N	-1.611556188	0.663157875	-1.168309958
C	-2.347598830	1.814653426	-1.139428374
C	-1.896856376	2.992290652	-1.776409956
C	-0.668055262	2.952281089	-2.388510185
C	0.112592225	1.773196575	-2.376200448
N	3.476333082	-1.689462244	-0.438194811
N	3.590301012	-0.400043013	0.082477988
B	2.384053634	0.509790424	-0.399295873
C	4.784642723	-0.284754707	0.647319303
O	5.523113490	-1.352678328	0.568804682
B	4.819102793	-2.486444484	-0.189092802
N	-3.476323578	1.689467314	-0.438105853
N	-3.590282327	0.400037120	0.082543300
B	-2.384030535	-0.509778344	-0.399260570
C	-4.784623900	0.284732236	0.647385228
O	-5.523098408	1.352654494	0.568891308
B	-4.819093046	2.486441081	-0.188978936
F	2.830072192	1.484749496	-1.260622347
F	1.625354897	1.005710591	0.630818800
F	4.638652933	-3.572785828	0.615310694
F	5.466025743	-2.771347651	-1.358403020
C	5.293326736	0.910625959	1.319840064
C	4.443914764	1.942518287	1.753644020
C	4.986212084	3.056960340	2.387059541
C	6.364316294	3.150948717	2.594315017
C	7.208254044	2.120284504	2.173451498
C	6.678251385	0.999940013	1.542268973
F	-2.830046521	-1.484729822	-1.260597068
F	-1.625304874	-1.005704325	0.630831786
F	-4.638642355	3.572762205	0.615451630
F	-5.466020451	2.771372374	-1.358279743
C	-5.293323985	-0.910660863	1.319874667
C	-4.443931570	-1.942565341	1.753689932

C	-4.986254815	-3.057011421	2.387076559
C	-6.364365031	-3.150992898	2.594293776
C	-7.208283202	-2.120316085	2.173422991
C	-6.678254560	-0.999967345	1.542269984
H	2.515212607	-3.880553077	-1.748382072
H	0.283171442	-3.837946641	-2.883529466
H	-1.095437192	-1.753504868	-2.823972847
H	-2.515228461	3.880588818	-1.748259816
H	-0.283206614	3.838012010	-2.883446422
H	1.095408240	1.753572364	-2.823957644
H	3.371801186	1.862231144	1.621917499
H	4.328797048	3.850790170	2.727106264
H	6.779598988	4.023645918	3.089507307
H	8.278834971	2.189515652	2.338311351
H	7.319646014	0.190833664	1.212652418
H	-3.371813992	-1.862283713	1.622002141
H	-4.328854723	-3.850849422	2.727133104
H	-6.779667517	-4.023692930	3.089464534
H	-8.278868944	-2.189540433	2.338254745
H	-7.319634478	-0.190851055	1.212648682

The ground states of 1b optimized at B3LYP/6-31G(d,p) level.

C	-2.130597676	-2.058313281	1.242440790
N	-1.527499133	-0.832969986	1.281548788
C	-0.305799524	-0.680270149	1.877386691
C	0.299936284	-1.750534305	2.499439479
C	-0.346543506	-3.007946334	2.503964802
C	-1.558178232	-3.180944638	1.880470349
C	0.305785263	0.680105549	1.877435862
N	1.527473532	0.832852995	1.281589725
C	2.130583113	2.058193507	1.242588986
C	1.558186212	3.180767802	1.880741431
C	0.346562480	3.007718873	2.504241842
C	-0.299928564	1.750312373	2.499609668
N	3.259929814	2.058188850	0.528717193
N	3.528888601	0.778846938	0.039874466
B	2.407983902	-0.248889497	0.489015268
C	4.753222718	0.773702954	-0.472725496
O	5.371719213	1.915497348	-0.386561123
B	4.529867617	2.976468077	0.337478029
B	-2.407998513	0.248825579	0.489038273

N	-3.528898036	-0.778877276	0.039816150
N	-3.259938069	-2.058262856	0.528554599
B	-4.529971261	-2.976443576	0.337441281
O	-5.371722705	-1.915492295	-0.386732248
C	-4.753216871	-0.773695884	-0.472810566
C	-5.361441479	0.393003975	-1.119251867
C	5.361479474	-0.392952077	-1.119216793
C	4.527568871	-1.254845027	-1.820059205
C	5.045130616	-2.375437332	-2.497368909
C	6.395961358	-2.630299800	-2.469719128
C	7.287421660	-1.785188456	-1.758483632
C	6.781507519	-0.634911975	-1.063160645
C	8.678392370	-2.070877457	-1.719799484
C	9.544842008	-1.268761818	-1.016177637
C	9.047278867	-0.145608214	-0.317657347
C	7.705287427	0.166520176	-0.337652269
C	-4.527503089	1.254905708	-1.820048918
C	-5.045034173	2.375541712	-2.497310959
C	-6.395858433	2.630437111	-2.469653589
C	-7.287344135	1.785320449	-1.758455236
C	-6.781462486	0.634999284	-1.063183262
C	-8.678306802	2.071046418	-1.719756949
C	-9.544777131	1.268923862	-1.016168911
C	-9.047244840	0.145726621	-0.317696239
C	-7.705262450	-0.166438739	-0.337705948
F	-2.934821092	1.204522076	1.323214665
F	-1.693421967	0.774141457	-0.558113486
F	-4.290405201	-4.045514416	-0.473201018
F	-5.100310377	-3.312604064	1.534857788
F	2.934796814	-1.204640701	1.323128753
F	1.693407515	-0.774128799	-0.558177125
F	4.290202611	4.045385551	-0.473341995
F	5.100156932	3.312876945	1.534841658
H	1.271440402	-1.624433891	2.954494548
H	0.128737038	-3.847205973	3.001280119
H	-2.074979682	-4.131723756	1.846074537
H	2.075011199	4.131537999	1.846452354
H	-0.128696249	3.846932161	3.001656285
H	-1.271420843	1.624172244	2.954677828
H	3.463297674	-1.058056815	-1.860364572
H	4.370356591	-3.025191850	-3.044755195
H	6.804489210	-3.489767072	-2.994604553
H	9.042460496	-2.943322563	-2.255482655
H	10.606145876	-1.496295779	-0.991356404

H	9.731445411	0.483351815	0.243909608
H	7.351986100	1.036421371	0.198431534
H	-3.463235591	1.058092767	-1.860345908
H	-4.370242670	3.025304147	-3.044666393
H	-6.804361467	3.489939250	-2.994501337
H	-9.042352173	2.943525275	-2.255400723
H	-10.606074490	1.496486743	-0.991335898
H	-9.731428954	-0.483236821	0.243845394
H	-7.351983930	-1.036370946	0.198343058

The ground states of 1c optimized at B3LYP/6-31G(d,p) level.

C	-1.127425872	-3.184786015	-2.660413981
C	0.092307661	-2.819631466	-3.173526372
C	0.559424952	-1.489476737	-3.060854116
C	-0.225159489	-0.546401773	-2.432949331
N	-1.452366945	-0.892093790	-1.935066191
C	-1.892173549	-2.185631385	-2.016473850
C	0.196470374	0.880083965	-2.330508469
N	1.368451662	1.161287908	-1.682151465
C	1.802124927	2.454063048	-1.564534587
C	1.103538906	3.522909417	-2.171760618
C	-0.055303422	3.223582475	-2.843590538
C	-0.528691933	1.892625979	-2.920166275
N	2.897045018	2.564510855	-0.814055529
N	3.296678332	1.312349576	-0.340979670
B	2.383908290	0.170379495	-0.938403293
C	4.462186201	1.456492135	0.286676098
O	4.918958821	2.679393807	0.285124387
B	3.997641852	3.641484105	-0.462019521
N	-3.072321106	-2.370363257	-1.423445312
N	-3.494452270	-1.190493920	-0.805309955
B	-2.503585223	-0.001985100	-1.112838847
C	-4.508915722	-1.480711948	0.004897572
O	-4.823094266	-2.747057823	0.033666522
B	-3.938853270	-3.581582135	-0.892317368
C	-5.244524471	-0.522208475	0.803097343
C	5.207421769	0.400649093	0.940493294
C	4.654556847	-0.860784055	1.234181921
C	5.409122837	-1.836759785	1.858239962
C	6.761267283	-1.602965149	2.221542290
C	7.303570509	-0.322390525	1.936929974
C	6.541282744	0.649261818	1.316897569

C	-5.187170886	0.865377002	0.571720946
C	-5.898993911	1.745535136	1.365236540
C	-6.706626663	1.282363499	2.436846981
C	-6.774357699	-0.119778495	2.647760157
C	-6.063685936	-0.993129274	1.846368474
N	-7.402745416	2.157680931	3.234125194
C	-7.315353540	3.591290627	2.999622228
C	-8.253232159	1.656982551	4.303391692
N	7.513974294	-2.576579874	2.831427584
C	8.883135439	-2.297056603	3.237265491
C	6.929576393	-3.875660077	3.129933888
F	-4.685587394	-4.163195621	-1.877778726
F	-3.176494897	-4.476915172	-0.191548492
F	-1.940445648	0.544937777	0.004956001
F	-3.110282663	0.943775923	-1.923716667
F	1.737342911	-0.578824733	0.014080015
F	3.093751552	-0.602018794	-1.832947846
F	4.603096080	4.136559717	-1.585500696
F	3.524526535	4.616867611	0.369953769
H	-1.510946559	-4.196083849	-2.707574162
H	0.713840424	-3.559997894	-3.666837505
H	1.533680516	-1.209742721	-3.433847605
H	1.488493240	4.530129215	-2.073953289
H	-0.624083903	4.016888891	-3.317918401
H	-1.460886079	1.662566948	-3.414396129
H	3.617015023	-1.069519408	1.002756242
H	4.941140349	-2.787492854	2.077997378
H	8.326611421	-0.089615832	2.202639581
H	6.973092861	1.621427592	1.107717088
H	-4.611806300	1.255661617	-0.259196588
H	-5.837664914	2.803394419	1.145467345
H	-7.384474196	-0.524569948	3.444779571
H	-6.126487475	-2.060957432	2.023504367
H	-7.705028659	3.870257553	2.011613542
H	-7.904474453	4.113639515	3.753283097
H	-6.281042951	3.949883155	3.071760866
H	-7.679706311	1.087739409	5.046151769
H	-8.719809485	2.499391959	4.813793336
H	-9.052164919	1.008958543	3.920129841
H	9.512826891	-2.027950519	2.379787878
H	8.935043335	-1.479279550	3.968086508
H	9.308720315	-3.188176644	3.698417692
H	6.089535398	-3.797241718	3.832820697
H	6.568191460	-4.373275538	2.221568452

H	7.688677400	-4.514043867	3.581781836
---	-------------	--------------	-------------

The ground states of 1d optimized at B3LYP/6-31G(d,p) level.

C	0.158062331	-0.728745103	-2.411545747
N	1.322416036	-1.131384927	-1.817091764
C	1.664873664	-2.454323345	-1.787385976
C	0.873209624	-3.433602342	-2.427186972
C	-0.280168260	-3.013877136	-3.043820440
C	-0.655930700	-1.650543692	-3.033389182
C	-0.158072577	0.728739382	-2.411548832
N	-1.322430191	1.131383795	-1.817104803
C	-1.664881104	2.454324361	-1.787400475
C	-0.873207042	3.433600352	-2.427193618
C	0.280174616	3.013870463	-3.043816715
C	0.655931314	1.650535516	-3.033381863
N	2.774810889	-2.685118806	-1.081922645
N	3.277737485	-1.495082550	-0.556763222
B	2.416360339	-0.255872498	-1.045173195
C	4.441783174	-1.756046829	0.021389231
O	4.814833074	-2.999608041	-0.051560047
B	3.801605462	-3.860425836	-0.822452667
N	-2.774819091	2.685125664	-1.081940156
N	-3.277753551	1.495091202	-0.556785109
B	-2.416386475	0.255876065	-1.045195717
C	-4.441796160	1.756060275	0.021369324
O	-4.814839794	2.999623815	-0.051575030
B	-3.801609632	3.860436780	-0.822470575
F	3.148163409	0.530801479	-1.903055195
F	1.847608807	0.452976305	-0.016669968
F	3.284254277	-4.836438206	-0.024102052
F	4.342863473	-4.329213298	-1.985190595
C	5.287284384	-0.777463621	0.703312728
C	4.802395413	0.473537733	1.120265977
C	5.650215621	1.368008037	1.764453752
C	6.979572689	1.010553102	1.992416600
C	7.474970279	-0.232276261	1.595921990
C	6.624894549	-1.126115063	0.955838995
F	-3.148196011	-0.530785657	-1.903083384
F	-1.847652041	-0.452982203	-0.016689743
F	-3.284253949	4.836448599	-0.024122246
F	-4.342867347	4.329224549	-1.985208619
C	-5.287290380	0.777474221	0.703295778

C	-4.802392873	-0.473530388	1.120228262
C	-5.650201809	-1.368008995	1.764419112
C	-6.979556338	-1.010558579	1.992404689
C	-7.474962500	0.232273481	1.595928589
C	-6.624898041	1.126120640	0.955842250
Br	8.138633216	2.239763757	2.872378711
Br	-8.138602312	-2.239781088	2.872369239
H	1.184517048	-4.470176524	-2.397661379
H	-0.919200826	-3.736408909	-3.540922229
H	-1.581866248	-1.326651766	-3.485861712
H	-1.184509052	4.470176169	-2.397668438
H	0.919215818	3.736399929	-3.540910767
H	1.581871408	1.326640209	-3.485842974
H	3.763269370	0.740143920	0.969746355
H	5.281194935	2.331870888	2.094262916
H	8.508992255	-0.493906347	1.786720477
H	6.988423285	-2.097813542	0.642343762
H	-3.763268560	-0.740133310	0.969686214
H	-5.281174805	-2.331875037	2.094211867
H	-8.508982624	0.493899067	1.786743507
H	-6.988433180	2.097821120	0.642360986

The ground states of (*P*)-2a optimized at B3LYP/6-31G(d,p) level.

F	-4.830385376	-0.010546245	1.893877103
F	-5.758309282	-0.665554037	-0.088697960
F	-0.790290550	-1.000924399	-2.015925088
F	0.787759225	-0.998800451	2.013381905
F	5.758617792	-0.662326775	0.092484963
F	4.833422287	-0.007416850	-1.891387985
O	-4.240105184	1.179509058	-0.097945578
O	0.000485841	-0.078298109	-0.002580350
O	4.239804331	1.182232992	0.099705962
N	-2.452068881	-0.065427742	-0.468579023
N	-3.336228151	-0.923096719	0.186967662
N	-1.452560068	-2.140528523	0.047080364
N	1.454381379	-2.139521377	-0.047630515
N	3.337064394	-0.920603188	-0.186744833
N	2.451860597	-0.063483237	0.468151908
C	-3.035256505	3.533718254	-1.018509996
H	-3.882333727	3.600805445	-0.345607047
C	-2.513201405	4.670885321	-1.626114208
H	-2.956201467	5.641118958	-1.424263293

C	-1.424358254	4.562388956	-2.494458757
C	-0.861394742	3.311861639	-2.759291718
H	-0.024819069	3.225281468	-3.445351103
C	-1.372596739	2.167034816	-2.154831364
H	-0.952525912	1.196746059	-2.389956341
C	-2.459878092	2.276994192	-1.271695132
C	-3.042270358	1.110170418	-0.607879014
C	-2.745959981	-2.083208361	0.476467538
C	-3.349695643	-3.182191459	1.131923598
H	-4.376931820	-3.103683955	1.464749486
C	-2.587541014	-4.310876153	1.314258996
H	-3.014488045	-5.172233551	1.817819785
C	-1.247228278	-4.363316031	0.867128250
H	-0.636005319	-5.238078356	1.045422454
C	-0.700039528	-3.260900526	0.239414457
C	0.702746111	-3.260438914	-0.240057361
C	1.251027231	-4.362573574	-0.867325226
H	0.640553423	-5.237838676	-1.045724101
C	2.591534698	-4.309220537	-1.313757479
H	3.019366064	-5.170353352	-1.816953104
C	3.352840575	-3.179984488	-1.131173447
H	4.380195753	-3.100849327	-1.463483778
C	2.747968770	-2.081311515	-0.476252660
C	3.041441476	1.112338425	0.608311367
C	2.457851100	2.278880211	1.271567579
C	1.369412733	2.168522518	2.153225375
H	0.949350144	1.198068494	2.387699819
C	0.857075576	3.313143571	2.757118139
H	0.019576601	3.226244512	3.442010968
C	1.420040755	4.563858471	2.493187414
C	2.510022860	4.672757343	1.626322053
H	2.953036982	5.643132848	1.425178818
C	3.033208716	3.535806334	1.019290353
H	3.881126224	3.603213361	0.347487288
B	-4.666528223	-0.143186117	0.543060219
B	-1.025422803	-0.749836939	-0.671753697
B	1.025331430	-0.748554414	0.669481236
B	4.667591319	-0.140241947	-0.540844485
H	1.014328729	5.451991115	2.968634868
H	-1.019539447	5.450691456	-2.970349233

The ground states of (*P*)-2b optimized at B3LYP/6-31G(d,p) level.

F	3.934020157	0.131330301	3.677555520
F	5.131861481	1.514065482	2.307108685
F	1.607343513	1.336059559	-1.436379611
F	-1.607195100	1.336482170	1.436426226
F	-3.933477946	0.131120606	-3.677501380
F	-5.131579768	1.514125554	-2.307557342
O	4.274327399	-0.544091152	1.419659250
O	0.000037051	0.385329789	0.000124123
O	-4.274239984	-0.543875925	-1.419547742
N	2.415979675	0.390472425	0.675200017
N	2.776409285	1.172126374	1.778674485
N	1.242864873	2.437780344	0.730074259
N	-1.242511313	2.437826276	-0.730178639
N	-2.776240239	1.172246952	-1.778586250
N	-2.415895144	0.390669335	-0.675038137
C	2.021804771	-1.973919358	-0.987468274
C	1.885165273	-2.964988900	-1.977512419
C	3.003934356	-3.566962116	-2.502874696
C	4.304877553	-3.198130457	-2.071824700
C	4.467119387	-2.188876337	-1.062160706
C	3.272238270	-1.585661582	-0.524309267
C	3.324364166	-0.564340633	0.526861302
C	2.148117772	2.351380569	1.743349946
C	2.367620632	3.437989497	2.621442331
C	1.629356303	4.579969690	2.417981182
C	0.676284370	4.654549778	1.376733773
C	0.497066370	3.563392212	0.549057507
C	-0.496577574	3.563375648	-0.549313121
C	-0.675652067	4.654437989	-1.377143748
C	-1.628726365	4.579832416	-2.418389427
C	-2.367133085	3.437918962	-2.621694785
C	-2.147769399	2.351401582	-1.743450257
C	-3.324329960	-0.564101164	-0.526692649
C	-3.272427007	-1.585298127	0.524605149
C	-4.467457103	-2.188389997	1.062239532
C	-4.305517852	-3.197542266	2.072049109
C	-3.004696736	-3.566402770	2.503445091
C	-1.885770065	-2.964559361	1.978264565
C	-2.022119457	-1.973592035	0.988074769
B	4.107569598	0.610137304	2.412147479
B	1.222744617	1.067443932	-0.141558317
B	-1.222591187	1.067619698	0.141657288
B	-4.107277059	0.610169986	-2.412215891
C	5.452723602	-3.813136954	-2.639595344

C	6.717895915	-3.447669418	-2.246461871
C	6.881319820	-2.443133739	-1.266358056
C	5.791437153	-1.829158847	-0.688295990
C	-5.791652529	-1.828646550	0.687983897
C	-6.881716756	-2.442490990	1.265841056
C	-6.718595805	-3.446916844	2.246110016
C	-5.453542134	-3.812415156	2.639604287
H	1.132157129	-1.515682045	-0.572776168
H	0.893584303	-3.250294824	-2.313070856
H	2.908754403	-4.337094033	-3.263731450
H	3.108031638	3.347149581	3.405852414
H	1.772226884	5.435058713	3.070850539
H	0.062338331	5.535905927	1.245290552
H	-0.061595185	5.535734791	-1.245820724
H	-1.771484554	5.434848842	-3.071378367
H	-3.107556538	3.347062240	-3.406091401
H	-2.909739382	-4.336457936	3.264407389
H	-0.894282727	-3.249890326	2.314078701
H	-1.132347823	-1.515463240	0.573532479
H	5.307536151	-4.576809242	-3.398831296
H	7.588930346	-3.922313539	-2.687867427
H	7.880998139	-2.148399834	-0.961501287
H	5.945292581	-1.069156731	0.064486087
H	-5.945263423	-1.068732431	-0.064942702
H	-7.881300405	-2.147740405	0.960690026
H	-7.589768933	-3.921462437	2.687347542
H	-5.308588420	-4.576012862	3.398959880

The ground states of (*P*)-2c optimized at B3LYP/6-31G(d,p) level.

N	4.807032075	1.331932717	-3.220576071
N	4.808716742	-1.328872432	3.220361437
F	-0.789647440	-4.592957023	-2.376109392
F	-1.523836661	-5.730236482	-0.536501671
F	-1.844869527	-0.977887091	1.923525671
F	-1.846319266	0.976294347	-1.923448866
F	-1.527837468	5.729689577	0.535121809
F	-0.794337475	4.593321700	2.375566335
O	0.331620243	-4.244304867	-0.293584978
O	-0.913081902	0.000007815	0.000119004
O	0.328320582	4.244581415	0.293664926
N	-0.906924337	-2.486718772	0.227409383
N	-1.751491793	-3.290429029	-0.542202116
N	-2.975386968	-1.439226500	-0.200182952

N	-2.976688173	1.437261284	0.200443122
N	-1.754465171	3.289733923	0.541574269
N	-0.909360368	2.486594003	-0.228055822
C	2.649144315	-3.247800563	0.915451711
H	2.724663195	-4.069438202	0.212100206
C	3.770603925	-2.830326832	1.608148493
H	4.710127417	-3.337905484	1.431098327
C	3.696886915	-1.758243026	2.534732246
C	2.430167483	-1.150592738	2.732866257
H	2.315121725	-0.348206792	3.449845766
C	1.314175132	-1.571605824	2.033620209
H	0.360228654	-1.103401897	2.242672835
C	1.401824077	-2.622958905	1.101060843
C	0.262739429	-3.103808666	0.344182716
C	-2.910776696	-2.677732777	-0.771174212
C	-4.007192998	-3.207138049	-1.494307919
C	-5.137185348	-2.432724695	-1.594496243
H	-5.996144239	-2.804146899	-2.144298313
C	-5.195522880	-1.149294550	-1.002014018
H	-6.071047480	-0.523683755	-1.114814715
C	-4.096440990	-0.672754049	-0.314343917
C	-4.096947365	0.669717450	0.315164305
C	-5.196174620	1.145250726	1.003299723
H	-6.071049755	0.518811741	1.116543971
C	-5.138784463	2.428771419	1.595677272
H	-5.997818715	2.799379768	2.145910870
C	-4.009600337	3.204286302	1.494874430
C	-2.913025858	2.675910783	0.771226294
C	0.260077105	3.104199416	-0.344363336
C	1.399462692	2.624010248	-1.101194455
C	1.312352693	1.572735179	-2.033898054
H	0.358637628	1.104092499	-2.243038999
C	2.428576618	1.152326953	-2.733128422
H	2.313978850	0.349912285	-3.450145693
C	3.694990635	1.760585032	-2.534865811
C	3.768194332	2.832478789	-1.608030714
H	4.707510541	3.340369164	-1.430753679
C	2.646494698	3.249352042	-0.915358137
H	2.721606540	4.070882232	-0.211837106
B	-0.966629253	-4.577258725	-1.017854817
B	-1.586522061	-1.088892338	0.562572863
B	-1.587722219	1.088024138	-0.562610149
B	-0.970458443	4.577103126	1.017215333
C	6.075377790	2.025740569	-3.062887961

C	4.697748120	0.253986969	-4.192268735
H	6.827882708	1.542407120	-3.686051286
H	6.009624500	3.079598124	-3.365571008
H	6.427733213	1.992648899	-2.024096823
H	5.687282053	0.030641297	-4.591368538
H	4.306377744	-0.661303399	-3.732532120
H	4.043130833	0.519083710	-5.033721242
C	4.698786408	-0.251105260	4.192170747
C	6.077250019	-2.022520907	3.063421732
H	5.688335433	-0.026535807	4.590557294
H	4.306037801	0.663681061	3.732645718
H	4.045046957	-0.516930041	5.034092460
H	6.829661220	-1.538179449	3.685916520
H	6.011889379	-3.076058315	3.367341926
H	6.429467750	-1.990507572	2.024565843
H	-3.928610182	4.189170625	1.937200997
H	-3.925483581	-4.191958664	-1.936645002

The ground states of (*P*)-2d optimized at B3LYP/6-31G(d,p) level.

Br	-5.154034849	-0.008765368	1.931153814
Br	-5.154082083	0.008830850	-1.930974275
F	1.481630134	-4.974055517	1.588629573
F	1.725095252	-5.754473699	-0.545972785
F	2.145263369	-0.689604497	-2.075837885
F	2.145665660	0.690235245	2.076466860
F	1.724627533	5.754852273	0.544592018
F	1.481505148	4.973018166	-1.589536292
O	-0.007498705	-4.174990468	-0.118835902
O	1.293434601	-0.000014328	0.000523429
O	-0.007615404	4.174718418	0.118267118
N	1.255432695	-2.420581554	-0.588272838
N	2.161928250	-3.374202963	-0.123309754
N	3.353895347	-1.463557170	-0.086635935
N	3.353957980	1.463648575	0.086819270
N	2.162067265	3.374395070	0.123464496
N	1.255624103	2.420781091	0.588618951
C	-2.401435572	-2.732208035	-0.457873163
H	-2.409763943	-3.613541789	0.173226915
C	-3.587193731	-2.070608328	-0.755746102
H	-4.530510281	-2.415419356	-0.351125222
C	-3.541106171	-0.935904195	-1.565838321

C	-2.340062325	-0.468797554	-2.100788328
H	-2.333043540	0.402341034	-2.744915824
C	-1.154749066	-1.127761598	-1.793125570
H	-0.221110508	-0.776562707	-2.216903310
C	-1.178005903	-2.254530575	-0.955117070
C	0.044814702	-2.950208037	-0.558755453
C	3.322195799	-2.797251010	0.201168648
C	4.436779444	-3.454412010	0.771057486
H	4.369983760	-4.510047711	1.001444739
C	5.558286526	-2.701681519	1.022606225
H	6.429950624	-3.166909894	1.471418892
C	5.587008838	-1.321744652	0.720750235
H	6.456934378	-0.722500039	0.953984065
C	4.471070225	-0.722500155	0.166732724
C	4.471097355	0.722542664	-0.166522378
C	5.587042229	1.321703922	-0.720602504
H	6.456943850	0.722418313	-0.953815167
C	5.558382095	2.701650203	-1.022483689
H	6.430053814	3.166818823	-1.471339896
C	4.436917580	3.454429388	-0.770912899
H	4.370205961	4.510096814	-1.001188866
C	3.322281160	2.797305970	-0.201048160
C	0.044896383	2.950126877	0.558652882
C	-1.177872831	2.254385644	0.955092151
C	-1.154653719	1.127791486	1.793300188
H	-0.221053257	0.776654292	2.217217102
C	-2.340004348	0.468875706	2.101015837
H	-2.332994004	-0.402155798	2.745285942
C	-3.541003405	0.935876926	1.565927213
C	-3.587071893	2.070430477	0.755610516
H	-4.530364837	2.415131272	0.350866495
C	-2.401304706	2.731960851	0.457685403
H	-2.409582414	3.613190791	-0.173556579
B	1.383999117	-4.702876107	0.252021298
B	1.943976048	-0.988479854	-0.738081673
B	1.944052462	0.988740644	0.738604109
B	1.383893118	4.702719571	-0.252763369

References

- 1 H. Shimada, T. Sakurai, Y. Kitamura, H. Matsuura and T. Ihara, *Dalton Trans.*, 2013, **42**, 16006–16013.
- 2 P.-E. Doulain, C. Goze, E. Bodio, P. Richard and R. A. Decréau, *Chem. Commun.*, 2016, **52**, 4474–4477.
- 3 CrysAlisPro, Rigaku Oxford Diffraction, Tokyo, Japan. 2015.
- 4 G. M. Sheldrick, *Acta Cryst.*, 2015, **A71**, 3–8.
- 5 G. M. Sheldrick, *Acta Cryst.*, 2015, **C71**, 3–8.
- 6 O. V. Dolomanov, L. J. Bourhis, R. J. Gildea, J. A. K. Howard and H. Puschmann, *J. Appl. Cryst.*, 2009, **42**, 339–341.